Reconstruction of the Pollution, and Limnological History of Douglas Lake (Michigan) using Biomarkers

BY

Nnamdi Lionel Mojekwu

B.S., University of Illinois at Chicago, 2012

THESIS

Submitted as partial fulfillment of the requirements

for the degree of Master of Science in Earth and Environmental Sciences

in the Graduate College of the

University of Illinois at Chicago, 2015

Chicago, Illinois

Defense Committee:

Fabien Kenig, Advisor

Kathryn L. Nagy

Max Berkelhammer

ACKNOWLEDGMENTS

I had the utmost privilege of working with Fabien Kenig, my advisor and thesis committee chair. Work at Douglas Lake was completely funded by the organic geochemistry laboratory (OGL), and with this action I was denied one of life's great pleasure, grant writing. I am eternally grateful for the tutelage provided to me by all the professors in the EAES department and especially to Fabien, a true inspiration. I am also grateful to Neil Sturchio and the isotope geochemistry laboratory (IGL) for determining lead concentrations in Douglas Lake sediment, necessary values for sediment dating. I appreciate the efforts of my committee members (and Roy Plotnick) for their input into this thesis, any contributions they made were either crucial or the final linchpin required during the inception of a hypothesis. I would also like to extend my thanks to the OGL family: Joey Pasterski, Luoth Chou, and Ioana Stefanescu. In one way or another, each one was instrumental to my understanding of organic geochemistry and the completion of this study. Staff at the University of Michigan Biological Station (UMBS) were a pleasure to work with; we were graciously provided a modifiable pontoon boat and extra coring tools. I would especially like to thank Bob Vande Kopple for all the assistance with coring, and for collecting surface water samples for our analysis.

Finally, I would like to thank UIC for aiding me on this informative journey. Accepting me into the institution may have been as easy as the stroke of a pen but that decision has shaped my life for the better.

NML

TABLE OF CONTENTS

TABLE OF CONTENTS (CONTINUED)

TABLE OF CONTENTS (CONTINUED)

LIST OF TABLES

LIST OF FIGURES

LIST OF FIGURES (CONTINUED)

LIST OF FIGURES (CONTINUED)

LIST OF ABBREVIATIONS

UMBS: University of Michigan Biological Station

OM: Organic Matter

PAH: Polycyclic Aromatic Hydrocarbon

BPA: Bisphenol A

GC-MS: Gas Chromatography – Mass Spectrometry

DCM: Dichloromethane

MeOH: Methanol

HPLC: High Pressure Liquid Chromatography

TLE: Total Lipid Extract

SIM: Single Ion Monitoring

CPI: Carbon Preference Index

TOC: Total Organic Carbon

CRS: Constant Rate of Supply

CIC: Constant Initial Concentration

TIC: Total Ion Chromatogram

HMW: High Molecular Weight

LMW: Low Molecular Weight

MMA: Monomethyl Alkane

OEP: Odd over Even Predominance

HBI: Highly Branched Isoprenoid

FAME: Fatty Acid Methyl Ester

PEE: Phenyl Ethyl Ester

EPA: Environmental Protection Agency

TRI: Toxic Release Inventory

ECHO: Enforcement and Compliance History Online

HYSPLIT: Hybrid Single-Particle Lagrangian Integrated Trajectory

SUMMARY

In order to reconstruct the pollution and paleolimnologic history preserved in the sedimentary record of Douglas Lake, a core was collected, dated, and analyzed using gas chromatography – mass spectrometry (GC–MS). The total lipid extract from the sediment samples were separated into three fractions for enhanced analytical resolution and target compounds within the fractions were quantified. Target compounds included polycyclic aromatic hydrocarbons (PAHs), Bisphenol A (BPA), and numerous *n*-alkanes. In interpreting the analyses of these compounds, a few points were highlighted: (1) forest fires were the principal sources of PAHs in the lake; (2) the concentration profiles of biomarkers reflected the response of the ecosystem to natural or anthropogenic environmental perturbations; and (3) the anomalously large, intermittent inputs of BPA were transported to Douglas Lake following fugitive releases into the atmosphere.

Although further work is needed to assess the extent of contamination, the results from this study support the use of sediment cores in reconstructing the pollution history of lakes, especially where contamination monitoring is lacking.

CHAPTER I

1. INTRODUCTION

The history of human settlement around Douglas Lake, Michigan (Figure 1) has been reported by several researchers (Gold, Gannon, & Paddock, 1976; Stoermer, 1977; Voss, 1956; Wilson & Putzcer, 1942), most notably, by Kilburn (1957). Anthropogenic perturbations since modern settlement have affected the lacustrine ecosystem. These influences include but are not limited to:

I. increased eutrophication via delivery of surplus nutrient during excessive logging and uncontrolled fires (Francis, 1997); and

II. the introduction of contaminants like polycyclic aromatic hydrocarbons, which may have deleterious effects on the health of the ecosystem around the lake (Drooge, 2004; El-Shahawi et al., 2010; Rezg et al., 2014; Rosner & Markowitz, 2013; Tsai, 2006).

Despite the tenuous environmental track record of recent anthropogenic processes, modern Douglas Lake is one of the least disturbed lakes in Michigan because it is managed by the University of Michigan Biological Station (UMBS; Lind, 1987). However, as a result of global agriculture and manufacturing, even the most remote locations may receive measurable quantities of anthropogenic contamination via atmospheric transport (Rice et al., 1986).

In an effort to quantify the concentration of any atmospherically transported contaminants and potential ecological responses, a core from Douglas Lake was collected, dated and analyzed. Lipid biomarkers within the lake sediments were extracted, analyzed and quantified by gas chromatography–mass spectrometry (GC-MS). Variations in the concentration of lipid biomarkers have been frequently used to reconstruct ecosystem dynamics because biomarkers contain useful information about their precursor molecules, the organisms synthesizing them, as well as processes such as changes in primary productivity or anthropogenic perturbations (Castañeda &

Schouten, 2011; Das et al., 2009; George et al., 2008; Holtvoeth et al., 2010; Lu & Meyers, 2009; Meyers, 2003; Muri & Wakeham, 2006; Xu & Jaffé, 2008). In Douglas Lake, characterization of lipid within accumulated sediments is one of the few means of reconstructing lake history and contaminant record.

2. STUDY AREA

Douglas Lake is a 15 square kilometer mesotrophic kettle lake located in northwestern Cheboygan County, Michigan. It is a moderately productive lake undergoing a steady, natural transition to a more eutrophic state, especially in the shallower areas (Bazin & Saunder, 1971; Haynes & Barre Hellquist, 1978). There are several depressions in the lake including Maple Bay, Grapevine Point, North and South Fishtail Bay, which act as separate sub–basins and currently have anoxic bottom waters (Francis, 2001). Although the shorelines of both North and South Fishtail Bays remain mostly undeveloped, residential development continues along the shore of the western half of the lake.

There are three main reasons for choosing Douglas Lake:

1. The quantification of atmospherically transported contaminants to a relatively undisturbed lake was a major goal. As such, the selected lake should not be in the vicinity of any large, industrial pollutant source that may skew the results. The nearest industrial plants are H & H Tube (metal tubing plant), 17 kilometers northeast of the lake (Cheboygan County, MI), and Cornillie Concrete Plant, 23 kilometers southwest of the lake (Emmet County, MI). According to the EPA Toxic Release Inventory (TRI), neither company releases organic contaminants in quantifiable amounts. Thus, the river catchment proximal to Douglas Lake will not include high concentrations of industrial contamination

2. Douglas Lake has been extensively studied. Investigations include the composition and succession of the benthic fauna, historical reconstruction using pollen as proxies, and several limnological and paleolimnological studies (Francis, 1997; Goad & Stoermer, 1986; Nichols, 1922; Phinney, 1946; Stoermer, 1977; Wilson & Putzcer, 1942). However, the lacustrine sedimentary record has never been studied for native lipids and organic contaminants.
3. The UMBS provides local support including a cold storage facility in which sediment cores can be stored for the duration of lake sampling.

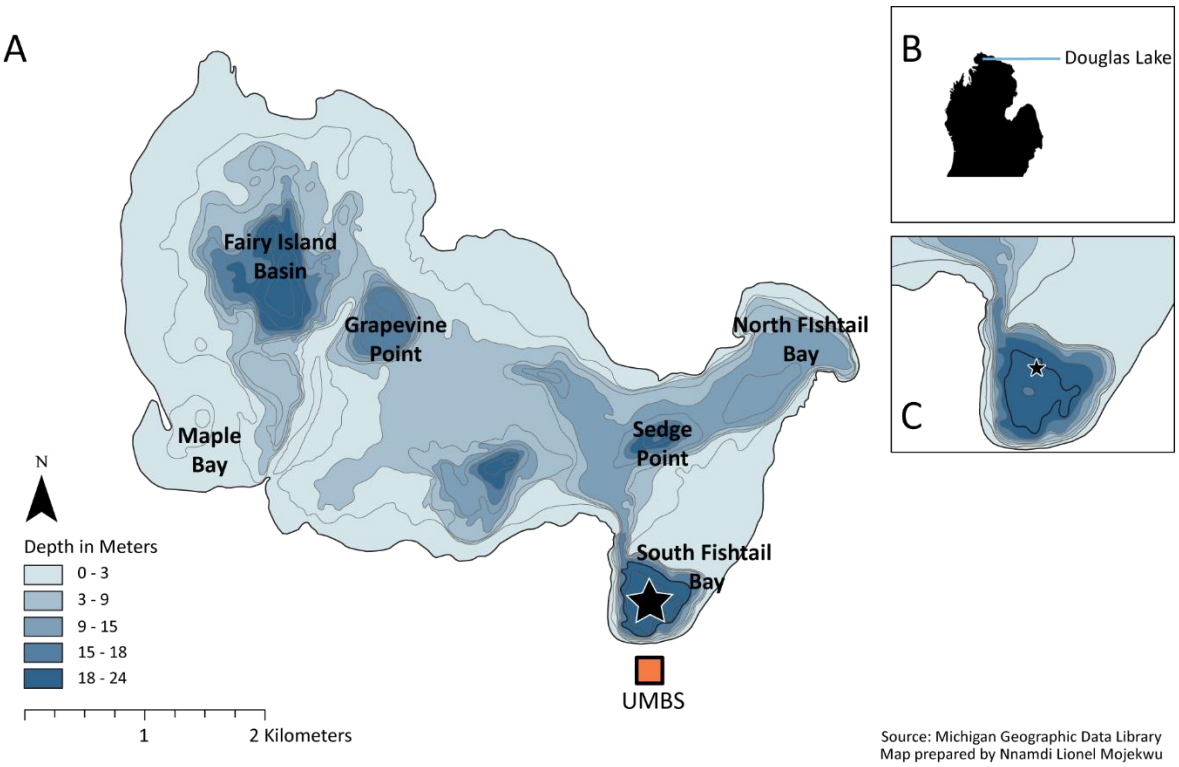

Figure 1. A) Simplified bathymetric map of Douglas Lake with the UMBS. B) Location of Douglas Lake in the State of Michigan. C) Large scale image of coring location in Douglas Lake.

3. HISTORY OF DOUGLAS LAKE

Phinney (1946) described two long cores (83 and 92 feet) collected from South Fishtail depression. Phinney noted that diatomaceous ooze at 83 feet dated to "a probable 15,000 years". However, the landscape in and around Douglas Lake was shaped by the action of retreating glaciers roughly 12,000 years ago. Glacial retreat created seven kettle depressions (maximum depth of ~24 meters) within the modern lake. Present day landscapes were further shaped by, fluctuating lake levels (Cwalinski, 2004; Gold et al., 1976; Kilburn, 1957). Around ~11,000 years ago, postglacial vegetation, spruce, pine, fir, and tamarack reemerged in Cheboygan County, MI (Cwalinski, 2004; Gold et al., 1976; Kilburn, 1957).

In the mid-19th century, following modern settlement around Douglas Lake, logging increased rapidly and by 1872 there were six mills in operation in the area. By 1880, the population of pine trees around the Douglas Lake region had declined significantly (Voss, 1956). In the period between 1880 and 1920 there were numerous uncontrolled fires. According to Kilburn (1957), there have been nine major fires, the largest ones occurred in 1892, 1901, 1911, and 1923. There have also been several incidences of controlled fires for research purposes between 1911 and 1954. Ecology classes led by Professor Frank Gates of the UMBS, clear-cut and burned three adjacent plots of 0.1 acres for insight into community succession following the event of a fire.

The combination of rapid logging and subsequent fires radically changed the landscape around Douglas Lake. Soil and air temperatures increased, and soil moisture decreased, increasing soil erosion (Kilburn, 1957). Major forest fires at Douglas Lake ceased once fire control measures were established in the 1920s (Francis, 2001).

4. RESEARCH ON DOUGLAS LAKE

Most of the research performed at UMBS and Douglas Lake has focused on ecological and taxonomic questions. For example, Eggleton (1931) estimated that ~80% of the surface area of Douglas Lake is underlain by shallow, highly organic sediments. Studies of hypolimnetic benthic fauna in the depressions of the lake have described simple communities well adapted to the cold, oxygen-deficient sediment. Fuller et al. (1977) reported on the community composition and population dynamics of rotifers in the lake from 1941 to 1974.

Changes in water quality as a result of the heavy logging around the lake were evident from decrease of diatom species diversity and by the increased abundance of eutrophic indicators, especially the diatom *Melosira granulata* (Stoermer, 1977). These changes were determined by the analysis of population diversity from a sediment core collected from the lake by Andresen (1976). Andresen interpreted the changes as direct consequences of the uncontrolled fires that recycled nutrients bound in the soil. It is likely that such variations will be reflected in the biomarker record.

5. BIOMARKERS

Although lipid biomarkers represent only a minor fraction of sedimentary organic matter (OM), they are important diagnostic geochemical fossils that convey information regarding the origin and the state of preservation of organic matter (OM) in sediments. This information includes, but is not limited to: determination of the types of organisms incorporated into sediments, history of the ecosystem in and around the sediment (community succession), and characterization and reconstruction of the depositional environment (George et al., 2008; Lu & Meyers, 2009). For example, it is possible to determine the percentage of contribution to OM derived from terrestrial plants (C_{29} *n*-alkane) relative to phytoplankton (C_{14} – C_{17} *n*-alkanes) or macrophytes (C_{23} and C_{25} *n*-

alkanes) (Ficken et al., 2000; Xu & Jaffé, 2008a). Biomarkers can also be used to detect anthropogenic contamination in recent sediment (Lu & Meyers, 2009; Tissot & Welte, 1984).

Resolution and accuracy of sediment characterization using biomarkers depends on the preservation of features that can be linked to the precursor molecule. Unfortunately there is a bias towards relatively inert (unreactive) molecules like *n*-alkanes, which rarely undergo alterations. Conversely, molecules like *n*-alkanols, ketones and fatty acids may lose functional groups or incorporate elements like sulfur (Kenig et al., 1990; ten Haven et al., 1992; Wakeham et al., 1995). There is also the possibility of a biomarker having such a wide distribution in nature that its usefulness as a unique biomarker is diminished. This is most evident with some sterols which are widely distributed (Volkman, 1986), although there remain several sterols that can only be found in a limited number of organism classes (Volkman et al., 1998).

6. CONTAMINANTS

Industrially produced anthropogenic contaminants including insecticides, polycyclic aromatic hydrocarbons (PAHs) and plasticizers, are ubiquitous in the environment. Many of these xenobiotic compounds are toxic (e.g. chlorinated pesticides) because of their potential for bioaccumulation, carcinogenicity, or potential for disruption of the endocrine system (e.g. Bisphenol A (BPA), Magliano & Lyons, 2013; Sheehan, 2000). PAHs also have carcinogenic, mutagenic, teratogenic and neurologic effects (El-Shahawi et al., 2010; Ritter et al., 2007). Pollutants can be deposited in lake sediment by runoff, leaching, spray drift from contaminated water bodies, or dry and wet atmospheric deposition (Fu & Kawamura, 2010; Hogarh et al., 2012; Turusov et al., 2002). Some pollutants have long residence times in the atmosphere and can be deposited at locations far from their sources. The resistance of some contaminants to degradation results in their persistence in

sediment long after contribution from their point sources have ceased. Thus, these resistant compounds have been aptly named persistent organic pollutants (POPs).

It is possible to detect the presence of contaminants within Douglas Lake using GC-MS. If these contaminants cannot be detected directly, their influence on the dynamics of an ecosystem can be inferred from lipid biomarkers.

CHAPTER II: RECONSTRUCTION OF THE LIMNOLOGICAL HISTORY OF DOUGLAS LAKE FROM BIOMARKERS

1. INTRODUCTION

Compared to proteins or carbohydrates, lipids usually make up a smaller portion of biogenic organic matter. However, lipids are often more resistant to degradation. Because of this property, they tend to be more easily preserved and may provide some information about their source organisms. Biomarkers may also provide proxies for information that may not have been otherwise preserved in the sedimentary record. For example, *n*-alkanes have been investigated in various organisms and sedimentary settings (Ficken et al., 2000; Kenig et al., 1990; Nichols et al., 2006; Tissot & Welte, 1984). Generally, the carbon number of algal *n*-alkanes ranges between $C_{15} - C_{21}$. There are exceptions to the trend, for example, planktonic green algae *Botryococcus braunii* have *n*-alkane values ranging from $C_{27} - C_{31}$ (Gelpi et al., 1968).

The analysis of the lipid composition of sediments from Douglas Lake aided in the determination of responses to natural or anthropogenic forcing.

2. FIELD METHOS AND SAMPLES

Field work was carried out in South Fishtail Bay in Douglas Lake (N 45° 33', 47.0" ; W 84° 40', 29.3"), August 20th 2013, in Cheboygan county, Michigan. The pontoon boat used for transportation and coring at the site was provided by the UMBS. The tripod used for coring was constructed out of recycled material: three aluminum pipes were wedged onto two glued chipboard bases. A 10 inch aluminum plate acted as the grip for the ratchet cable puller and held the pipes steady. Several polycarbonate core tubes were cleaned three times each with dichloromethane (DCM) in the laboratory and once more with native water from Douglas Lake

prior to use. Water depth at the sampling location was determined using a Hondex digital depth sounder.

Two surface sediment samples were collected with a Wildco (6''x 6''x 6'') Ekman dredge. These surface samples were used for testing extraction methodology (results not shown). However, the soft nature of the collected mud induced mixing in the Ekman dredge prior to sample recovery. Thus, the sample could not be used for dating. The retrieved core, termed DL–L2 (Douglas Lake Location 2), was obtained over the deepest portion (22.6 m) of the South Fishtail bay subbasin using a percussion corer. The core measured 95 cm from end to end. Prior to dewatering, sediment within the core was equally divided between soft, highly organic black mud (top 50 cm) and flocculent brown mud (bottom 45 cm; Fig. 2). When the core was dewatered, compaction occurred, affecting mainly the less consolidated black mud. The core was re-measured to be 65 cm long (Fig. 2), the length of the black mud was ~22 cm and the brown mud was ~40 cm. The depth of 90 cm was shown to correspond to the end of the fire and deforestation horizon of 1880, at lower depths industrial-scale contamination was minimal (Francis, 1997; Jarman & Ballschmiter, 2012). Since we are interested in the last 100 years of limnological history of Douglas Lake, the collected core did not need to exceed a length of ~90 cm below the sediment-water interface.

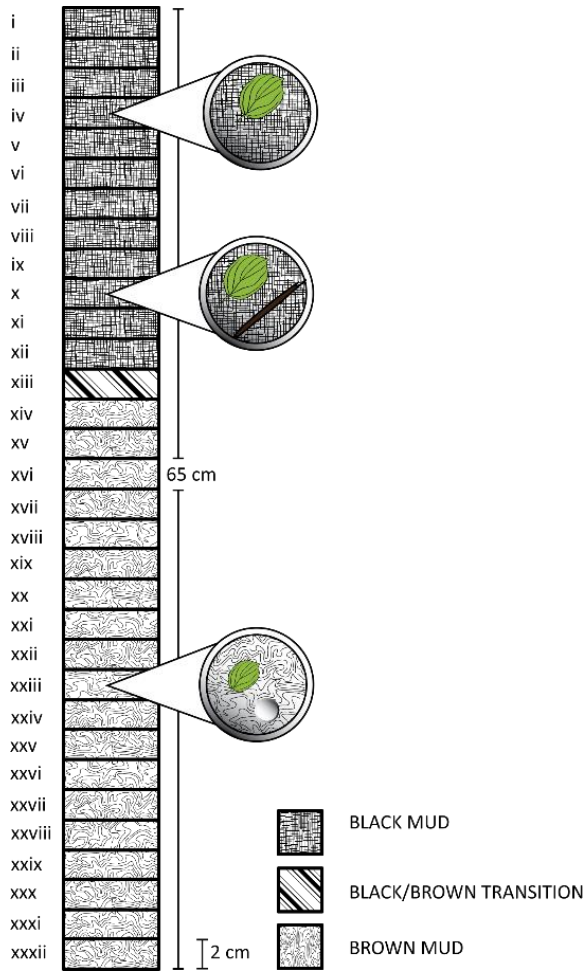

Figure 2. Cross section of DL–L2. Subsections iv, x, and xxiii contain visible plant debris and spherical carbonaceous materials.

3. LABORATORY METHODS

The core was stored in the cold storage facilities at UMBS and transported cold within an insulated container to the organic geochemistry laboratory at UIC, where it was kept refrigerated until use. Figure 3 presents an analytical flow diagram employed in the characterization of Douglas Lake sediment.

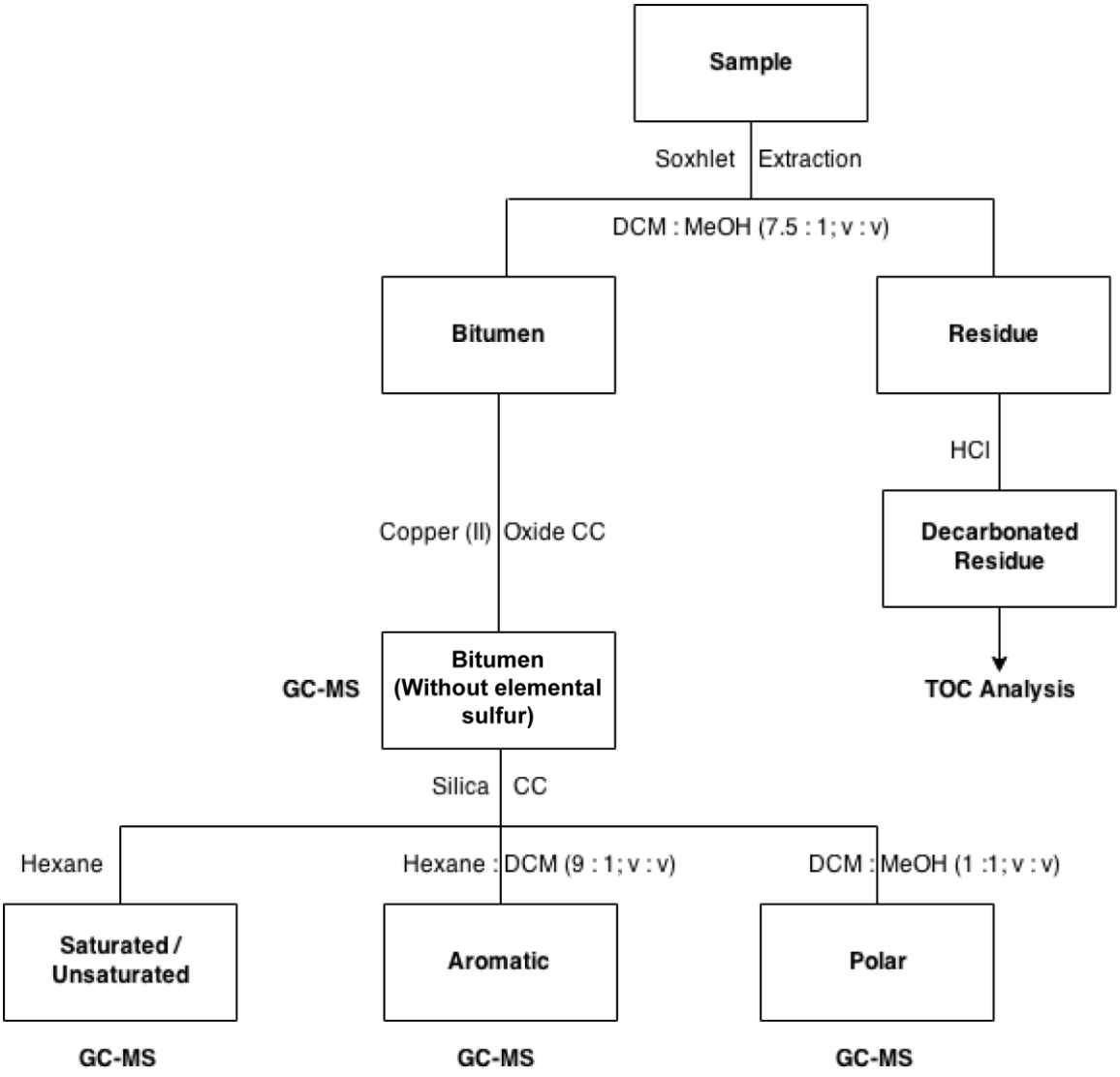

Figure 3. Analytical flow diagram. CC – Column Chromatography. (v:v) – Volume per volume.

3.1. CORE SAMPLING

All materials that came in contact with the core and sediment samples were rinsed successively with DCM and MeOH prior to cutting and sectioning. The polycarbonate tube containing the sediment was carefully halved using a corded Dremel (4000 series). The sediment was halved along the core length using a sharp putty knife. Then, half of the core was sectioned into thirty two, 2 cm thick subsamples and stored in clean (baked at 500 °C for 12 hours), pre-weighed 100 mL jars. The sectioned sediment samples were labelled DL–L2 I to XXXII and weighed. All samples were freeze dried in a Labconco freeze dry system for 48 hours and then pulverized using a thoroughly cleaned 80 mL porcelain mortar and pestle (three rinses with tap water and three with dichloromethane/methanol (DCM:MeOH 1:1, v/v) and weighed again.

Between 0.79 and 1.52 grams of subsections DL-L2 i – DL-L2 xiv (0-28 cm of the core) were stored in separate pony plastic vials, which were used to date the sediment by measuring gamma emissions from radionuclides, including lead (^{210}Pb) and cesium (^{137}Cs).

3.2. CHEMICALS AND REAGENTS

DCM, hydrochloric acid (HCl), High Pressure Liquid Chromatography (HPLC) grade cyclohexane and MeOH were purchased from Thermo Fisher Scientific (California, USA). In-house distillation of these solvents removes potential pollutants. The solvents are tested after distillation with the GC–MS and distillation was repeated until blank readings were obtained. Copper powder (-40 +100 mesh) used in clean up procedures was purchased in bulk from Alfa Aesar (Massachusetts, USA). Any ultra-pure, deionized water used was purified in a Milli-Q water purification system. High grade hydrogen (H_2), helium (He), and nitrogen (N_2) gas used in various experiments in the lab were ordered from Praxair.

3.3. EXTRACTION

All samples (sediment weight pre-extract given in Appendix A) were extracted for 24 hours using a Soxhlet extractor with an azeotropic mixture of DCM and methanol (MeOH) (a 7.5:1 ratio, respectively; Fig. 3). Once extracted, excess solvent was evaporated with a Büchi R-114 rotatory evaporator. The total lipid extract (TLE) was transferred from round bottom flasks into pre-weighed 2 mL vials and evaporated to dryness under a gentle flow of nitrogen.

3.4. ELEMENTAL SULFUR REMOVAL

TLE was analyzed by GC-MS but was found to contain abundant amount of elemental sulfur that interfered with peak identification. Elemental sulfur was removed on activated (1 M HCl) copper (II) oxide powder and the TLE was weighed again before further separation into subfractions by column chromatography. The abundance of elemental sulfur was obtained by the difference of TLE mass before and after removal of elemental sulfur (Appendix B).

3.5. COLUMN CHROMATOGRAPHY

Aliquots of TLE were separated by microscale flash column chromatography using a method modified from Grice et al. (1998). Briefly, 1 g of activated silica (SiO_2) was used as the stationary phase in a Pasteur pipette. The aliquot of TLE (re-evaporated and dissolved in 1 µL of hexane) was deposited at the head of the column. TLE was separated into three fractions using 2.5 mL of hexanes (to elute saturated/unsaturated fractions), 2.5 mL of hexanes/DCM (9:1, v/v; to elute aromatic fractions) and 2.5 mL of DCM/MeOH (1:1, v/v; to elute polar fractions). All fractions were analyzed by GC-MS.

3.6. GAS CHROMATOGRAPHY-MASS SPECTROMETRY (GC-MS)

Chromatographic analysis was performed with a Hewlett-Packard (HP) 6890 GC system coupled to a HP 5973 mass selective detector. Before analysis, the dried samples were diluted by adding 100 µL of cyclohexane for every 1 mg of TLE. Then, using a 10 µL syringe, ~1 µL of sample was injected into the GC. A HP-5ms column (0.25 mm diameter x 30 m length x 0.25 µm film thickness) was used with a split/splitless injector in pulsed splitless mode. Helium was used as a carrier gas and the oven temperature was maintained at 60 °C, then increased to 130 °C at a 10 °C/min, then increased to 315 °C at a 4 °C/min rate, and then kept at 315 °C for 60 minutes. Mass scans were made over the interval from 38 to 530 mass to charge (*m/z*). Compounds were identified by interpretation of characteristic fragmentation patterns, comparisons and references to mass spectral libraries (Geo and published mass spectra.

3.7. COMPOUND QUANTIFICATION

Quantification was performed by integrating peak areas of specific compounds. Target peak areas were compared against internal standard peak areas and when necessary, Single Ion Monitoring (SIM) was used to increase sensitivity and reproducibility.

Concentrations for all analytes were calculated using equations 1–3:

$$A = \frac{Area\ of\ Analyte}{Area\ of\ Standard} \qquad \text{Equation 1}$$

Once lipid aliquots had been spiked with known amounts of standard, S, a raw amount (R, in µg) can be calculated, where:

$$R = A \times S \qquad \text{Equation 2}$$

Since the samples are aliquots of the original TLE it is necessary to use an aliquot correction factor, F, which is the mass of the original TLE divided by the mass of the aliquot. The raw calculated amount, R, is then multiplied by F to produce a corrected amount that can be divided by the dry sediment weight, D in grams. All final concentration values are reported in µg per g of dry sediment weight.

$$C_S = \left(\frac{R \times F}{D}\right) \qquad \text{Equation 3}$$

For the purpose of this study, there were three deuterated compounds that served as internal standards: *n*-eicosane ($C_{20}D_{42}$), Bisphenol A ($((CD_3)_2C(C_6D_4OH)_2$), and pyrene ($C_{16}D_{10}$).

3.7.1. n-EICOSANE D_{42} STANDARD PREPARATION

A 40 µg/mL standard solution was prepared by dissolving 1 mg of n-eicosane D_{42} flakes in 25 mL DCM. The solution was mixed overnight with a magnetic stirrer and several working calibration standards were prepared. 1 µL (0.04 µg/µL) of the standard was injected into the saturated/unsaturated fraction of the samples.

3.7.2. BISPHENOL A D_{14} STANDARD PREPARATION

A stock solution at 20 µg/mL was prepared by dissolving 5 mg of BPA D_{14} flakes in 250 mL DCM and stirring overnight. 1 µL (0.02 µg/µL) of the authentic standard was injected into the polar fraction of the samples. This standard was prepared for the quantification of BPA within lipid extracts and the polycarbonate core tube.

3.7.3. PYRENE D_{10} STANDARD PREPARATION

A stock solution of 40 µg/mL prepared by dissolving 1 mg of pyrene crystals in 25 mL cyclohexane and mixing overnight. 1 µL (0.04 µg/µL) of the standard was injected into the polar fraction of the samples. This standard was prepared for the quantification of aromatic compounds, mainly PAHs within TLE.

3.8. CARBONATE CONTENT

A known amount of powdered sample was added to a tared polycarbonate centrifuge tube, 1 M HCl was added, drop-wise, to eliminate carbonates. All samples evolved CO_2 as HCl reacted with carbonates present in the lacustrine sediment. The solution was mixed thoroughly using a Thermolyne vortexer and HCl was added as needed until evolution of CO_2 ceased. Then the centrifuge tube was spun in a Thermo Centra CL3 centrifuge, the mixture was decanted and rinsed with deionized water. The rinsing process was repeated until the mixture returned to neutral pH. The decarbonated sediment was placed in a Heratherm oven at 50°C for three days to achieve complete dehydration. The dry sediment was weighed and sent for TOC analysis. Carbonate content was obtained by mass difference between digested and undigested samples.

4. SEDIMENT DATING

A reliable method for dating recent lacustrine sediment is the use of lead-210 (^{210}Pb) geochronology. ^{210}Pb has a half-life of about 22 years and reaches secular equilibrium with radium in 7 half-lives i.e. in roughly 150 years. In general, ^{210}Pb cannot be used to date sediment older than 150 years because it reaches background levels of *in situ* radionuclides.

Another geochronological method used is based on the Cesium-137 (^{137}Cs) radionuclide. Unlike ^{210}Pb, ^{137}Cs has no natural sources and is produced exclusively during nuclear fission (Roger, Ritchie,

& Gill, 1973). Using ^{137}Cs for dating is fundamentally different from using ^{210}Pb since it does not produce a useable concentration slope but rather it peaks at reference points for known dates (Jeter, 2000). More specifically, the two major peaks of ^{137}Cs activity in North American lakes usually correspond to 1951 and 1964, periods when above ground nuclear bomb testing occurred (Ritchie & Mchenry, 1990).

4.1. RADIONUCLIDE PROFILING

For both ^{137}Cs and ^{210}Pb profiling, a high purity Germanium gamma detector was used following the method described by Heusser et al. (2006). The well spectrometer (model GWL–170–15–LB, referred to as Well #1 Large) was provided by the University of Illinois at Chicago (UIC) Isotope Geochemistry Laboratory; Well #1 is a 15 mm diameter well-format spectrometer that has been calibrated with certified radionuclide standards. Calibration for ^{137}Cs gamma spectrometry measurements used certified standard reference material NIST 4357. ^{210}Pb calibration used certified standard reference material (Uranium-Thorium Ore, DL–1A). Five vials of standard DL–1A and four vials of NIST 4357 of various masses and heights were prepared and gamma emissions were measured in each. Gamma emissions from fourteen (of thirty two) Douglas Lake samples were measured for at least 24 hours and any samples with nonsufficient signals were re-measured for another 24 hours.

4.2. DATING MODEL

Sediment age was calculated using both the Constant Initial Concentration (CIC) and the Constant Rate of Supply (CRS) models. The CIC model assumes that the initial concentration of ^{210}Pb in sediment is constant and subject to change as a function of sedimentation rates. The CRS model assumes that, in a closed system, the only variable is local sedimentation rate but the flux

of ^{210}Pb into the system is constant (Appleby & Oldfield, 1983; Turner & Delorme, 1996). The assumption made by the CIC model is compromised by variable sedimentation rates, which is true of Douglas Lake and of most depositional system (Francis, 1997; Noller, 2000). For this reason, only results from the CRS method were used in this study.

The CRS model employs the following formulas for the calculation of sediment age:

$$A(m) = A(0)\, e^{-\lambda t} \qquad \text{Equation 4}$$

Where A (m) is the cumulative excess ^{210}Pb activity per unit area, λ is the ^{210}Pb decay constant 0.03114 yr^{-1} and m corresponds to the depth below the sediment water interface. A (m) is given as:

$$A(m) = \int_{m}^{\infty} C\,(m) \times dm\,(m) \qquad \text{Equation 5}$$

A (0) is the cumulative excess for the entire core and is given as

$$A(0) = \int_{0}^{\infty} C\,(m) \times dm\,(m) \qquad \text{Equation 6}$$

C (m) is the cumulative excess of the sample and dm (m) is the dry mass per unit area at sediment depth, m. Once A (m) and A (0) have been calculated age, t, can be calculated using:

$$t = \frac{1}{\lambda} \ln\left(\frac{A(0)}{A(m)}\right) \qquad \text{Equation 7}$$

Dry mass sedimentation rate can be calculated using equation 8, where M is the slope of the line of cumulative dry mass to $\ln\left(\frac{A(0)}{A(m)}\right)$

$$r = \lambda \times M \qquad \text{Equation 8}$$

5. RESULTS

5.1. CONSTANT RATE OF SUPPLY (CRS) DATING MODEL

Activities and errors for ^{210}Pb, ^{226}Ra and ^{137}Cs for core subsections DL–L2 i–x were calculated by using the procedures described in section 4 (Appendix C). Any radionuclide activity below the detection limit of the spectrometer is denoted with "≤" and the adjusted detection limit for each sample (values fluctuate as a function of the total mass of the sample) and measured radionuclide. All ^{210}Pb activities are above the detection limit and almost all ^{137}Cs activities are above the detection limit except one value measured in subsection DL–L2 x (18–20 cm, Table I).

TABLE I. CALCULATED SEDIMENT DATES AND CESIUM ACTIVITY AS A FUNCTION OF DEPTH ALONG WITH ANALYTICAL ERRORS

Subsection	Depth (cm)	Date (years)	Age uncertainty (%)	Cs-137 (Bq/Kg)	Cs error (Bq/Kg)
DL-L2 i	1	2013	2.720	80.406	3.766
DL-L2 ii	3	1999	3.909	107.219	4.466
DL-L2 iii	5	1997	4.137	119.883	4.483
DL-L2 iv	7	1985	6.557	126.195	5.120
DL-L2 v	9	1982	4.760	159.938	4.167
DL-L2 vi	11	1976	5.466	202.239	4.602
DL-L2 vii	13	1969	6.083	197.144	4.174
DL-L2 viii	15	1954	6.470	14.462	1.483
DL-L2 ix	17	1945	9.225	2.847	0.956
DL-L2 x	19	1932	12.951	≤ 2.16[a]	1.033

[a] ^{137}Cs is less than or equal to the detection limit of the spectrometer.

The black organic matter–rich sediment from Douglas Lake is recent: ^{210}Pb dates range from 1932–2013, with an average sedimentation rate of 0.036 g cm^{-2} yr^{-1}. Francis (2001) measured a lower average sedimentation rate of ~0.012 g cm^{-2} yr^{-1} at South Fishtail Bay. In order to have confidence in the results, ^{210}Pb dates can be validated using another independent radionuclide tracer. In this case, ^{137}Cs was used for corroboration since its first detectable occurrence in sediment usually indicates a relative date of 1954 (Appleby, 2008; Ritchie & Mchenry, 1990). In Douglas Lake, the first detectable concentration of cesium is measured at subsection DL-L2 viii (14-16 cm) and it peaks at subsection DL-L2 vi (10-12 cm), 1954 and 1976 respectively (Table I and Fig. 4).

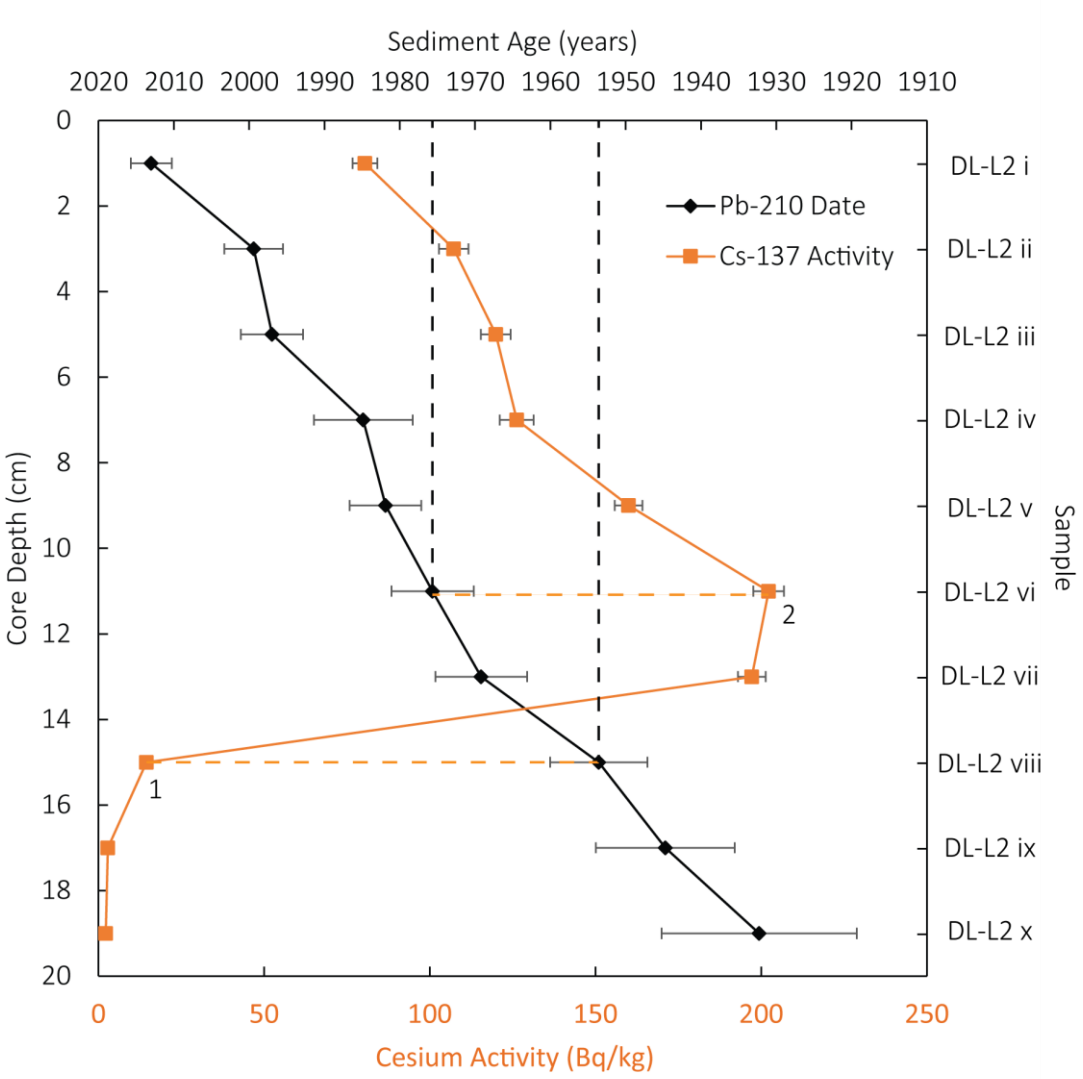

Figure 4. Sediment age (calculated from unsupported ^{210}Pb activity) vs. depth below sediment-water interface. ^{137}Cs activity peaks near the period of most frequent above-ground bomb testing. Lines are drawn from ^{137}Cs activity to corresponding sediment date. For example, line 1 represents sediment subsection DL-L2 viii, ^{137}Cs = 14.5 Bq/kg and sediment date = 1954. Line 2 represents subsection DL-L2 vi, ^{137}Cs = 202.3 Bq/kg and sediment date = 1976.

5.2. HYDROCARBON COMPOSITION OF DOUGLAS LAKE

Bulk lipid extracts of Douglas Lake sediment contained a complex suite of compounds ranging from monoterpenes and straight chain *n*–alkanes to functionalized hopanoids and steroids (Fig. 5). The distribution of compounds in the TLE of most samples analyzed have bimodal distributions. Generally, the first major cluster of peaks contained highly branched isoprenoids, neophytadiene isomers, and several functionalized alkanes, while the second cluster was made up of various esters, long chain *n*–alkanes, steroids and hopanoids. Steroid and hopanoids make up a large fraction of the lipid content. TLE from all subsections were separated into saturated/unsaturated hydrocarbons, aromatic, and polar fractions for further analysis.

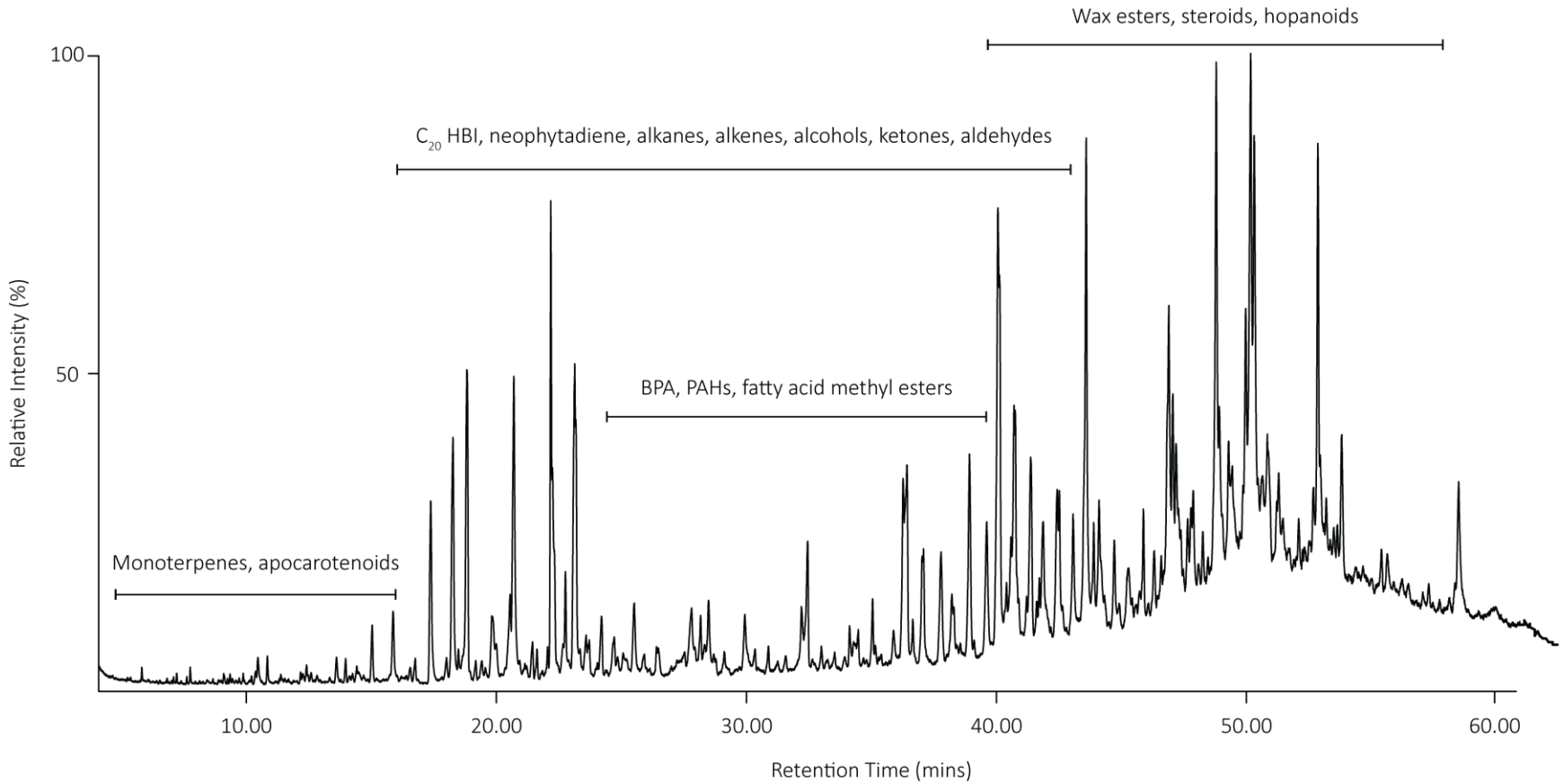

Figure 5. Representative total ion chromatogram (TIC) of total lipid extract from core subsection DL–L2 viii (~1954). The trace has been broadly labelled with compounds that correspond to the most intense peaks.

5.2.1. SATURATED/UNSATURATED HYDROCARBON FRACTION

Saturated/unsaturated hydrocarbon fractions include of low molecular weight (LMW) *n*-alkanes (C_{17}–C_{21}), high molecular weight (HMW) *n*-alkanes (C_{22}–C_{35}), C_{32}–C_{34} botryococcene, highly branched isoprenoids, C_{27}–C_{28} steroid hydrocarbon, C_{29}–C_{31} hopanoid hydrocarbon, and a few unidentified compounds. This fraction also contains minor amounts of aromatic compounds including 3-methyl-2-(3,7,11-trimethyldodecyl) thiophene, tetrahydrorimuene and fichtelite (Fig. 6, Table II).

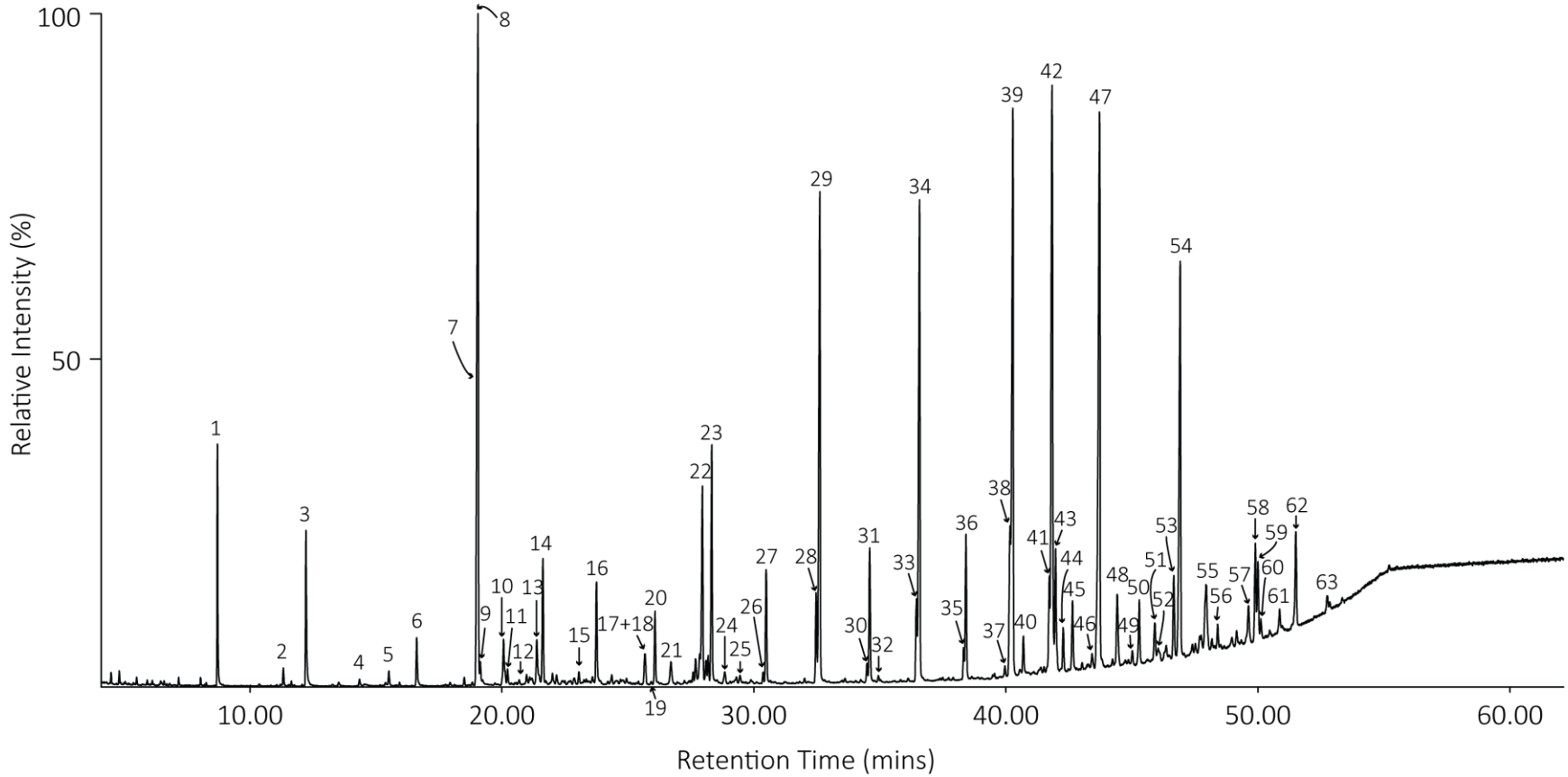

Figure 6. Representative TIC of the saturated/unsaturated hydrocarbon fraction from subsection DL-L2 xiv. All numbered peaks are identified in Table II.

TABLE II. IDENTIFICATION OF NUMBERED PEAKS IN FIGURE 6, WHICH SHOWS TIC OF THE SATURATED/UNSATURATED HYDROCARBON FRACTION OF SAMPLE DL–L2 XIV

Peak	Compound	Peak	Compound	Peak	Compound
1	Dodecane	27	Docosane	53	A'Neogammacer-17(21)-ene
2	5-methyl tridecane	28	Tricosene	54	Hentriacontane
3	Tetradecane	29	Tricosane	55	A'Neogammacer-22(29)-ene
4	Pentadecane	30	Tetracosene	56	Dotriacontane
5	5-methyl pentadecane	31	Tetracosane	57	17β,21β(H)-30-norhopane
6	Hexadecane	32	Des-A-lupane	58	Triacontane
7	Heptadecane	33	Pentacosene	59	Diploptene
8	C_{20} HBI	34	Pentacosane	60	Hop-21-ene
9	Pristane	35	Hexacosene	61	Homohop-30-ene
10	7-methyl heptadecane	36	Hexacosane	62	17β,21β(H)-31-homohopane
11	5-methyl heptadecane	37	$C_{33:5}$ Botryococcene	63	Tetratriacontane
12	3-methyl heptadecane	38	Heptacosene		
13	Octadecane	39	Heptacosane		
14	Phytane	40	$C_{33:5}$ Botryococcene		
15	Kaur-16-ene	41	$C_{34:2}$ Botryococcene		
16	Nonadecane	42	$C_{34:3}$ Botryococcene		
17	Tetramethylhydrorimuene	43	Octacosane		
18	Fichtelite	44	$C_{34:4}$ Botryococcene		
19	Eicosene	45	$C_{33:3}$ Botryococcene		
20	Eicosane	46	Ergosta-5,22-diene		
21	Elemental sulfur	47	Nonacosane		
22	$C_{25:2}$ HBI	48	Bisnorhopane		
23	Heneicosane	49	Stigmasta-5,22-diene		
24	3-methyl-2-(3,7,11-trimethyldodecyl)thiophene	50	Triacontane		
25	3-(4,8,12-trimethyltridecyl)thiophene	51	Stigmast-8-ene		
26	Docosene	52	17β,21α(H)-30-norhopane		

5.2.1.1. *n-ALKANES*

Straight chain aliphatic compounds comprise a major portion of TLE from sediments in Douglas Lake. The *n*-alkanes showing a pronounced OEP are typical of autotrophic organic matter contributors. The presence of long chain alkanes (C_{21}-C_{33}) with OEP indicate contribution from higher plant sources (epicuticular leaf waxes; Fig. 7). On the other hand, shorter chain alkanes with OEP usually indicates contribution from algae and bacteria (P. Cranwell, 1973; Szafranek & Synak, 2006). Generally, carbon preference index (CPI) proposed by Bray and Evans (1961) are used to further characterize *n*-alkane distributions within TLE. CPI measures the abundance of odd over even carbon chain lengths. Given that the vast majority of measured modern plants have CPI values greater than 1, measured CPI values greater than 1 likely indicate input to sediment *n*-alkanes from terrestrial plants (Bush & McInerney, 2013). In this study, we used a modified CPI equation proposed by Marzi et al. (1993, Equation 9) which corrects for errors that can be exacerbated if the peak areas for even *n*-alkanes are small relative to the odd *n*-alkanes.

$$CPI = \frac{(\sum_{odd}(C23 - C31) + \sum_{odd}(C25 - C33))}{2 \times \sum_{even}(C24 - C32)} \qquad \text{Equation 9}$$

CPI values range between 6 and 9 in lipid extracts from Douglas Lake, indicative of the contribution from terrestrial plants to OM in Douglas Lake sediments.

The depth profile of *n*-alkanes (C_{18}–C_{31}) in TLE was divided into two zones: all subsections above DL–L2 x fall into the post–logging zone at Douglas Lake while subsections below correspond to the period of increased logging activity (Fig. 8).

Concentrations of odd *n*-alkanes (C_{23}–C_{31} odd) range between 11 µg/g and 20 µg/g at subsection DL–L2 xii (20–22 cm, < 1932) and peak at DL–L2 ix (16–18 cm, 1945) with values ranging between 53 µg/g and 108 µg/g (Fig. 8). However, even numbered *n*-alkanes range between 0.6 and 3 µg/g at DL–L2 xii and peak at DL–L2 ix with values ranging between 2 µg/g and 19 µg/g (Fig. 8). The concentration of total *n*-alkanes (C_{18}–C_{33}) ranges between 105 µg/g (DL–L2 xii) to 487 µg/g (DL–L2 ix).

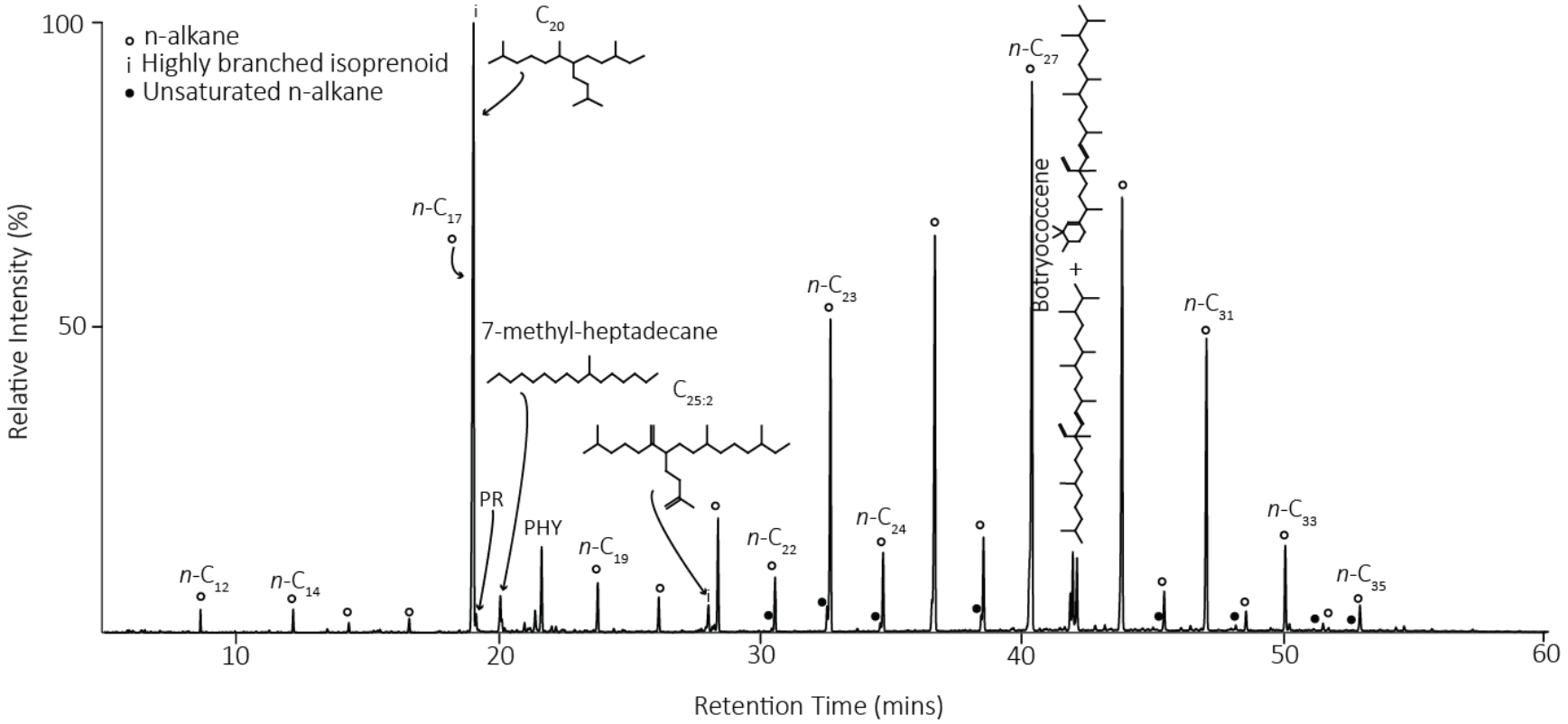

Figure 7. Partial selected ion chromatogram (m/z 57) of core subsection DL-L2 xiv with highly branched isoprenoids, botryococcene members and various n-alkanes indicated. Chromatogram also serves as representative trace and reference for Figure 12.

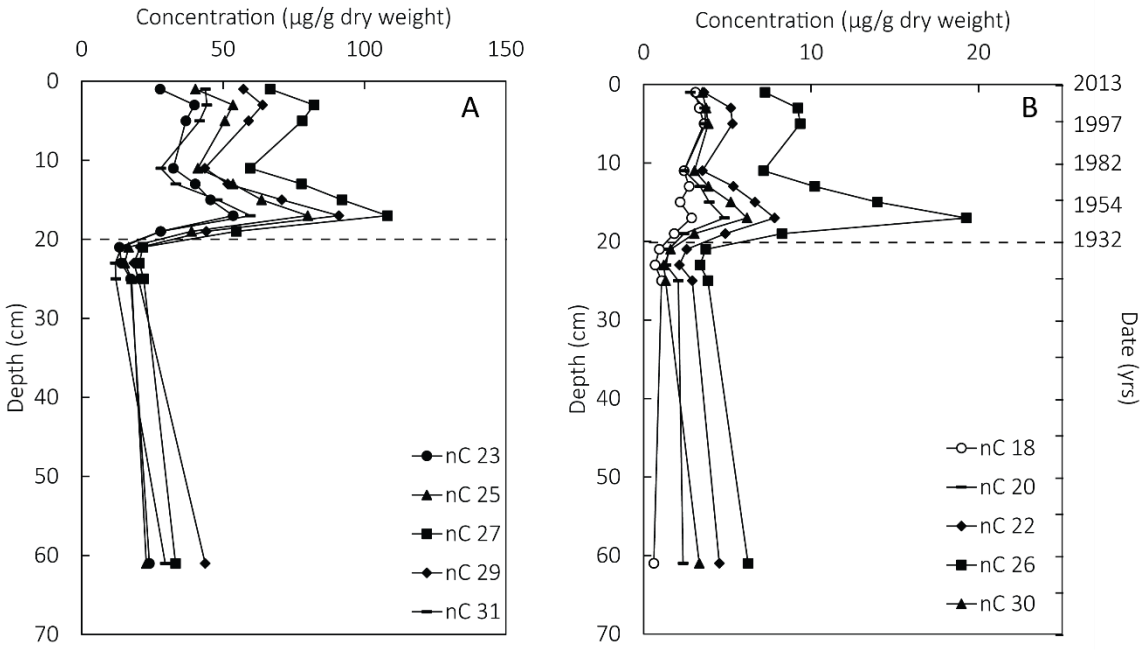

Figure 8. Historical profiles of selected n-alkanes. A) Historical profile for long chain odd n-alkanes. B) Historical profile of long chain even n-alkanes. The dashed line demarcates zones before (below line) and after (above line) fires and logging at Douglas Lake.

The depth profiles of all even numbered *n*-alkanes follow a similar trend from the bottom to the top of the core i.e. a decrease into the logging era followed by a sharp spike associated with fire and logging control measures, followed by a trough, a peak, and the current (~2013) downward trend. Nevertheless, the distribution of C_{18} varies significantly enough from HMW even *n*-alkanes to suggest input from different sources. It is likely that HMW even n-alkanes are related to diagenetic processes while C_{17}, C_{18}, and C_{19} are related to a general algal/bacterial source (Gelpi et al., 1970; Tissot & Welte, 1984).

In order to differentiate between the relative abundance of OM from algae and cyanobacteria, the concentration profiles of C_{17} monomethyl alkane (7-meythyl-heptadecane, MMA) and C_{18} can

be compared; 7-methyl-heptadecane is a biomarker that is almost exclusively cyanobacterial (Shiea et al., 1990). C_{17} coelutes with C_{20} HBI, the most abundant alkane in the saturated/unsaturated fraction and, as such, cannot be used as a biomarker for algal productivity. Relative to HMW *n*-alkanes, the concentration of C_{17} MMA is very low, ranging from 0.2 µg/g to 15 µg/g. Despite a decrease in concentration during the logging era and ~1976 (DL–L2 vi), C_{17} MMA has generally has a positive slope (Fig. 9). Additional *n*-alkane values useful for further resolution lipid input source include pristane to phytane ratios and P_{aq} ratios.

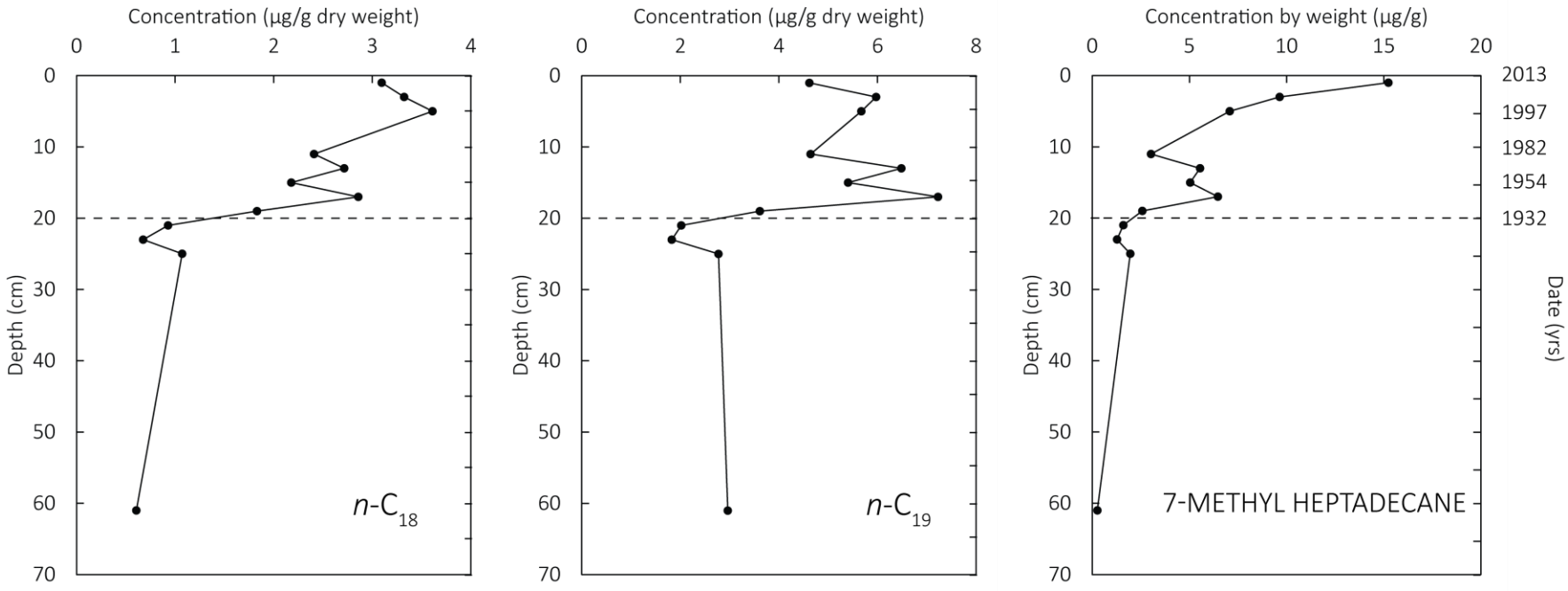

Figure 9. Historical profiles of selected cyanobacterial biomarker, monomethyl alkane (MMA), 7-methyl heptadecane and algal biomarkers n-C_{18} and n-C_{19}. The dashed line demarcates zones before (below line) and after (above line) major fires and logging at Douglas Lake.

PRISTANE PHYTANE RATIOS

Pristane and phytane ratios may reflect the extent of anoxia in a depositional environment. High pristane/phytane values i.e. values > 3, are associated with organic matter deposited under oxic conditions, and low values < 1 are common in anoxic depositional environments (Didyk et al., 1978). Pristane and phytane are acyclic diterpenoids formed as diagenetic products of phytol (ester side chain from chlorophyll). Oxidization of phytol promotes decarboxylation and, consequently, the formation of pristane, while diagenesis in reducing conditions preferentially produces phytane. There are some problems underscoring the usage of pristane/phytane ratios as highlighted by ten Haven et al. (1987). The two main problems are: (1) pristane/phytane ratios tend to increase with increasing sediment maturity; and (2) microbially mediated reactions can produce additional biological inputs of either pristane or phytane. As a precautionary measure, the ratio should be used in conjunction with other indicators of redox conditions, and may be used when pristane and phytane have the same isotopic composition (Kenig et al. 1994).

Pristane values in TLE from Douglas Lake range from 0.6 µg/g to 5.9 µg/g whereas phytane ranges from 0.2 µg/g to 12 µg/g. Pristane/phytane ratios vary between 0.23 (DL–L2 i, ~2013) and 0.54 (DL–L2 ix, ~1945) however, lower subsection DL–L2 xxxi (60–62 cm, <1932) has a high value of 2.5 (Fig. 10). The value for DL–L2 xxxi may be as a result of analytical error since the integrated peak area for phytane was small.

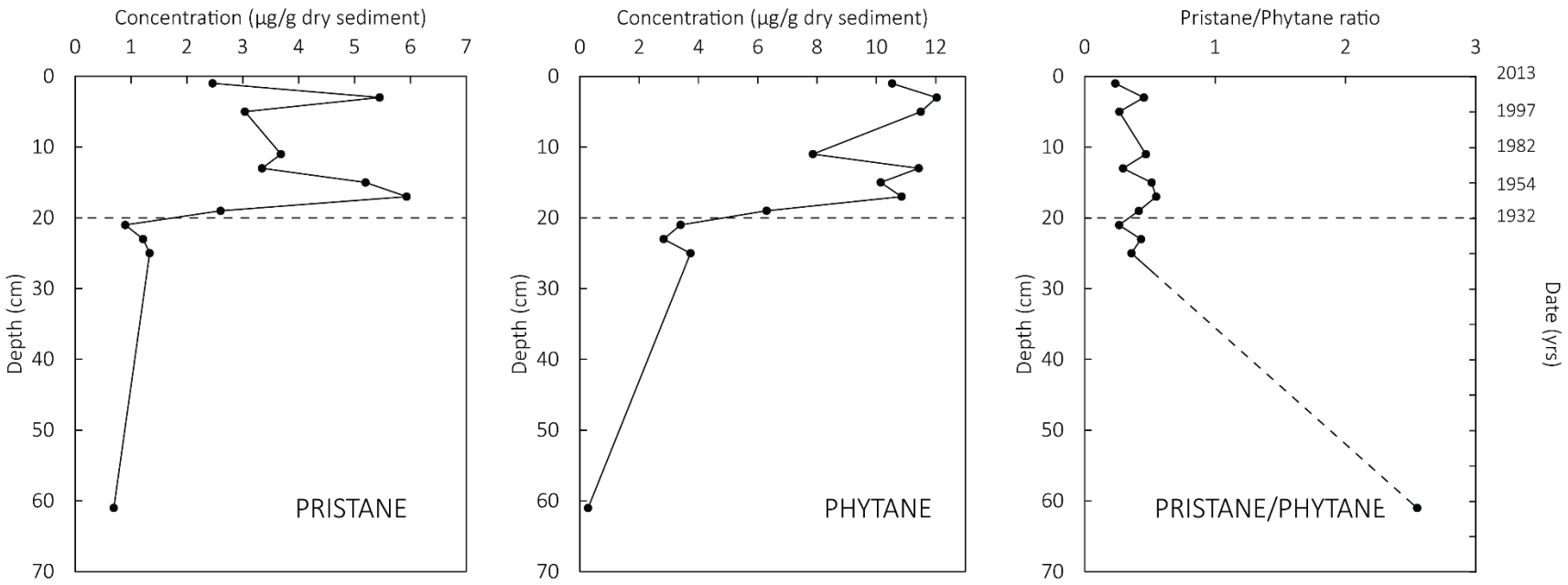

Figure 10. Historical profiles and ratio of Pristane and Phytane. Dashed lines demarcate zones before (below line) and after (above line) fires and logging at Douglas Lake.

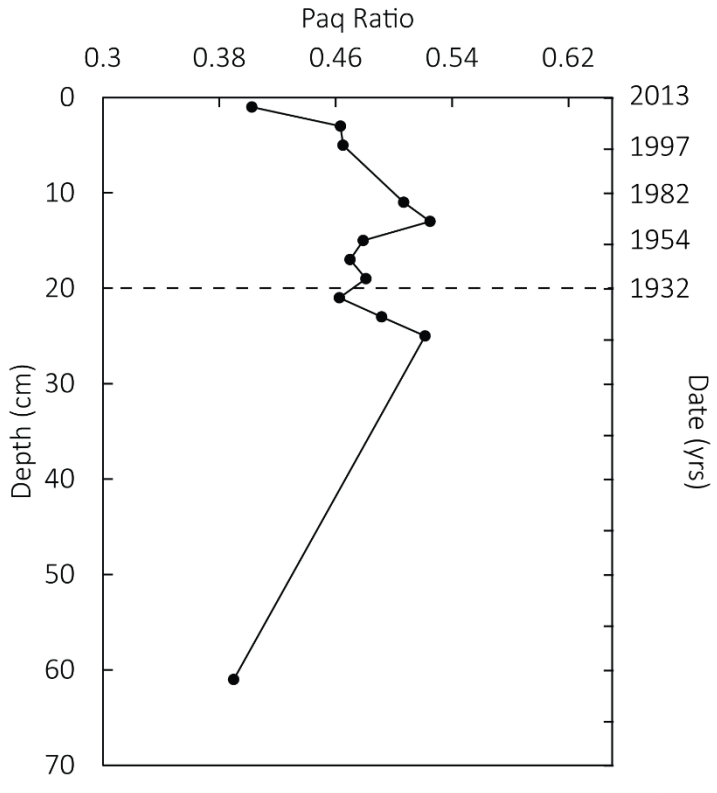

Figure 11. Historical profile of P_{aq} ratio in Douglas Lake sediment. The dashed line demarcates zones before (below line) and after (above line) fires and logging at Douglas Lake. $P_{aq} = (C_{23} + C_{25})/(C_{23} + C_{25} + C_{29} + C_{31})$.

Ficken et al. (2000) proposed an aquatic macrophyte proxy (P_{aq}), defined in equation 10, to estimate relative contribution from terrestrial plants relative to floating or submerged plants. Terrestrial plants are dominated by long chain *n*-alkanes C_{27}, C_{29} (vascular vegetation type), C_{31}, and C_{33} (herbaceous vegetation type), while submerged plants contain abundant C_{23} and C_{25} *n*-alkanes

(Jaffé et al., 2001; Rao et al., 2011). P_{aq} values ranging from 0.01 to 0.23 define input from terrestrial plants, and values between 0.48 to 0.94 signify input from macrophytes (Nichols et al., 2006).

$$Paq = \frac{C23+C25}{C23+C25+C29+C31} \quad \text{Equation 10}$$

The P_{aq} ratio showed minute fluctuations ranging from a minimum of 0.39 to a maximum of 0.52. At subsection DL–L2 xiii (<1932) the P_{aq} value peaked at 0.521 steadily reducing to 0.46 near the border of the post logging era. Following fire and logging control measures, P_{aq} rose to its maximum value (0.52) at DL–L2 vii and had declined to 0.40 (Fig. 11). In general, P_{aq} values from Douglas Lake are indicative of mixed input from terrestrial plants and macrophytes. When values increase, it is likely that organic matter contribution from macrophytes also increased relative to that of terrestrial plants.

5.2.1.2. HIGHLY BRANCHED ISOPRENOIDS (HBI)

The structure of HBI alkanes were first identified by Yon and Maxwell (1982) in Rozel point crude oil. In Douglas Lake sediment, C_{20} HBI (peak 8, Fig. 6) is the most abundant alkane in the lipid extract. On average, C_{20} HBI is 19.3 % of total concentration in the saturated/unsaturated hydrocarbon fraction of TLE (Fig. 12). Robson & Rowland (1988) reported on the predominance of HBIs in recent lacustrine sediment relative to *n*-alkanes. According to these authors, HBIs and other branched alkanes were more resistant to biodegradation than straight chain alkanes, therefore HBIs would be better preserved and overrepresented in the sedimentary record. Although there are other HBI compounds (e.g. $C_{25:2}$, peak 22 Fig. 6), they are present in low concentrations.

HBI structures (Fig. 13) were tentatively identified on the basis of comparison of its mass fragmentation patterns with those in studies by Yon and Maxwell (1982), Belt et al. (2000) and Sinninghe Damsté et al. (1989). HBI is likely synthesized by diatoms (Belt et al., 2000; Sinninghe

Damsté et al., 2005; Smittenberg et al., 2004). Therefore, its significant intensity in most of the lipid extracts suggests a large algal contribution to the organic matter of sediment. According to Phinney (1946) and Stoermer (1977), planktonic species are predominant in Douglas Lake sediments (including diatoms *Melosira islandica*, *Gomphonema acuminatum, Navicula sp., Melosira granulata*, and *Stephanodiscus alpinus*).

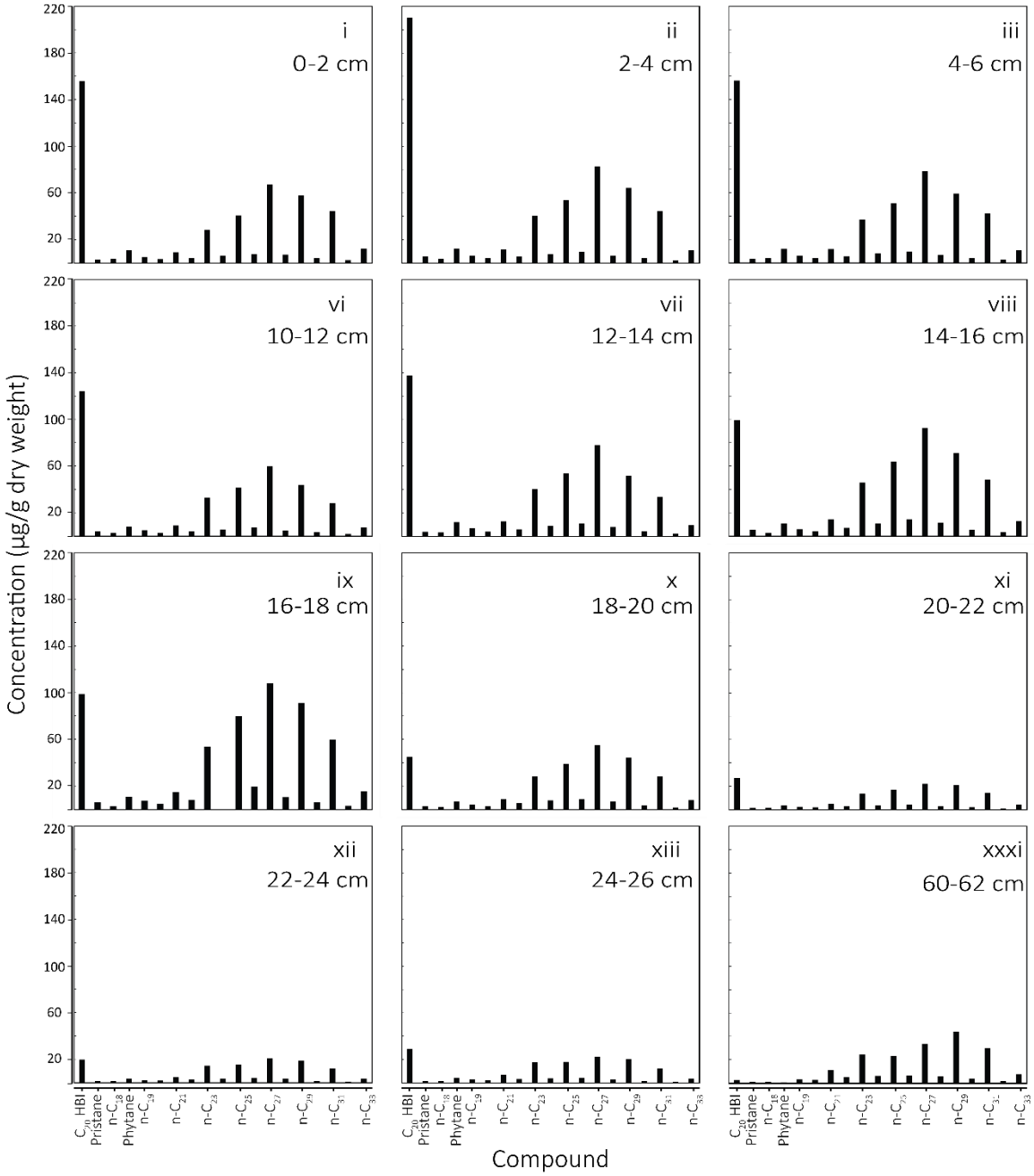

Figure 12. n-Alkane distribution from the uppermost subsection (DL-L2 i, 0-2 cm) to lower subsections (down to 62 cm). Abscissa is carbon number, C_{20} HBI, pristane and phytane are shown for comparison. Ordinate axis is concentration (µg/g dry sediment weight).

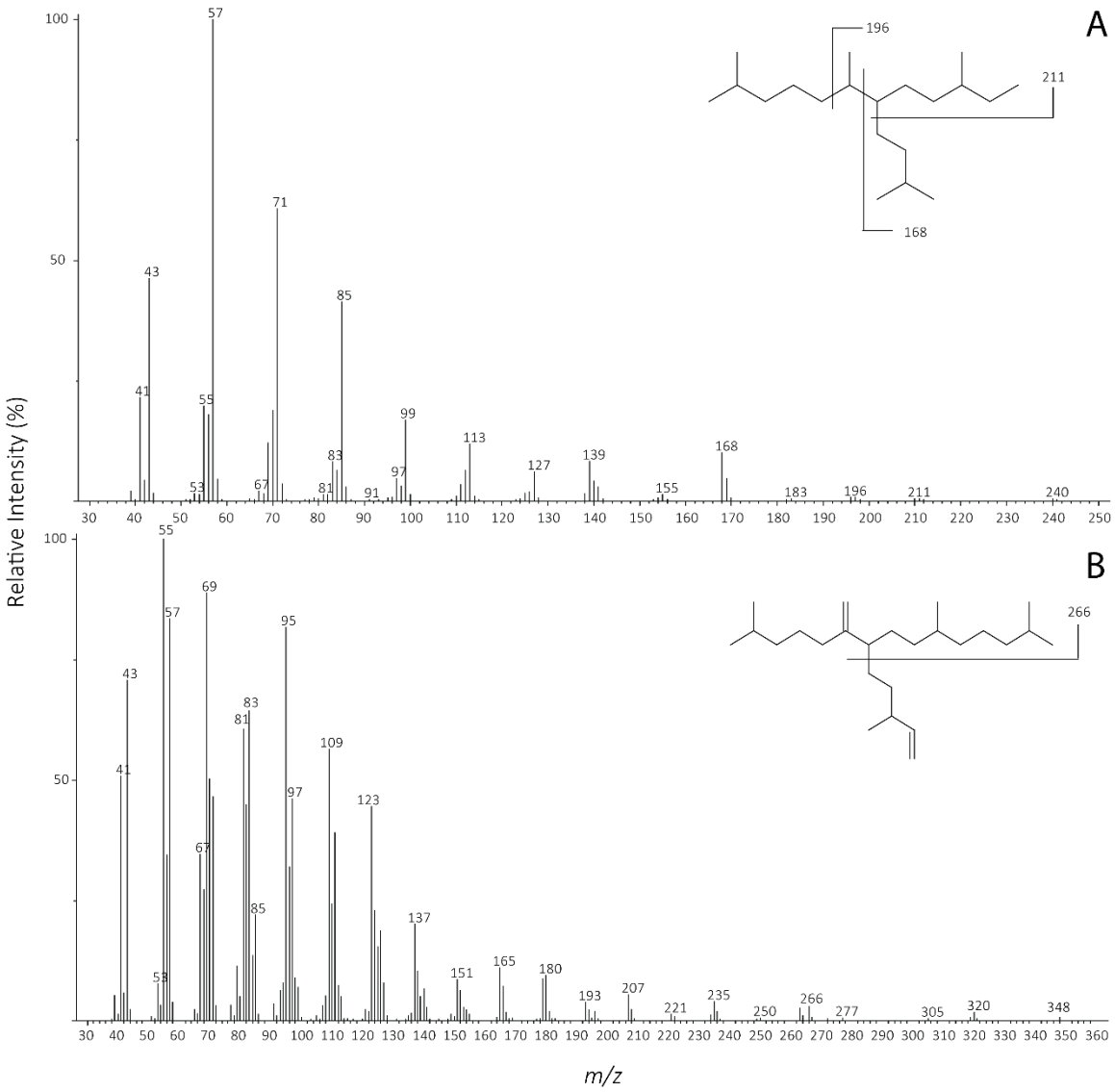

Figure 13. Mass spectra (subtracted for background) of A) C_{20} HBI alkane, and B) $C_{25:2}$ HBI alkene. These mass spectra are identical to those published by Yon and Maxwell (1982), Belt et al. (2000) and Sinninghe Damsté et al. (1989).

The historical profiles of C_{20} and $C_{25:2}$ HBIs differ minutely, i.e. as C_{20} HBI decreased down the core while $C_{25:2}$ HBI ultimately peaks at DL–L2 xxxi (Fig. 14). There are three potential explanations for this discrepancy: (1) the two HBIs may be synthesized by different diatom species. For example, several *Navicula* genera only produce C_{25} HBI (Sinninghe Damsté et al., 2004); (2) as a function of higher branching and unsaturation, $C_{25:2}$ HBI is less susceptible to biodegradation than C_{20} HBI (Rowland & Robson, 1990); (3) the small peak area of $C_{25:2}$ HBI at lower depths may give rise erroneous values as a result of peak integration errors.

The concentration of C_{20} HBI increased from 2.3 µg/g (DL–L2 xxxi) to 209 µg/g (DL–L2 ii, ~1999) and decreased to 157 µg/g by ~2013. Values for $C_{25:2}$ HBI were about two orders of magnitude lower than C_{20}, ranging from a minimum of 0.8 µg/g (DL–L2 xii) to a maximum of 5.7 µg/g (DL–L2 ii). As seen with other hydrocarbons, HBI concentrations decrease slightly during the period of increased fire and logging at Douglas Lake.

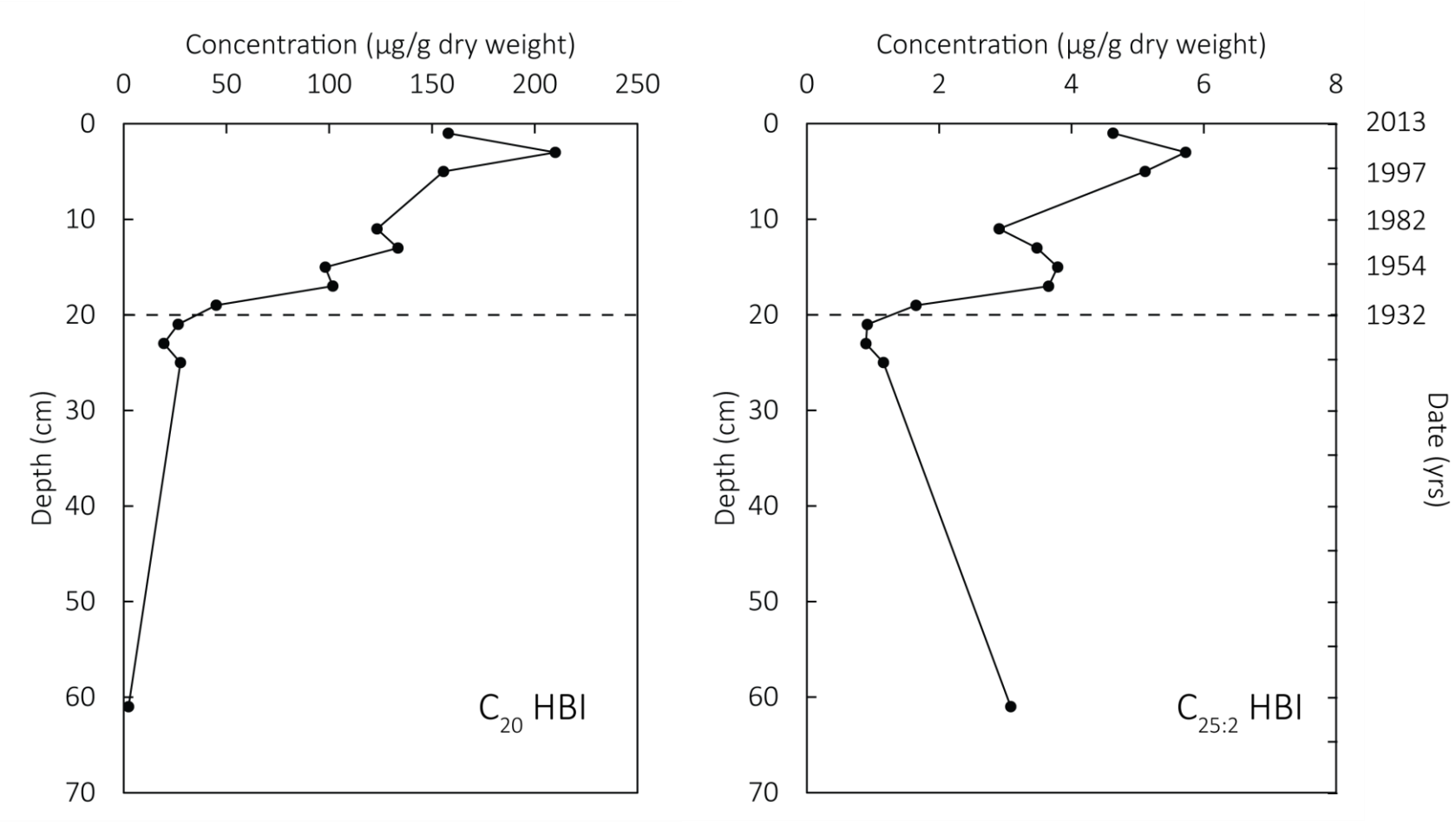

Figure 14. Historical profiles of C_{20} HBI and $C_{25:2}$ HBI. The dashed line demarcates zones before (below line) and after (above line) fires and logging at Douglas Lake.

5.2.1.3. BOTRYOCOCCENE

Several peaks eluting between *n*-C_{27} and *n*-C_{29} (Fig. 6) were tentatively identified as botryococcenes on the basis of comparison with published spectra (Gao et al., 2007b; Metzger et al., 1988; Metzger et al., 1985). Since there was no apparent trend in the succession (Fig. 15) of individual botryococcene members, for qualitative purposes, the average relative abundance of the group was used in this report. Botryococcenes eluted with both the saturated/unsaturated hydrocarbon and the aromatic fractions, however they were separated by order of saturation i.e. the most saturated botryococcenes ($C_{33:5}$–$C_{34:2}$) eluted with the saturated/unsaturated fraction.

Botryococcenes vary in chain length (C_{32}–C_{34}) and the number of end-chain cyclic moieties, the most common of which are $C_{34:3}$ botryococcene and $C_{32:2}$ botryococcene (Fig. 16). Although ~50 botryococcenes have been reported in literature (Gao et al., 2007; Y. Huang, Street-Perrott, Perrott, Metzger, & Eglinton, 1999; Metzger et al., 1988, 1985) only seven structures (labelled B_1–B_7) were tentatively identified in Douglas Lake: in order of retention time – botryococcenes $C_{32:2}$ (39.6 mins), $C_{33:5}$ (40.3 mins), $C_{34:3}$ (41.0 mins), $C_{34:2}$ (41.4 mins), $C_{34:3}$ (41.5 mins), $C_{34:4}$ (41.6 mins), and $C_{33:3}$ (41.9 mins). There were several botryococcene – related peaks that could not be identified as a result of their weak intensities and incomplete mass spectrum. The distribution of botryococcene groups through all analyzed core subsections (DL–L2 i – DL–L2 xiv and DL–L2 xxxi, Fig. 17) may reflect ecological succession.

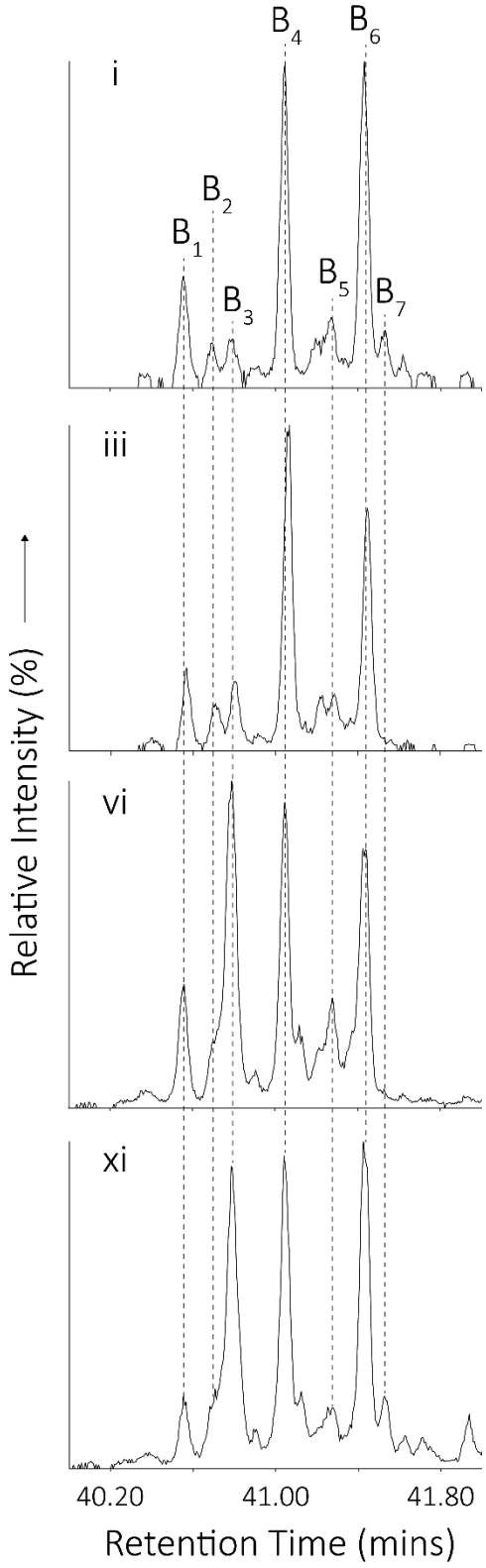

Figure 15. Partial selected ion chromatogram (m/z 95) from DL–L2 i, iii, vi and xi. The relative abundance of individual botryococcenes shows no apparent trend or successive pattern down-section. B1 – $C_{32:2}$, B2 *– $C_{33:5}$, B3 – $C_{34:3}$, B4 – $C_{34:2}$, B5 – $C_{34:3}$, B6 – $C_{34:4}$, and B7 – $C_{33:3}$.*

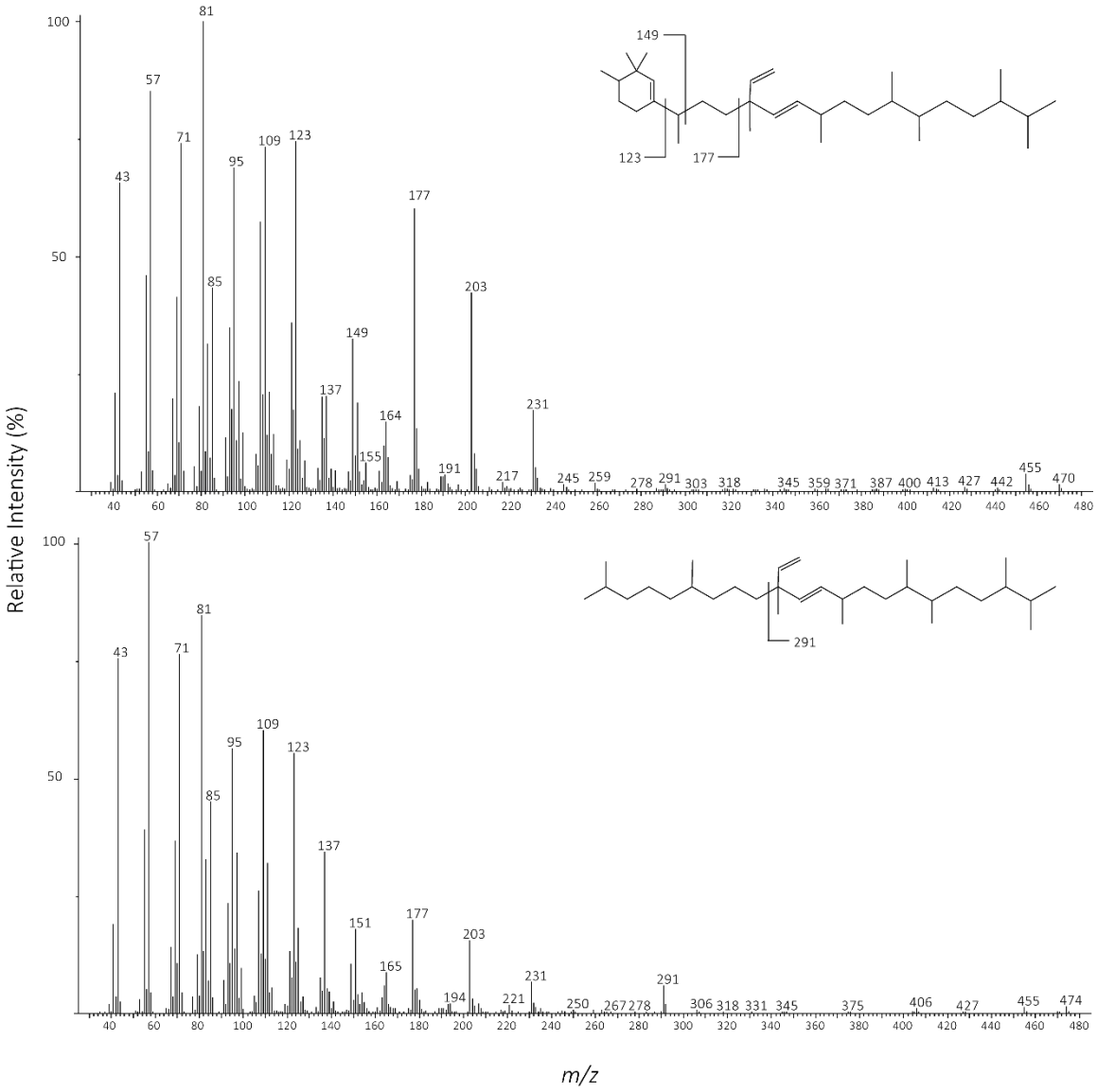

Figure 16. Mass spectra (subtracted for background) of the most abundant botryococcene members in Douglas Lake sediment. Mass spectra are identical to those published by (De Mesmay et al., 2008; and Metzger et al., 1988)

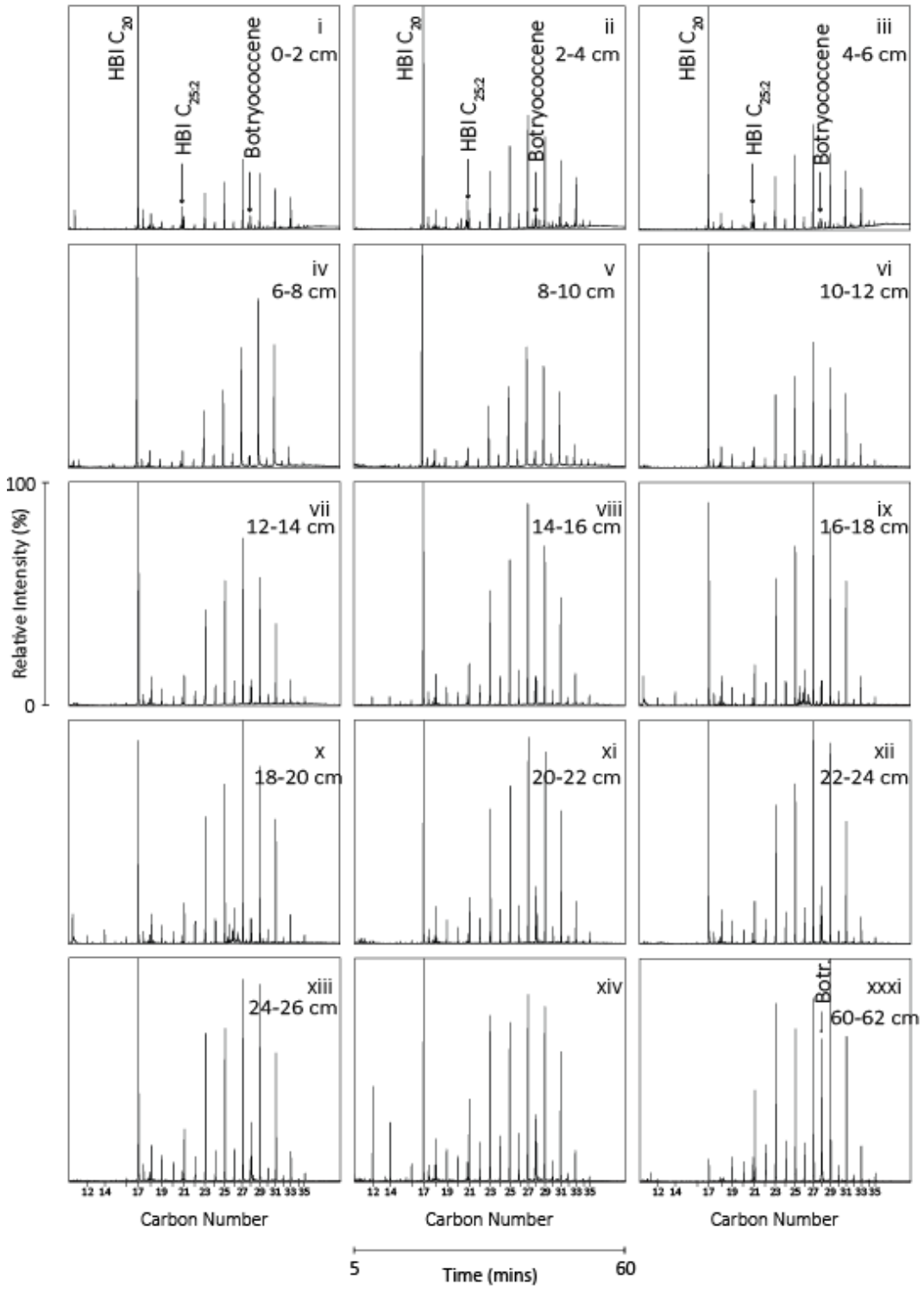

Figure 17. Partial selected ion chromatogram (m/z 57) distribution from the uppermost subsection, DL-L2 i (0-2 cm) to DL-L2 xiv (26-28 cm) and lower subsection DL-L2 xxxi (60-62 cm) showing changes in relative abundance and community succession. The community of Botryococcus braunii in lower sections of the core is succeeded by a diatomic population following logging and fire at Douglas Lake.

5.2.1.4. TRICYCLIC DITERPENOIDS (RESINS)

The tricyclic diterpenoids fichtelite, tetrahydrorimuene, dehydroabietane and kaurene have been tentatively identified in Douglas Lake sediment extract on the basis of comparison with published spectra (Brophy et al., 2000; Hautevelle et al., 2006; Livsey et al., 1984). These diterpenes are diagenetic products of compounds synthesized by vascular plants of a restricted number of taxa (Hautevelle et al., 2006). For example, kaurene (Fig. 6, peak 15), was isolated from the essential oils in pine needles (Brophy et al., 2000); while fichtelite (Fig. 6, peak 18) is known to be major component of conifer resins (Livsey et al., 1984).

5.2.1.5. TETRA AND PENTACYCLIC TRITERPENOIDS

Polycyclic triterpenoids comprise compounds like steroids and hopanoids, which function as biomarkers for various organisms. In the saturated/unsaturated fraction these compounds include: erogosta-5,22-diene (C28 steroid), diploptene (C_{30} hopanoid), neogammacerene (C_{30} hopanoid), and homohopanes (C_{32} hopanoid) (Fig. 6). These triterpenoids both widespread in nature and unique to certain organisms (Kenig & Sinninghe Damsté, 1995; Rashby et al., 2007; Summons at al., 1999; Volkman, 2003). For example, the detection of hopanoids like neogammacerene and diploptene in TLE is evidence for contribution to organic matter from unspecified bacteria (De Mesmay et al., 2008; Volkman, 2005).

Triterpenoids were not quantified in this study, but their presence is used as diagnostic biomarkers for contribution to organic matter.

5.2.2. AROMATIC FRACTION

The aromatic fraction of TLE consists of PAHs, phenanthrene, fluoranthene and pyrene, along with concomitant amounts of botryococcene, and squalene. Non-aromatic compounds like botryococcene and squalene elute with the aromatic fraction due to the solvent mixture used during extraction (DCM/hexanes 9:1, v/v). Other aromatic compounds like benzo(a)pyrene, perylene, coronene, and BPA eluted with the polar fraction of TLE.

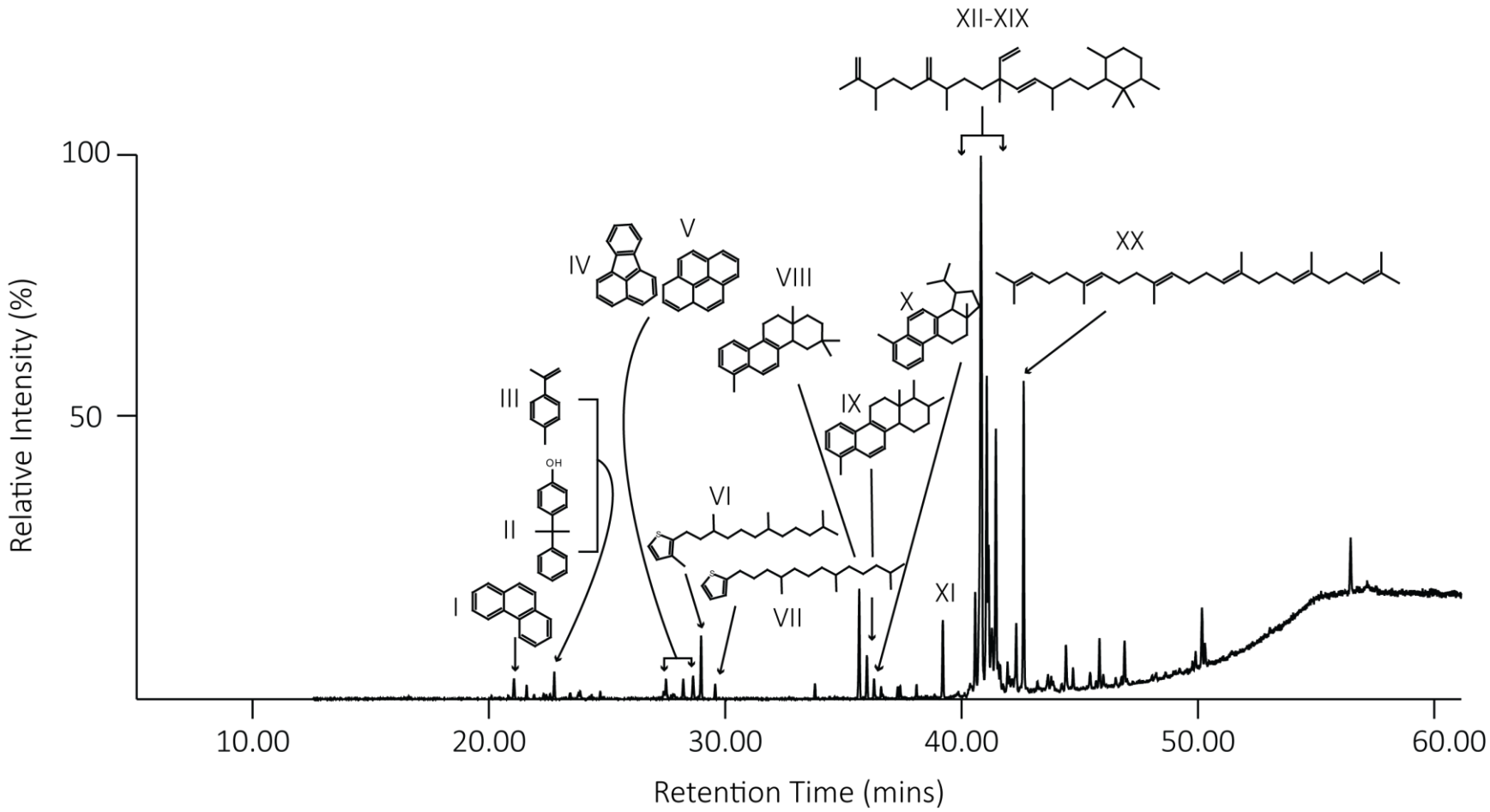

Figure 18. Representative chromatogram of the aromatic fraction of total lipid extract. Labelled compounds have been tentatively identified following comparisons with various authors described in the text. I) Phenanthrene. II) Dimethylphenol-2-ylphenylmethane. III) 1-methyl-4-(1-methyethen-1-yl) benzene. IV) Fluoranthene. V) Pyrene. VI) 3-methyl-2-(3,7,11-trimethyldodecyl)thiophene. VII) 3-(4,8,12-trimethyltridecyl)thiophene. VIII) Tetramethyloctahydrochrysene. IX) Des-A-26,27-dinor-ursa-5,7,9,11,13-pentaene. X) Des-A-26,27 dinor-lupa-5,7,9,13-pentaene. XI) 3,3,7-Trimethyl-1,2,3,4-tetrahydrochrysene. XII) $C_{32:2}$ Botryococcene. XIII) $C_{33:5}$ Botry. XIV) $C_{34:3}$ Botry. XV) C34:2 Botry. XVI) $C_{34:4}$ Botry. XVII) $C_{34:4}$ Botry. XVIII) Botry. XIX) $C_{33:3}$ Botry. XX) Squalene.

5.2.2.1. TETRAMETHYLOCTAHYDROCHRYSENES AND TRIMETHYLTETRAHYDROCHRYSENE

Tetramethyloctahydrochrysenes (Fig. 19) elute in the saturated/unsaturated hydrocarbon fraction of TLE. As previously discussed they are the oxidation products of pentacyclic triterpenoids like β–amyrin. Structures for tetramethyloctahydrochrysene, des-a-26,27-dinor-ursa-5,7,9,11,13-pentaene, and des-a-26,27-dinor-lupa-5,7,9,13-pentaene (Fig. 18 and Fig. 19) were tentatively identified by comparison with spectra from literature (Spyckerelle et al., 1977; ten Haven et al., 1992). These tetracyclic compounds are likely either naturally aromatized pentacyclic triterpenoids (β–amyrin) or resins that have been altered by increased temperatures (forest fires) (Laflamme & Hites, 1979; Spyckerelle et al., 1977).

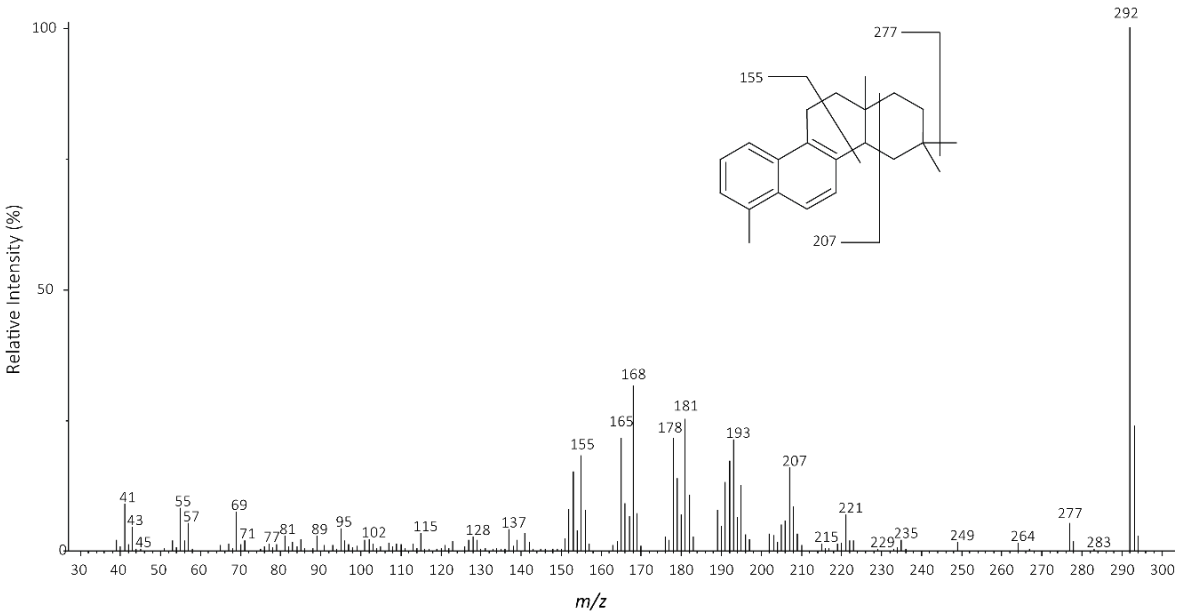

Figure 19. Mass spectra (subtracted for background) of tetramethyloctahydrochrysene. Tentatively identified by comparison with spectra from Spyckerelle et al. (1977).

5.2.2.2. ISOPRENOID THIOPHENES

The fragmentation patterns of mass spectra in the literature (Brassell et al., 1986; Fukushima et al., 1992) enabled identification of isoprenoid thiophenes (compounds VI and VII, Fig. 18) The presence of acyclic isoprenoid thiophenes signifies the diagenesis of pigment–derived compounds like phytol in an anoxic environment with reduced sulfur species (Brassell et al., 1986). Isoprenoid thiophenes were not quantified in this study, they are diagnostic for the reduced conditions in the lower water column and the sediment of Douglas Lake. To further validate this point, a ratio of all botryococcenes versus 3-methyl-2-(3,7,11-trimethyldodecyl)-thiophene (C_{20}) was used to create a historical profile. Botryococcenes were used in the ratio because the green algae that synthesize them are very sensitive to eutrophication, and by extension, increased anoxia in the hypolimnetic zone (Smittenberg et al., 2005).

5.2.2.3. BOTRYOCOCCENE

Botryococcene also elutes with two hydrocarbon fractions. See previous discussion in section 5.2.1.6 for representative results.

5.2.2.4. 4-(1-METHYL-1-PHENETHYL)-PHENOL

4-(1-methyl-1-phenethyl)-Phenol (Fig. 20) is used as an intermediate for resins, insecticides and lubricants. According to Fiege et al. (2000), it is a phenol derivative generally produced in the high boiling point still bottoms of industrial manufacturing plants (especially phenol-acetone plants). It is also likely that 4-(1-methyl-1-phenethyl)-phenol is derived from the photochemical transformation of BPA (Mill & Mabey, 1985).

4-(1-methyl-1-phenethyl)-phenol coelutes with 1-methyl-4-(1-methyethen-1-yl) in all samples analyzed. 1-methyl-4-(1-methyethen-1-yl) has been produced via pyrolysis of synthetic organic polymers in experiments by Moldoveanu (2005).

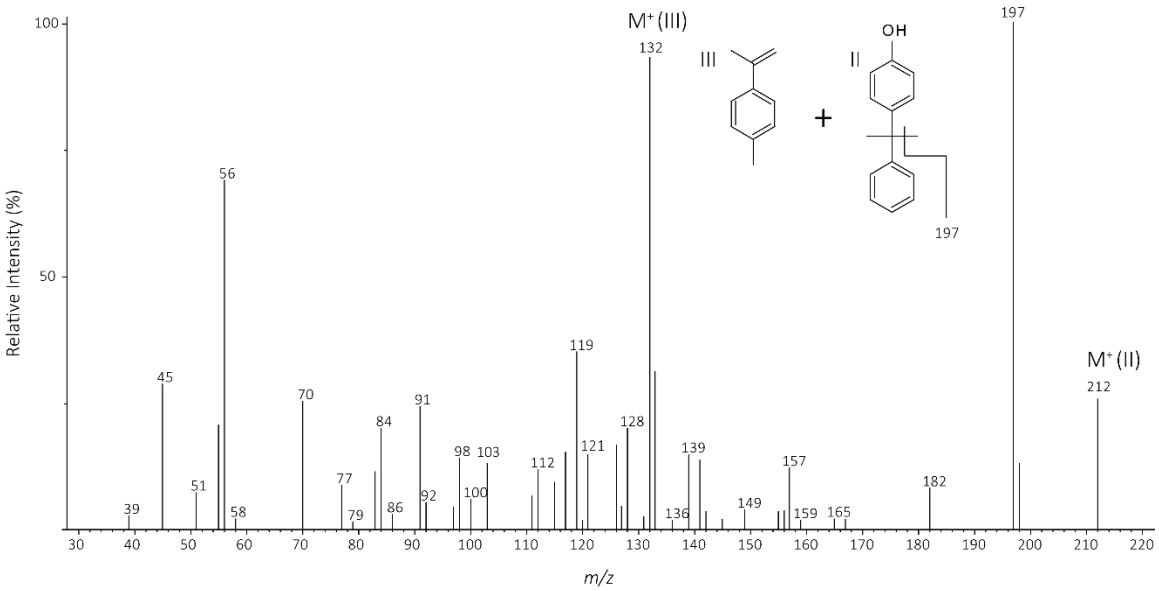

Figure 20. Mass spectra (subtracted for background) of 4-(1-methyl-1-phenethyl)-phenol and 1-methyl-4-(1-methyethen-1-yl) benzene. Both compounds coelute in every fraction of TLE, as such, they are characterized together.

5.2.3. POLAR FRACTION

The polar fraction of TLE from Douglas Lake is comprised of a diverse group of compounds, most of which are functionalized with carboxyl or hydroxyl groups (Fig. 21). Broadly divided, these groups include: degraded carotenoids, fatty acids, fatty acid methyl esters (FAME), phenylethyl esters (PEE), wax esters, carbonyl–grouped alkanes, tetracyclic, and pentacyclic triterpenoids. Triterpenoids were the most intense peaks in the TIC of all samples analyzed. Subsections DL–L2 i and ii were dominated by C_{29} hopanols, however, all subsections proceeding DL–L2 iii were dominated by C_{29} and C_{29} sterols (ergost-5-en-3β-ol, stigmasta-5-en-3β-ol, and stigmastan-3β-ol). Alcohols are the second most abundant compounds, they coelute with the wax esters convoluting

the analysis of both groups. Of all analyzed samples, DL–L2 xxxi is the only exception to the described relative abundances. In sample DL–L2 xxxi, the most abundant compounds in its TIC are C_{22}, C_{24}, C_{26} alcohols, and FAMEs; compounds like steroids and hopanoids were low in abundance in this sample.

Target contaminants, PAHs and BPA, elute in the polar fraction. BPA predictably elutes in this fraction due to its high polarity but the presence of PAHs in a fraction other than the aromatics suggests that the solvent mixture used for aromatic separation (Hexanes/DCM 9:1, v/v) could not elute higher molecular weight aromatics (m/z > 202). BPA will be further discussed in Chapter III.

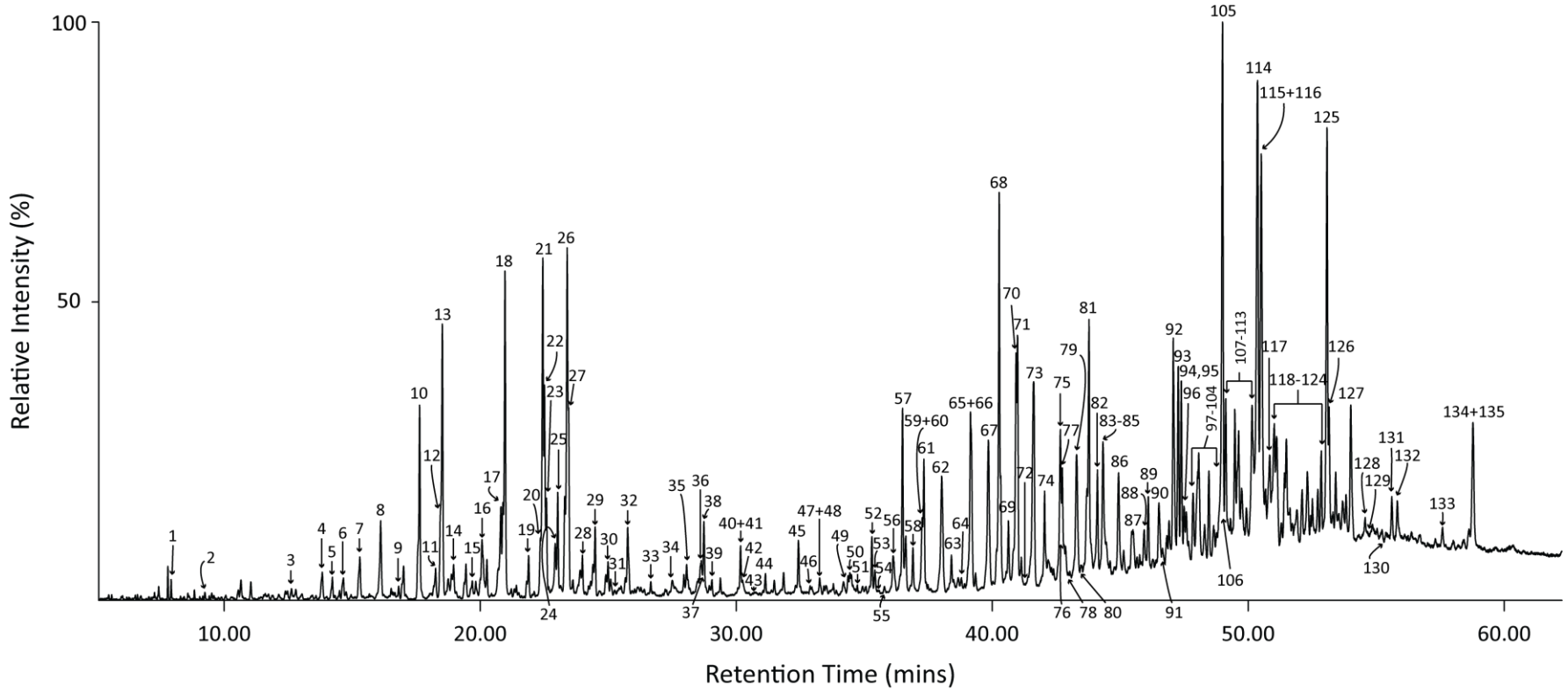

Figure 21. Representative total ion chromatogram (TIC) of the polar fraction in core subsection DL-L2 viii (14-16 cm, 1954). All identifiable peaks have been numerically designated. For information about peak identities, see table III.

TABLE III. IDENTIFICATION OF NUMBERED PEAKS IN FIGURE 21, WHICH SHOWS TIC OF THE POLAR FRACTION OF SAMPLE DL–L2 VIII.

Peak	Compound	Peak	Compound	Peak	Compound
1	Ketoisophorone	26	Hexadecanol	51	Docosanone
2	Methylethyl maleimide	27	3,7,11,15 Tetramethyl-2-hexadecen-1-ol	52	Docosanal
3	Pinanediol (1R,2R,3S,5R)-	28	9-Hexadecenoic acid methyl ester	53	C_{23} Wax ester
4	14-Methyl-8-hexadecenal	29	Hexadecanoic acid methyl ester	54	Benzo(a)anthracene
5	Beta-ionone	30	Isophytol	55	Chrysene + Triphenylene
6	4-Methyl-5-decanol	31	Hexadecanoic acid	56	C_{23} Wax ester
7	Dihydroactinidiolide	32	Heptadecanol	57	Docosanol
8	Tridecanol	33	Pentadecanal	58	Tricosanone
9	Dihydrojasmone	34	Fluoranthene	59	Tricosanal
10	12-Methyl-1-tridecene	35	Octadecanol	60	Docosanoic acid methyl ester
11	4-(6,6-Dimethyl-2-methylenecyclohex-3-enylidene)pentan-2-ol	36	9-Octadecenoic acid	61	C_{24} Wax ester
12	3-(1-hydroxy-2-isopropyl-5-methylcyclohexyl)-Ppropiolic acid	37	Pyrene	62	C_{24} Wax ester
13	Tetradecanol	38	Phytol	63	Tricosanol
14	4-Hydroxy-beta-ionone	39	Octadecanoic acid methyl ester	64	Tetracosanone
15	Tetradecanoic acid methyl ester	40	Unknown benzene structure	65	Tetracosanal
16	Isololiolide	41	Bisphenol A	66	C_{25} Wax ester
17	Loliolide	42	Nonanol	67	C_{25} Wax ester
18	Pentadecanol	43	Eicosanone	68	Tetracosanol
19	Hexadecanal	44	Eicosanal	69	Pentacosanone
20	Transpinane	45	Eicosanol	70	Pentacosanal + Tetracosanoic acid methyl acid
21	Neophytadiene	46	Heneicosanone	71	C_{26} Wax ester
22	Methyl pentadecanol	47	Heneicosanal	72	Benzo(b)fluoranthene
23	2-Pentadecanone	48	Eicosanoic acid methyl ester	73	C_{26} Wax ester
24	9-Hexadecen-1-ol	49	Benzo(g,h,i)fluoranthene	74	Pentacosanol
25	Neophytadiene	50	Heneicosanol	75	C_{27} Wax ester

TABLE III (CONT.). IDENTIFICATION OF NUMBERED PEAKS IN FIGURE 21, WHICH SHOWS TIC OF THE POLAR FRACTION OF SAMPLE DL–L2 VIII.

Peak	Compound	Peak	Compound	Peak	Compound
76	Benzo(e)pyrene	101	C_{30} Wax ester	126	Fern-7-en-3β-ol
77	Hexacosanal	102	4-Methyl-cholestan-3-ol	127	Oleanan-3-ol
78	Benzo(a)pyrene	103	Cholesta-3,5-diene-7-one	128	Dotriacontanoic acid methyl ester
79	C_{27} Wax ester	104	4-Methyl-cholest-8(14)-en-3-ol	129	Coronene
80	Perylene	105	Ergost-5-en-3β-ol	130	C_{24} Phenylethyl ester
81	Hexacosanol	106	Benzo(g,h,i)perylene	131	C_{28} Branched fatty acid methyl ester
82	Heptacosanone	107	Epiergostanal	132	βα/αβ C_{32} Hopanol
83	C_{28} Wax ester	108	Stigmasta-5,22-dien-3β-ol	133	βα C_{32} Hopanone
84	Hexacosanoic acid methyl ester	109	Stigmast-22-en-3β-ol	134	C_{26} Phenylethyl ester
85	Heptadecanal	110	C_{20} Phenylethyl ester	135	ββ C_{32} Hopanol
86	C_{28} Wax ester	111	5α-Ergostan-3-one		
87	Heptadecanol	112	Tricontanol		
88	C_{29} Wax ester	113	Norhopan-22-ol		
89	Octacosanal	114	Stigmast-5-en-3β-ol		
90	C_{29} Wax ester	115	Stigmastan-3β-ol		
91	Cholesta-5,22-dien-3β-ol	116	Triacontanoic acid methyl ester		
92	Octacosanol	117	β-amyrin		
93	Cholest-5-en-3β-ol	118	Stigmast-8(14)-en-3β-ol		
94	Nonacosanone	119	Stigmasta-3,5-dien-7-one		
95	Dihydrocholesterol	120	Tocopherol Isomer		
96	Tocopherol Isomer	121	4-Methyl-stigmastan-3-ol		
97	Octacosanoic acid methyl ester	122	Stigmast-4-en-3-one		
98	Epiergostanol	123	C_{22} Phenylethyl ester		
99	Ergosta-5,22-dien-3β-ol	124	C_{26} Branched fatty acid methyl ester		
100	Indeno(c,d)pyrene	125	Hopenol		

5.2.3.1. POLYCYCLIC AROMATIC HYDROCARBONS

PAHs ranging from MW 128 to 300 were identified in sediments from Douglas Lake. Structures were identified on the basis of comparison with spectra from in–house libraries and literature (Killops & Massoud, 1992; Simoneit, 2002). PAHs eluted in the polar fraction of TLE. Consequently, SIM (selected ion monitoring) of *m/z* 128, *m/z* 178, *m/z* 202, *m/z* 226, *m/z* 228, *m/z* 252, *m/z* 276 and *m/z* 300 was used to aid compound quantifications (Fig. 22). Samples DL–L2 i to DL–L2 v contain miniscule amounts of PAHs relative to all other samples, and their SIM traces could not be used for quantitation.

PAHs concentrations in all analyzed samples ranged between ~0 and 0.1 µg/g with a mean concentration of 0.0102 µg/g, and a median of 0.005 µg/g. The total concentration for quantified PAHs in the 9 subsections analyzed was 1.47 µg/g dry sediment weight. PAH distribution in lipid extract favors the predominance of 3–, 4–, and 5–ring. While fluoranthene and pyrene were the tallest peaks in the TIC (0.025 µg/g and 0.015 µg/g, average concentrations respectively), benzo[b]fluoranthene was, overall, the most abundant by weight (0.0261 µg/g average, Table X Appendix D). The preference for peri-condensed PAHs, and the distinct lack of alkylated homologues is more typical of pyrogenic sources (vegetation burning) rather than petroleum combustion or coal burning (Killops & Massoud, 1992; Page et al., 1999; Yunker et al., 2002).

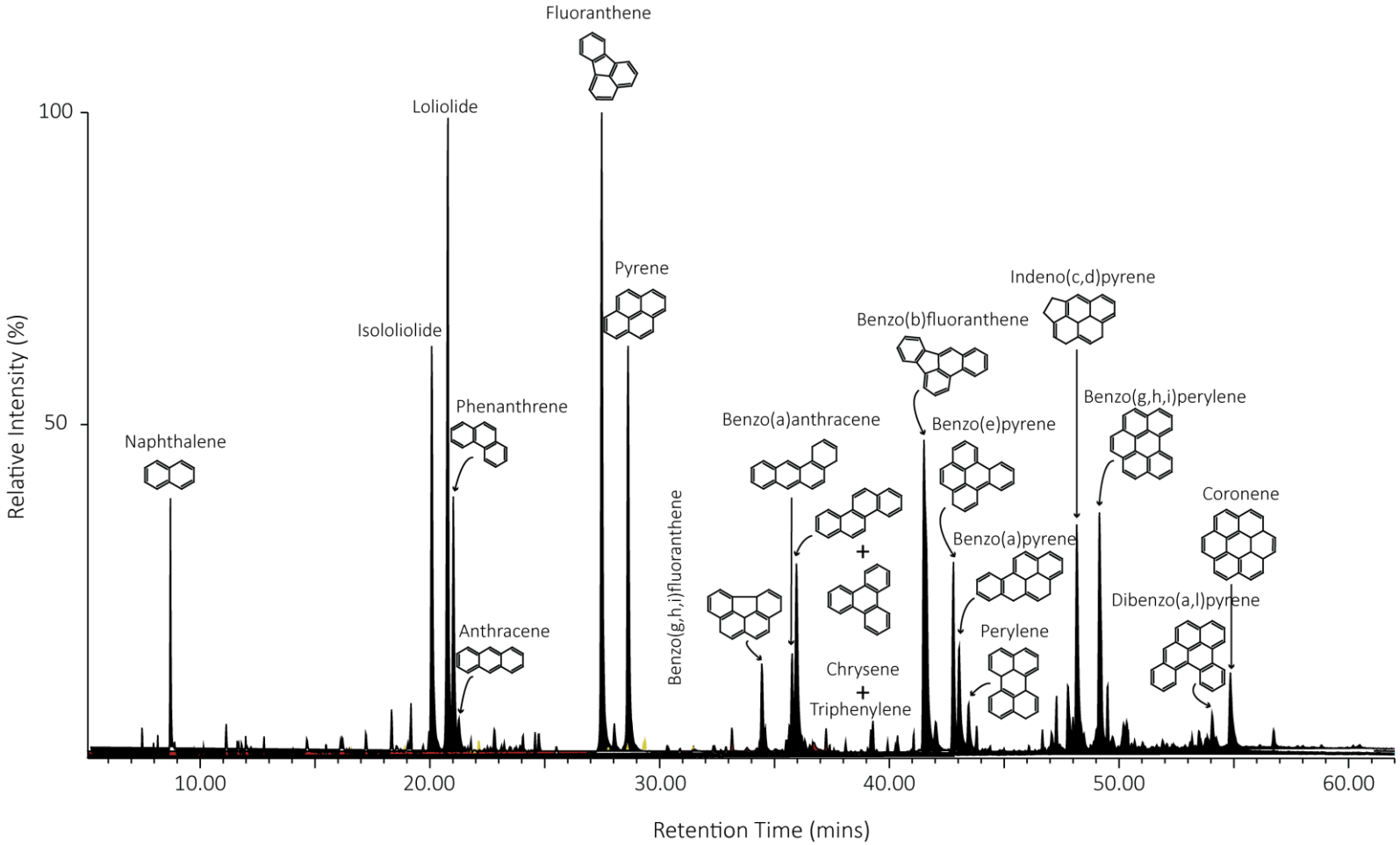

Figure 22. Selective ion chromatogram (m/z 128, m/z 178, m/z 202, m/z 226, m/z 228, m/z 252, m/z 276, m/z 300) PAH distribution in Douglas Lake sediment exhibiting typical pyrolytic distribution. PAHs were identified by their mass spectra and retention time.

PAH ratios were used to confirm that PAHs were derived from forest fires. The use of PAH ratios to determine the source of parent PAHs within sediments has been widely used in the literature (Bakhtiari et al., 2009; Barreca, Bastone et al., 2014; Lima et al., 2003; Yunker et al., 2002). The general difference between PAH distributions derived from wood/grass burning and PAHs derived from petrogenic combustion is the increased proportion of thermodynamically stable isomers like fluoranthene/pyrene (wood burning) relative to less stable (kinetic) isomers like phenanthrene/anthracene (Yunker et al., 2002). For this study, PAH ratios for *m/z* 178, *m/z* 202, *m/z* 276 were used to confirm that PAHs were derived from the forest fires reported at Douglas Lake (Francis, 1997; Gold et al., 1976; Wilson & Putzcer, 1942).

For anthracene/phenanthrene, *m/z* 178, (A/[A+P]) a ratio of < 0.1 usually indicates a petroleum source while > 0.1 indicates combustion. For mass 202, fluoranthene/pyrene (Fa/[Fa+Py]), a ratio of ~0.5 demarcates the boundary between petrochemical combustion (below) and wood/grass burning (above). However, this ratio is adaptive given that MW 202 ratios can vary up to ±0.1 between the vapor and particulate phases depending on the extent temperature–driven partitioning of fluoranthene/pyrene (Yunker et al., 2002). PAHs of mass 276 are used less frequently given their low concentration in refined crude oil and in burned biomass. This low concentration increases the likelihood for analytical errors.

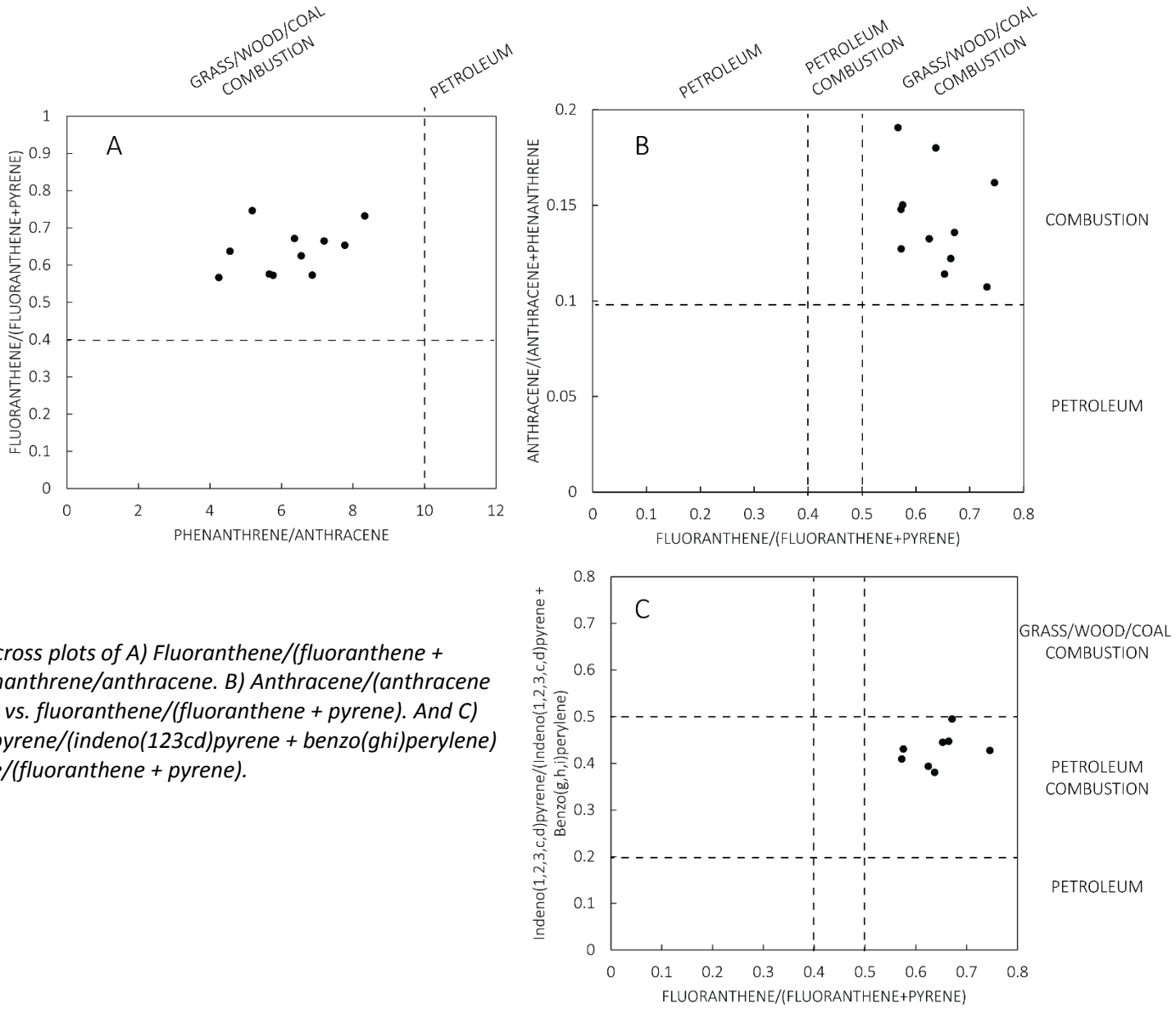

Figure 23. PAH cross plots of A) Fluoranthene/(fluoranthene + pyrene) vs. phenanthrene/anthracene. B) Anthracene/(anthracene + phenanthrene vs. fluoranthene/(fluoranthene + pyrene). And C) Indeno (123cd)pyrene/(indeno(123cd)pyrene + benzo(ghi)perylene) vs. fluoranthene/(fluoranthene + pyrene).

The phenanthrene/anthracene ratios, denoted by *m/z 178,* for all analyzed samples vary between 0.10 and 0.19, and range from 4.2 – 8.3 with ratios used by Bakhtiari et al. (2009). For pyrene/fluoranthene, denoted by *m/z* 202, values exhibit more scatter, ratios fall between 0.57 and 0.74 (Fig. 23). *m/z* 178 and *m/z* 202, although varied, fell within values that signify combustion from wood/grass or other biomass. However, the highest value for indeno(c,d)Pyrene/ benzo(g,h,i)perylene, denoted by *m/z* 276, was 0.49, and the lowest value was 0.38, well below the 0.5 threshold necessary to classify the PAHs as wood/grass combustion products. Yunker et al. (2002) referenced values from wood combustion experiments as low as 0.27, suggesting that the threshold value for *m/z* 276 may be too high. Overall, it is unlikely that there were PAH contributions from other sources given the ratios and overall composition and distribution of PAHs at Douglas Lake. From several reports, major forest fires occurred at Douglas Lake between 1880 and 1923 (Francis, 1997; Gold et al., 1976; Kilburn, 1957; Voss, 1956). These forest fires have been shown to be to the only detected source of PAHs in the lake. The reported occurrences of forest fires correspond well with ^{210}Pb dates from this study.

The historical profile of PAHs has two maxima (Fig. 24). The highest concentration of PAHs occurs around 1969 (subsection DL-L2 vii), and a second concentration spike occurs at ~1932.

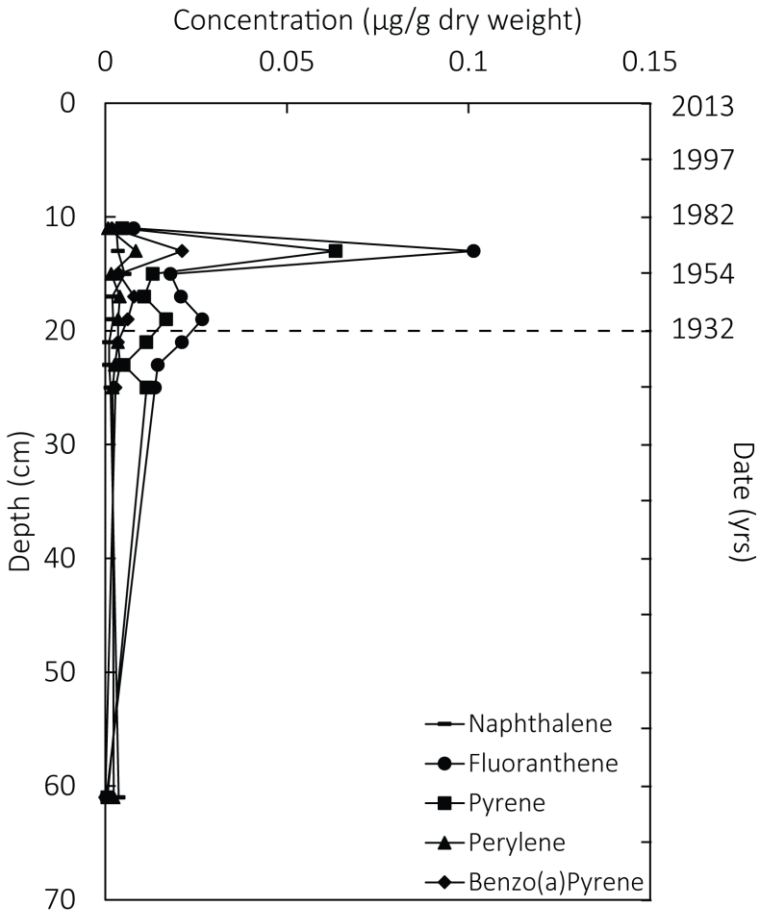

Figure 24. Historical profile of selected PAHs in the lipid extract of Douglas Lake. The dashed line demarcates zones before (below line) and after (above line) fires and logging at Douglas Lake. According to this profile, there may be other instances of major fires around 1964.

5.2.3.2. FUCOXANTHIN DEGRADATION PRODUCTS

Apocarotenoids and apofucoxanthinoids were detected in relatively low abundances in the polar fraction. These compounds are derived from the degradation of pigments from photosynthetic organisms. Pigment–derived compounds include: ketoisophorone, isololiolide,

loliolide, 4-hydroxy-β-ionone, dehdydroactinidiolide, methylethyl maleimide. Structures were identified on the basis of comparison of mass spectra with published characteristic fragmentation patterns (Castañeda & Schouten, 2011; El Hattab et al., 2008; Grice et al., 1996; Ide & Toki, 1970; Percot et al., 2009; Repeta, 1989). Apocarotenoids (4-hydroxy-β-ionone) are affiliated with higher plant, algae and some bacteria; apofucoxanthinoids (loliolide and ketoisophorone) are degradation products of fucoxanthin, a diatom specific pigment. While chlorophyll a derivatives (methylethyl maleimide) are biomarkers for photosynthetic algae and higher plants (Castañeda & Schouten, 2011). Pigment compounds were not quantified in this study, they were instead used as source proxies.

5.2.3.3. ESTERS, ALCOHOLS, KETONES, AND ALDEHYDES

A homologous series of ketones (C_{19} – C_{33}), alcohols (C_{18} – C_{30}), aldehydes (C_{18} – C_{30}) and esters (C_{23} – C_{28}) were identified using their characteristic fragmentation patterns. SIM (scanned ions – *m/z* 58, *m/z* 74, *m/z* 88, *m/z* 125, *m/z* 152) was used to deconvolute the ion current for ease of identification (Fig. 25). *m/z* 125 (for alcohols) does not show the true relative abundance of alcohols in the TIC, and use of other alcohol fragment ions (*m/z* 83, *m/z* 97, and *m/z* 111) preferably shows wax esters.

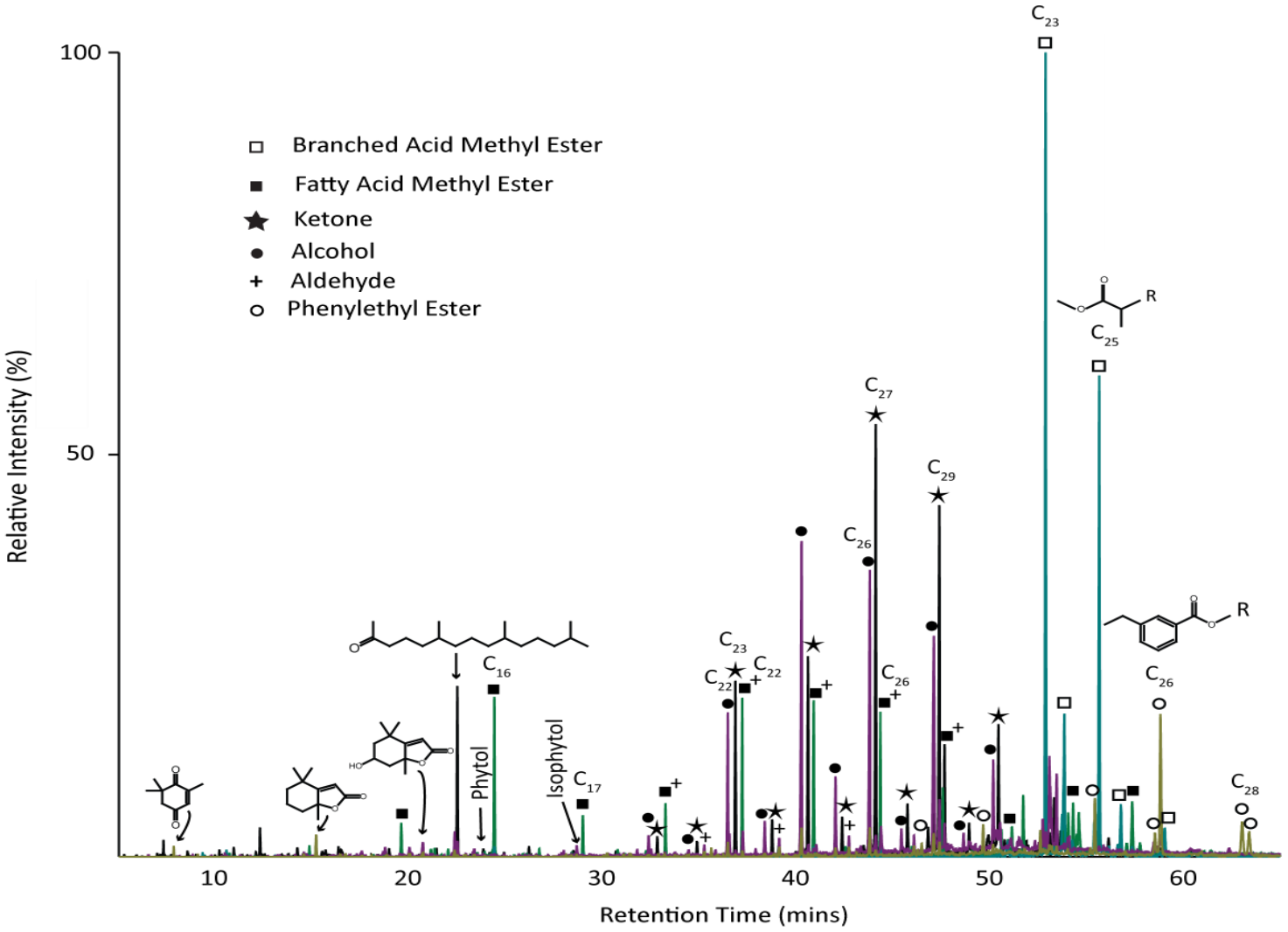

Figure 25. Summed ion chromatogram (m/z 58, m/z 74, m/z 88, m/z 125, m/z 152) from core subsection DL-L2 xxxi. This chromatogram was selected due to the dilution of wax ester signals during the peak of logging and uncontrolled fires at Douglas Lake. Wax esters coelute with most of the carbonyl compounds and some FAME compounds, convoluting representation. For the general trend in the relative abundance of labelled compounds see figure 26.

Detected *n*-alkanols ranged from C_{13} to C_{32}, the dominant *n*-alkanols for all analyzed samples were C_{24} and C_{26}. *n*-Alkanols derived from higher plants usually display even-over-odd predominance (Cranwell et al., 1987). However, the distribution of alcohols was bimodal, with higher plants contributing *n*-alkanols range from C_{22} to C_{30} and algae contributing C_{14} to C_{20} (Rielley et al., 1991).

Ketones cover a range from C_{21} to C_{33} with OEP, the most abundant of which was C_{27}similar to *n*-alkanes found in the saturated/unsaturated hydrocarbon fraction. *n*-Alkanones have been reported as components of epicuticular leaf waxes and may form microbially mediated oxidation of corresponding *n*-alkanes (Cranwell et al., 1987; Rielley et al., 1991; Szafranek & Synak, 2006). Given the ubiquity of alkenones in all samples from Douglas Lake, this process must occur rapidly in sediments upon deposition. Extracts also contained long chain aldehydes with carbon numbers from C_{20} to C_{30} that maximized around C_{24}.

Fatty acid methyl esters (FAMEs) ranging from C_{14} to C_{36}, they were dominated by palmitic acid methyl ester. FAMEs were identified by their characteristics fragmentation ions, *m/z* 74 and *m/z* 87, they tend to coelute with aldehydes and wax esters in the polar fraction. Esters also include phenylethyl ester and monomethyl branched FAME (BFAME) (Fig. 26). Esters and 6,10,14-trimethyl-2-pentadecanone (a derivative from essential oils in plants) are biomarkers for organisms with waxes like terrestrial plants (Al-Qudah, 2013; Szafranek & Synak, 2006).

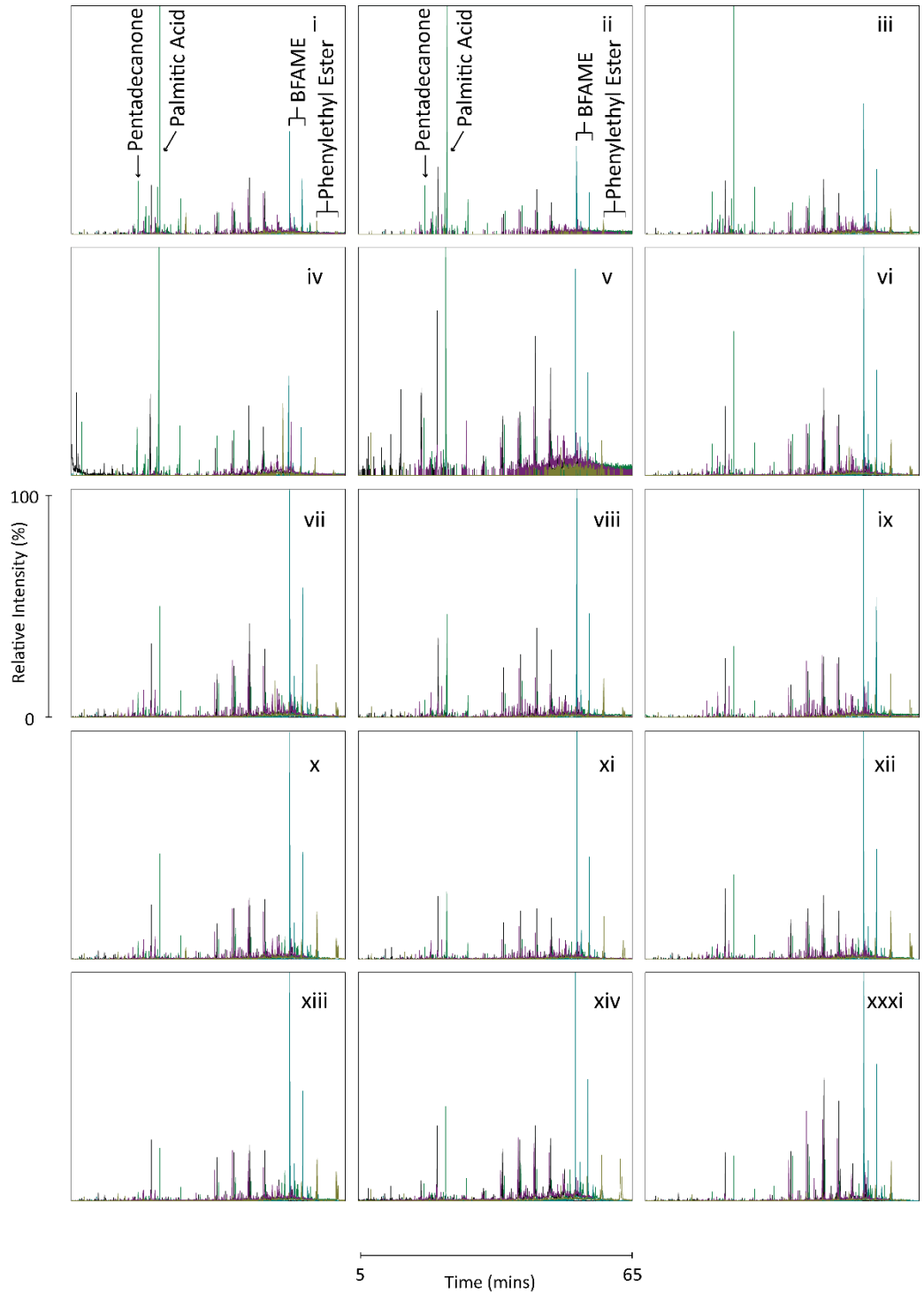

Figure 26. Summed ion chromatograms (m/z 58, m/z 74, m/z 88, m/z 125, m/z 152) showing the distribution of fatty acids, alcohols, aldehydes, and ketones from the uppermost subsection, DL-L2 i (0-2 cm) to DL-L2 xiv (26-28 cm) and lower subsection DL-L2 xxxi (60-62 cm).

5.2.3.4. EPICUTICULAR WAX ESTERS

Esters of long chain fatty acids with long alcohol moieties are biomarkers for waxes used by some higher plants, insects and birds (Dekker et al., 2000; Szafranek & Synak, 2006). Wax esters were tentatively identified on the basis of comparison with known fragmentation patterns and mass spectra from literature (Dekker et al., 2000; Szafranek & Synak, 2006). The distribution pattern of wax esters increased in complexity with increasing molecular weight (Fig. 27 B). This is due to the number of possible combination of fatty acid and alcohol moieties, and multiple branched isomers for wax ester. Since several wax esters of the same molecular weight (and different chain lengths) partially coelute, it can be difficult to identify specific fatty acid fragments or entire compounds. To overcome this issue, fatty acid ions (*m/z* 143, *m/z* 159, *m/z* 173, *m/z* 187, *m/z* 201, *m/z* 215, and *m/z* 229) were selectively monitored and unmerged. This allowed increase control during background subtraction and peak identification (Fig. 27 A).

Wax esters ranged in carbon number from C_{22} to C_{29} (and possibly up to C_{32}) and were predominantly branched C_{26} (denoted BR). As an example, the coeluting peaks within C_{26} wax esters in summed ion current mode included: (1) C_{10} acid, C_{16} alcohol; (2) C_{11} acid, C_{15} alcohol; and (3) C_{12} acid, C_{14} alcohol (peaks 27, 28, and 29, Fig 27 and Table IV). Wax esters were not quantified in this study.

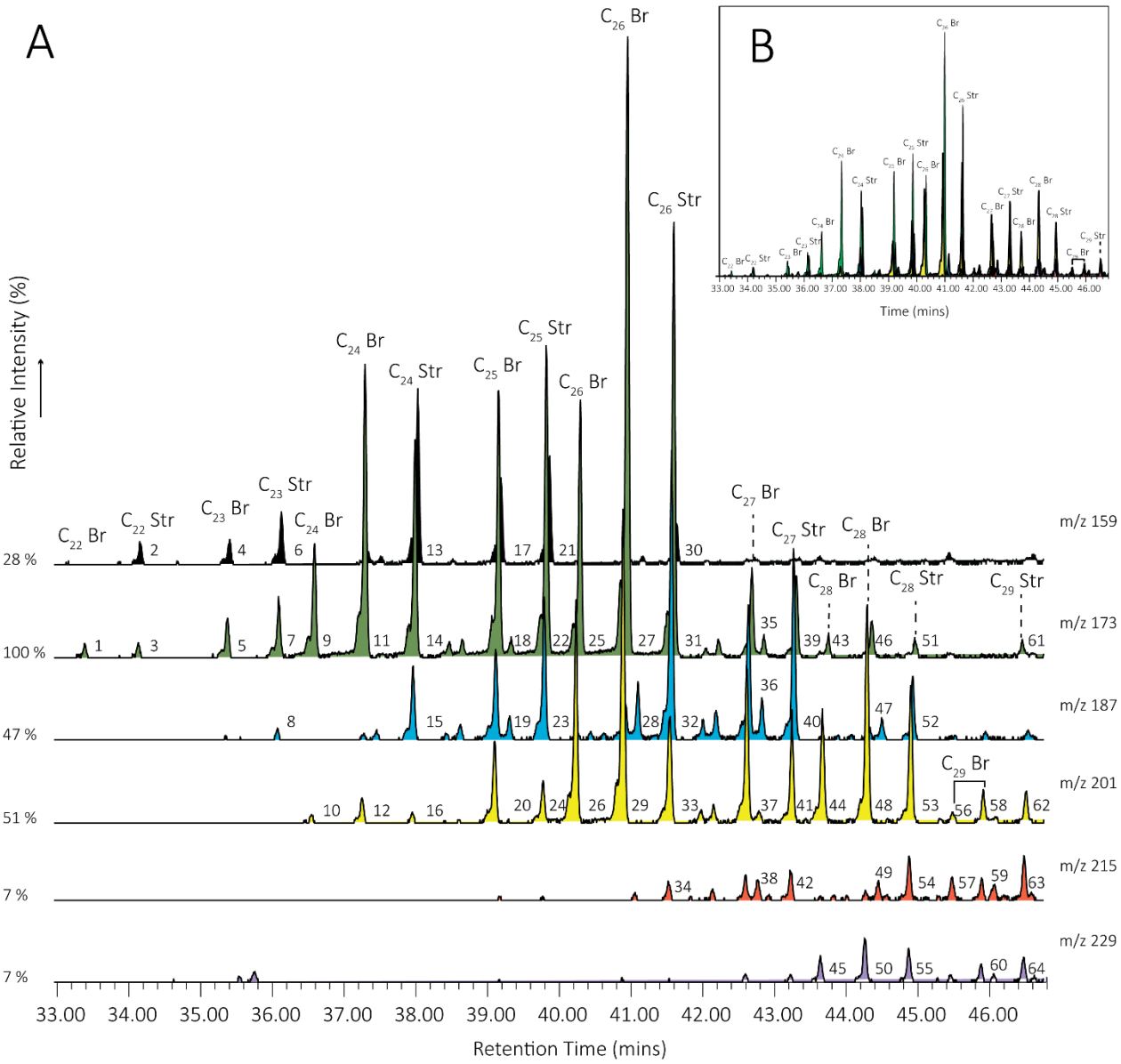

Figure 27. (A) Selected ion chromatogram m/z 159, m/z 173, m/z 187, m/z 201, m/z 215, and m/z 229 showing wax ester distribution in the polar fraction of sample DL-L2 viii (14-16 cm, ~1954). The relative intensity of ion chromatograms is respected. Peaks are numbered in order of increasing retention time. Identification of numbered peaks is given in Table IV. (B) Summed mass chromatogram of the m/z shown in A.

TABLE IV. IDENTIFICATION OF NUMBERED PEAK IN FIGURE 27, WHICH SHOWS A SELECTED ION CHROMATOGRAM OF THE POLAR FRACTION OF SAMPLE DL–L2 VIII.

Peak	Compound	MW[a]	Peak	Compound	MW	Peak	Compound	MW
1	Branched C_{22} wax ester[b]	340	23	Tetradecyl undecanoate	382	45	Branched C_{28} wax ester	424
2	Tridecyl nonanoate	340	24	Tridecyl dodecanoate	382	46	Octadecyl 7-methylnonanoate	424
3	Dodecyl decanoate	340	25	Hexadecyl 8-methylnonanoate	396	47	Heptadecyl 8-methyldecanoate	424
4	Branched C_{23} wax ester	354	26	Branched C_{26} wax ester	396	48	Hexadecyl 9-methylundecanoate	424
5	Branched C_{23} wax ester	354	27	Branched C_{26} wax ester	396	49	Branched C_{28} wax ester	424
6	Tetradecyl nonanoate	354	28	Pentadecyl 7-methyldecanoate	396	50	Branched C_{28} wax ester	424
7	Tridecyl decanoate	354	29	Branched C_{26} wax ester	396	51	Octadecyl decanoate	424
8	Dodecyl undecanoate	354	30	Heptadecyl nonanoate	396	52	Heptadecyl undecanoate	424
9	Branched C_{24} wax ester	368	31	Hexadecyl decanoate	396	53	Hexadecyl dodecanoate	424
10	Branched C_{24} wax ester	368	32	Pentadecyl undecanoate	396	54	Pentadecyl tridecanoate	424
11	Tetradecyl 8-methylnonanoate	368	33	Tetradecyl dodecanoate	396	55	Tetradecyl tetradecanoate	424
12	Branched C_{24} wax ester	368	34	Tridecyl tridecanoate	396	56	Branched C_{29} wax ester	438
13	Pentadecyl nonanoate	368	35	Branched C_{27} wax ester	410	57	Branched C_{29} wax ester	438
14	Tetradecyl decanoate	368	36	Hexadecyl 6-methyldecanoate	410	58	Branched C_{29} wax ester	438
15	Tridecyl undecanoate	368	37	Branched C_{27} wax ester	410	59	Branched C_{29} wax ester	438
16	Dodecyl dodecanoate	368	38	Branched C_{27} wax ester	410	60	Branched C_{29} wax ester	438
17	Branched C_{25} wax ester	382	39	Heptadecyl decanoate	410	61	Nonadecyl decanoate	438
18	Pentadecyl 8-methylnonoate	382	40	Hexadecyl undecanoate	410	62	Heptadecyl dodecanoate	438
19	Branched C_{25} wax ester	382	41	Pentadecyl dodecanoate	410	63	Hexadecyl tridecanoate	438
20	Branched C_{25} wax ester	382	42	Tetradecyl tridecanoate	410	64	Pentadecyl tetradecanoate	438
21	Hexadecyl nonanoate	382	43	Branched C_{28} wax ester	424			
22	Pentadecyl decanoate	382	44	Hexadecyl 7-methylundecanoate	424			

[a] MW - Molecular weight of the compound

[b] Wax esters with unidentified branch locations designated as branched.

5.2.3.5. TETRACYCLIC TRITERPENOID ALCOHOLS AND KETONES

Sterols are one of the most abundant compounds (by relative intensity) in the TLE and the most abundant in the polar hydrocarbon fraction. Structures were identified on the basis of mass spectral fragmentation and comparison mass spectral libraries as well as literature (Volkman, 2003, 2005). Compounds identified ranged in carbon number from C_{27} to C_{30} with varying side chain lengths and functional group positions. The most prominent sterols detected in the polar fraction were ergost-5-en-3β-ol (C_{28}), stigmast-5-en-3β-ol (C_{29}), stigmastan-3β-ol (C_{29}), and cholest-5-en-3β-ol (C_{27}), see table III for the complete list of sterols identified. Although, these abundant sterols are widely distributed in nature and derive from both higher plants and microalgae, their relative abundance and distribution can be diagnostic of specific classes of organisms (Castañeda & Schouten, 2011; Pearce et al., 1998; Volkman, 2003). For example, C_{29} sterols (stigmasterols) are thought to originate largely from higher plants even though they are also synthesized by certain algal species (Duan, 2000). While C_{27} and C_{28} sterols mainly derive from a diverse group of microorganisms (Meyers & Ishiwatari, 1993; Volkman, 2003). The major sterols from Douglas Lake are dominant components of microorganisms like baccilariophyceae (diatoms), bangiophyceae, chrysophyceae (golden algae), haptophyceae, and thraustochytrids (Volkman, 2003). It is difficult to determine which group of organisms (higher plant or microalgae) the detected sterols definitively derive from based on the mass spectra alone. However, according to Duan (2000), the low abundance of fatty acids relative to sterols may indicate that microalgal input is dominant.

5.2.3.6. PENTACYCLIC TRITERPENOIDS

The relative contribution of identified triterpenoids to TIC is high compared to other hydrocarbons, however the concentrations of hopanols were not calculated in this study. Triterpenoids were identified by comparison of characteristic fragmentation pattern with in–house

libraries and from literature (Matsunaga & Morita, 1983; Meredith et al., 2008). Hopanols detected ranged in carbon length from C_{29} to C_{32}, the most dominant hopanol in all samples analyzed was $C_{30:1}$ hopenol which is largely derived from terrestrial plants (Matsunaga & Morita, 1983; ten Haven et al., 1992). The *m/z* 191 and *m/z* 205 chromatograms show a suite of hopanols and hopanones that have been listed in table III. Other degraded triterpenoids identified in samples include fernenol, oleananol, amyrin, and friedelane-type compounds biomarkers of higher plants (Volkman, 2003). The abundance of hopanols and other triterpenoids was drastically diminished in the lowest subsection analyzed. Hopanols were not quantified, they serve as evidence for contribution to organic matter by vascular plants.

6. DISCUSSION

Prior to its modern settlement (~11,000 years BP), Douglas Lake was heavily forested by hardwoods as described in several studies of the region (Voss, 1956; Wilson & Putzcer, 1942). The contribution to organic matter in sediments is primarily derived from higher plants. Sediment extracts contain high concentrations of *n*-alkanes dominated by the C_{27} and C_{29} *n*-alkanes, diagnostic of higher plant leaf waxes. Although, other biomarkers of higher plants were not quantified, the presence of wax esters, long–chain alcohols, β-amyrin, oleananol, dehydroabietane, fichtelite and sterols corroborate the evidence for higher plant contribution to sedimentary organic matter.

MACROPHYTES

Higher plants in Douglas Lake include aquatic plants (macrophytes), which are an important aspect of lacustrine ecosystems (Bromilow et al., 2012). Macrophytes provide shelter and are a source of food for fish and many invertebrates. They also oxygenate the littoral zones via photosynthesis and consume the limiting nutrients available to cyanobacteria and other phytoplankton, which could help reduce the effects of eutrophication in lakes (Bromilow et al., 2012). The P_{aq} ratios for Douglas Lake (Fig. 11) vary between ~0.4 and ~0.5, suggesting mixed contribution of higher plants and macrophytes to the *n*-alkane pool (Ficken et al., 2000) and possibly sedimentary organic matter.

BIOMARKER RECORD OF THE FIRE HISTORY

The historical profile of *n*-alkanes shows that prior to 1932 the concentrations of *n*-alkanes was low (Fig. 8). These low concentrations are largely caused by rapid deforestation by the expanding logging industry in the region. The removal of anchored tree roots and subsequent stump burnings

increased soil erosion and sediment runoff into the lake (Francis, 2001). As a result, sediment accumulation rates increased and the concentration of all biomarkers were diluted by the sediment runoff. Following the purchase of 1400 acres of woodland surrounding Douglas Lake by the University of Michigan, strict fire control measures were taken, and the population of trees made a resurgence that was denoted by the increase in leaf wax alkanes (i.e. C_{27} and C_{29} *n*-alkanes; Fig. 8). However, in the 1950s the concentration of *n*-alkanes fell again. This time, the reduced concentration was not associated with uncontrolled logging and increased sediment accumulation rate but coincided with the largest peak in the concentration of PAHs (Fig. 24). These PAHs are unambiguous evidence for the occurrence of forest fires (or one major proximal fire; Fig. 23) around 1952.

According to Kilburn (1957), there were nine major fires at Douglas Lake during the logging era between 1880 and 1920. PAHs including pyrene, benzo[a]pyrene, and coronene are compounds that tend to form via pyrogenic processes like incomplete combustion. They are also classified as persistent organic pollutants and can be toxic to humans in varying degrees (Blomqvist et al., 2011; Rosner & Markowitz, 2013). Peaks in the concentrations of PAHs detected at Douglas Lake coincide with reported dates of the major fires (~1880–1920). PAHs were not quantifiable in sediments deposited after 1982, thus, after their maxima at subsection DL–L2 vii. Counterintuitively, there were much higher PAH concentrations during the ~1950s than when forest fires were common, prior to fire control measures after 1923. The high abundances of PAHs relative to plant biomarkers (i.e. abietane, fichtelite) around 1950 may be an indication that the PAH source was proximal, i.e., the burning of biomass occurred close to Douglas Lake. However, there is no historical record of forest fire at Douglas Lake, and a distal forest fire may be considered to explain this high concentration of PAHs, and at present, the true source of this ~1950 deposition of PAHs remains unknown. It can be hypothesized as well that the fire may have occurred directly over South Fishtail

Bay (i.e. boat fire). The PAH ratios (Fig. 23) demonstrate that the source of the PAHs were strictly grass/wood (as opposed to petrogenic; Yunker et al., 2002). For further corroboration for PAH sources, aerosolized particles of burning plant matter were also deposited in the lake, their biomarkers (dehydroabietane, tetramethyloctahydrochrysene, and β-amyrin) were preserved, aided by the anoxic conditions.

BIOMARKER RECORD OF INCREASED EUTROPHICATION

The level of anoxia of lake sediments can be indirectly determined using a number of proxies based on preserved lipids, including relative ratios of pristane to phytane (Duan, 2000; Hughes et al., 1995), and the ratio of C_{20} isoprenoid thiophene to botryococcene[1], (Francis, 2001; Grice et al., 1996). A record of oxygen concentration in the hypolimnion of Douglas Lake exist for 1913 to present. It has been noted that the lake has undergone steady eutrophication since its modern inhabitation (Bazin & Saunder, 1971; Francis, 2001). Eutrophication can also be inferred from an increase in primary productivity. Eutrophication imposes stress on slow growing, non-competitive species like *Botryococcus braunii* (Smittenberg et al., 2005), the source of the botryococcenes identified in Douglas Lake (Fig. 16 and 17). As a consequence of increased primary productivity, oxygen is rapidly consumed and the hypolimnion becomes more anoxic. In anoxic environments (water column or sediments) phytol may undergo diagenesis by incorporating reduced sulfur species to form sulfur bearing lipids such as isoprenoid thiophene (Kenig & Huc, 1990). Therefore, the population of *B. braunni*, sensitive to eutrophication, should reduce relative to isoprenoid thiophene. The isoprenoid thiophene to botryococcenes ratio (Fig. 28) clearly shows that the process of eutrophication reported by Bazin & Saunders (1971) and Francis (2001) for Douglas Lake is now even more pronounced.

[1] Thiophene to botryococcene ratios are experimental and unique to this study.

The historical profile for the concentration of 7-methylheptadecane (a well-known cyanobacterial marker; Coates et al., 2014; Köster et al., 1999; Shiea et al., 1990) is showing the same general trend as the isoprenoid thiophene/botryococcenes ratio. Increase in population of cyanobacteria have served as evidence for eutrophication in lakes (Das et al., 2009), supporting the use of isoprenoid thiophene/botryococcenes ratio as a proxy for past eutrophication events.

As excess nutrients continue to enter Douglas Lake (likely as a result of anthropogenic activity) the primary productivity may also continue to increase. In the years since reforestation (and consequently, reduced sediment runoff; > 1920), the concentration of biomarkers from microalgae generally increased (*n*–C_{18} and *n*–C_{19}; Fig. 9), but then stabilized after 1932. Nonetheless, communities of microalgae will not increase simply as a function of nutrient content, there are many factors controlling their population growth. Similarly, an increase in cyanobacterial biomass is controlled by a variety of conditions including total phosphorus, pH, nitrates, light and temperature (Huszar & Caraco, 1998).

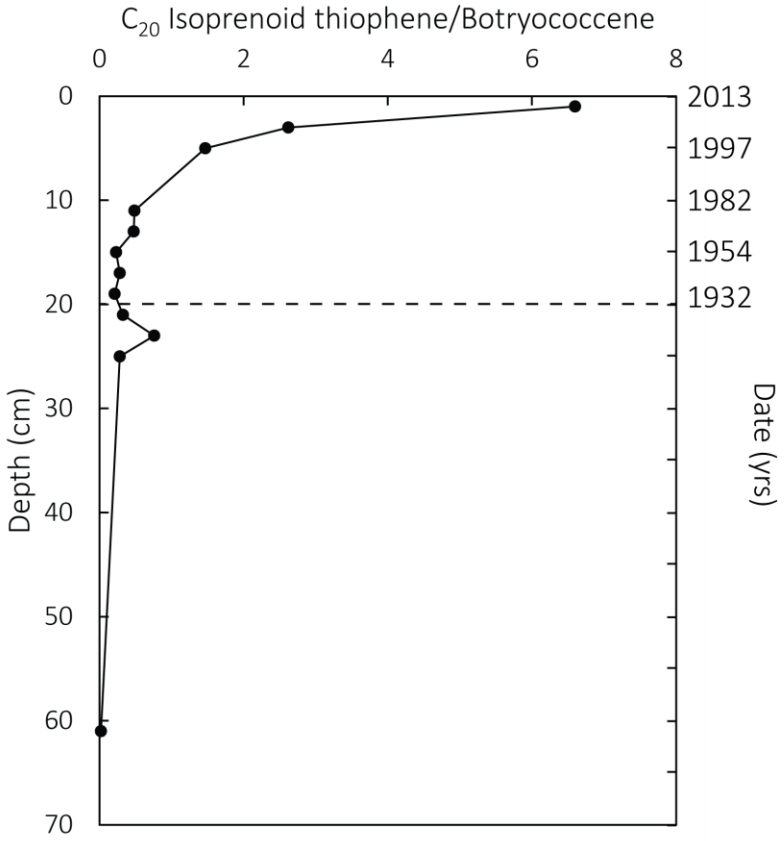

Figure 28. Historical profile of isoprenoid thiophene to botryococcene ratio. High values potentially signify increased eutrophication. Dashed line demarcates zones before and after logging and fires at Douglas Lake.

PRIMARY PRODUCER SUCCESSION

Primary producers in Douglas Lake include diatoms, golden and brown algae, cyanobacteria, and *Botryococcus braunii*, among other microalgae. Many of the primary producers generate recognizable lipids that can be found in the sedimentary record (Castañeda & Schouten, 2011; Castañeda, Werne, & Johnson, 2009; Meyers & Ishiwatari, 1993). No other species of microalgae

were more apparent in the Douglas Lake sediments than the Bacillariophyceae (diatoms) due to the prominence of C_{20} HBI (Fig. 7, 12 and 14). HBIs have been determined to derive almost exclusively from epiphytic diatoms (Belt et al., 2000; Grossi et al., 2004; Muschitiello et al., 2015; Sinninghe Damsté et al., 2005). Loliolide and other apofucoxanthinoids, all derived from degradation of fucoxanthin, a diatom pigment, were also detected.

The presence of another primary producer, cyanobacteria, was inferred from characteristic biomarkers including 7-methyl heptadecane and 2-methyl hopane, but only 7-methyl heptadecane was quantified (Fig. 9).

Based on the prominence of botryococcenes in the lower segment of the core, the profundal zone at Douglas Lake was likely dominated by green algae, *Botryococcus braunii*. However, Gao et al. (2007) reported on the possibility that botryococcene compounds may be produced by other species of green algae in addition to *Botryococcus braunii*. Notwithstanding, the population of green algae was likely affected by the environmental perturbations and was consequently succeeded by HBI–producing diatoms, proxy species for shifts in lacustrine trophic conditions (Muschitiello et al., 2015). Finely, a comparison of the C_{20} HBI profile (Fig. 14) to that of 7–methyl heptadecane (Fig. 9) shows that in the most recent sediments analyzed, cyanobacteria increases in concentration while C_{20} HBI concentration is decreasing. These trends may be a consequence of the progressive increase in eutrophication of Douglas Lake.

7. CONCLUSIONS

Sediment from Douglas Lake contain a well preserved record of ecosystem perturbations ranging from minor decreases in total biomass to the deforestation and burning of an entire region. The decrease in the concentration of *Botryococcus braunii* biomarkers, in response to increased eutrophication, parallels the increase in the concentration of cyanobacterial biomarkers. The

environmental significance of the shifts in dominance of Douglas Lake's primary producers warrants further investigation. Geochemical evidence for fires was also preserved in the form of PAHs and altered resin biomarkers. PAHs are considered toxic and can bioaccumulate along the food chain, their abundance in an environment usually requires remediation efforts. As of 2013 Douglas Lake sediments had below average concentrations of PAHs.

CHAPTER III: ABUNDANCE AND ORIGIN OF BISPHENOL A IN DOUGLAS LAKE (MICHIGAN, USA)

1. INTRODUCTION

Bisphenol A (BPA) is the common name for 4,4′-isopropyllidenediphenol. BPA is primarily used as an intermediate in the production of epoxy, polycarbonate, phenoxy resins and certain polyester resins, as well as a flame retardants and an additive to rubber. Because of the usefulness of polycarbonates, its shatter-resistance, lightweight and transparency as well as the durability and chemical resistance of epoxy resins, these BPA-containing products are widely used (Erler & Novak, 2010; Fu & Kawamura, 2010; Y. Q. Huang et al., 2012; Tsai, 2006a).

The German scientist Thomas Zincke was the first to synthesize BPA (Zincke, 1905). While Zincke reported on the physical properties of BPA he did not propose any industrial application. In the 1940s, BPA was commercially used a substitute for estrogen. Scientists in Germany and the United States would later develop manufacturing procedures for polycarbonates using BPA as an intermediate (Tsai, 2006). Commercial production for this purpose began during the late 50s in the United States and in Europe. In 1971, BPA (as an estrogen drug) was banned after studies reported the increased occurrence of vaginal cancers in women who were exposed to DES while in their mothers' wombs (Vogel, 2009), while the production of BPA as an intermediate in polycarbonate manufacturing did not cease.

In 2006, twelve nations commercially manufactured up to 3.2 million tonnes of BPA annually (Table V). In 2014, it was estimated that the global production of BPA would reach 5.4 million tonnes and that 53% of BPA production would occur in Asia (Tsai, 2006).

Table V. GLOBAL PRODUCTION OF BPA, ADAPTED FROM TSAI (2006).

Country	Production Capacity (10^3 metric tons/yr)	Percentage
USA	930	28.52
Brazil	22	0.67
Germany	280	8.59
The Netherlands	250	7.67
Belgium	140	4.29
Spain	210	6.44
Russia	20	0.61
China	30[a]	0.92
Japan	665	20.39
Korea	130	3.99
Singapore	210	6.44
Taiwan	374	11.47
Sum	3261	100

[a] Several new BPA producing plants are being planned to build in China which could increase total capacity to 175 000 in the future.

BPA enters the environment from various sources including polycarbonate manufacturing and intermediary companies as well as wastewater treatment plants. BPA is a soluble solid with low volatility at common temperatures but is soluble in water (120 mg/l at 25°C). As a result, BPA mainly resides in the aquatic compartment of the environment. Once in the aquatic system, BPA will adhere to sediment and organic substrates owing to its high polarity. Although, aerobic biodegradation of BPA is rapid (1–10 days), biodegradation is slow in anoxic conditions, including anoxic marine and freshwater sediments (Klečka et al., 2009) leading to BPA's environmental persistence.

Klečka et al. (2009) reported measurements of 85 observations of BPA in recent freshwater sediments. The median concentration of BPA in North America was ~0.6 ng/g dry weight in marine and fresh water sediments. The results of this analysis by Klečka et al., suggested that, except for highly urbanized and industrial regions, the frequency of locations with significant amounts of BPA was low. Several other studies have reported BPA in water bodies in Germany, Iran, Japan and Korea (Table VI, Heemken et al., 2001; Liao et al., 2012; Mortazavi et al., 2012). These studies also concluded that the concentration of BPA in sediments was greater near industrialized areas.

TABLE VI. COMPARISON OF BPA CONCENTRATION (ng/g dry weight) IN FRESH WATER AND MARINE SEDIMENTS.

Location	Year	Mean	Median	Range	Reference
Elbe River, Germany	1998	163	132	66-343	Heemken et al., 2001
Anzali Wetland, Iran	2010	671	N.D.[a]	10-6970	Mortazavi et al., 2012
Several rivers and bays, USA	1998-2012	6.65	1.11	<0.25-106	Liao et al., 2012
Saginaw River watershed and Michigan inland lakes, USA[b]	1999-2014	3.1	2.57	<0.25-13.4	Liao et al., 2012
Tokyo Bay, Japan	2012	8.17	8.3	1.88-23.0	Liao et al., 2012
Lake Shihwa, Korea	2008	567	6.02	<0.25-13370	Liao et al., 2012
Douglas Lake, MI	2013	357.27	111.18	1.48-1336	This study
Freshwater Sediment, USA	2009	N.D.	0.6[c]	N.D	Klečka et al., 2009

[a] N.D. – No data reported.

[b] Samples from Gratiot and Whitmore lakes, MI reported as ng/g wet weight (ww).

[c] Based on 35 sediment samples with concentrations above detection limit.

71 samples were analyzed

The aim of this study was to quantify anthropogenic contamination in a relatively clean lacustrine environment (with comparative references to values from other studies). Because Douglas Lake and, specifically, South Fishtail Bay remains relatively undeveloped, the presence of BPA in measurable concentrations could serve as evidence for atmospherically mediated transport of BPA as opposed to direct introduction via runoff or leaching.

2. SAMPLES AND METHODS

2.1. SAMPLES AND EXTRACTION METHODS

The samples analyzed were the same as those studied in Chapter II. Identical sample nomenclature is used here. Methods of extraction, elemental sulfur removal, separation and analysis of BPA are identical to methods described in Chapter II. The authentic standard used for quantification of BPA is BPA D14 purchased from Supelco (Bellefonte, PA).

To check for the presence and concentration of BPA in the coring material used, 1.98 g of the polycarbonate core tube used was sonicated in an azeotropic mixture of DCM and MeOH (7.5:1, v/v) for 30 minutes. The process was then repeated with ~3g of the low density polyethylene (LDPE) core tube cap. Total extract of the core tube and LDPE cap weighed 1 mg and 5 mg, respectively. After dissolution in cyclohexane (dilution factor = 100 µL cyclohexane/1 mg TLE) the extracts were injected into the GCMS. Peaks were integrated and concentrations calculated by comparison with the internal standard, as described in the method section of chapter II.

2.2. CHARACTERISTIC DIFFUSION MODEL (WITH POSSIBLE BIOTURBATION)

To estimate the diffusion of BPA in the sediments we used a characteristic diffusion model (equation 11).

$$Diffusion\ distance, x = \sqrt{D \times t} \qquad \text{Equation 11}$$

Diffusion distance can be calculated where D is defined as the diffusion coefficient in units of length squared per time. In this case, D = 10^{-6} cm^2/yr, a value used for very fine lacustrine/marine sediment. Time t is the difference between the date of the first occurrence of BPA in the core and the date of the core collection at Douglas Lake. For ease of calculation, properties such as compaction and porosity gradients are ignored. It should be noted that the core (especially in the upper 20 cm) compacted by a factor of ~2.27 following dewatering, from 50 cm (from the top of the water–sediment interface to the black– brown sediment transition zone) to 22 cm (see Chapter II).

2.3. HYBRID SINGLE-PARTICLE LAGRANGIAN INTEGRATED TRAJECTORY (HYSPLIT) MODEL

In order to make first order approximations of the concentrations and the mechanism of BPA transport from a potential point source to Douglas Lake, a simple HYSPLIT dispersion and trajectory model was created (Fig. 33). The parameters for modeling of the atmospheric dispersion of any compound include: 1) mass of release; 2) half-life in the atmosphere; 3) Henry's Law constant of wet deposition; 4) dry deposition velocity; 5) starting distance above ground level (AGL); and 6) a point source location.

In 2013, according to data from the Environmental Protection Agency's (EPA) Enforcement and Compliance History Online (ECHO) website, 713 lbs (323 kg) of BPA originating from Midland, MI (43.601976N latitude, -84.226026W longitude) was released into the atmosphere. This

information formed the basis of data used for the 'mass of release' for a single day (hypothetically), though the data for fugitive venting of BPA is provided for the entire year. Release time was set at eight hours, the average work period, (assuming the release occurred during a specific shift), and the released plume was monitored (modelled) for 24 hours. Diagnostic data (density and solubility) for BPA was extracted from reports by Huang et al. (2012) and Vandenberg et al. (2009). Meteorological data was retrieved from Global Data Assimilation System (GDAS) from 2006 – present.

3. RESULTS AND DISCUSSION

BPA (Fig. 31; see Fig. 21 for the position of BPA in the TIC of polar fractions) is present in the lipid extract of all Douglas Lake samples analyzed. The BPA depth profile is trimodal, with two major recent peaks at ~2013 and ~1997, and one major peak around 1932 (Fig. 30). Concentrations range between 0.0014 µg/g dw sediment and 1.34 µg/g dw, the total concentration from all samples measured was 4.28 µg/g dw. For reference, the core tube that contained the subsections from Douglas Lake was extracted and its BPA peak integrated. The core tube extract was found to contain 0.006332 µg/g (6.3 ng/g dry weight of core tube) of BPA.

BPA partly coelutes with a compound that has a fragmentation pattern similar to 11-phenyl-undecanol but with an additional carbon atoms, thus this compound was tentatively identified as 12-phenyl-dodecanol (Fig. 29), the source of this compound is unknown.

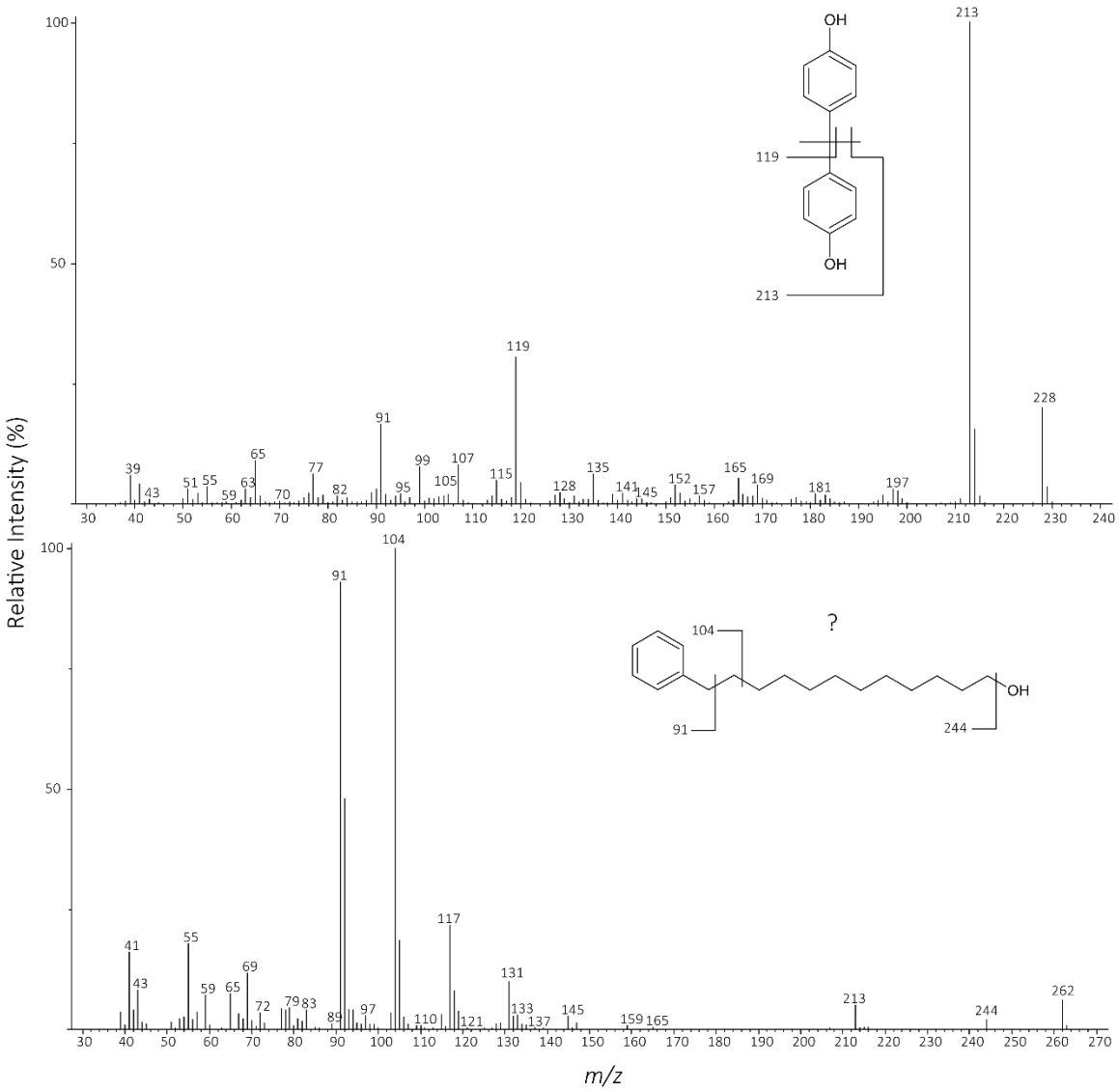

Figure 29. Mass spectra (subtracted for background) of A) Bisphenol A, and B) unknown coeluting benzene compound similar to 12-phenyl-dodecanol. Spectra was selected from the TIC of subsection DL-L2 i (0-2 cm, 2013).

3.2. SEDIMENT BPA CONCENTRATION

The concentration of BPA in the surface sediments of Douglas Lake is relatively high (0.0014 – 1.336 μg/g dw), the highest reported concentration of BPA from sediment in another Michigan inland lake is 0.0134 μg/g (Liao et al., 2012). However, concentrations as high as 12 μg/L were detected in surface water samples from Santa Cruz, AZ (Kolpin et al., 2002). This large variance in concentrations is likely a result of BPA's short half-life in oxygen-rich surficial waters (1–10 days); BPA is rapidly degraded in the photic zone before it can be incorporated into sediments.

At Douglas Lake, there were three major concentration spikes of BPA, the first and largest spike occurred in 2013 (DL-L2 i, 0-2cm) and the second occurred in 1997 (1.25 μg/g dw, DL-L2 iii, 4–6 cm). Evidence for the 2013 spike is corroborated by the EPA's nationwide ECHO reports (Fig. 31). According to ECHO, 713 pounds of BPA were released from a manufacturing plant in Midland, MI and a total of 1.4 million pounds were released nationally that year. In contrast, data that could corroborate the 1997 spike were not reported by ECHO (Appendix E).

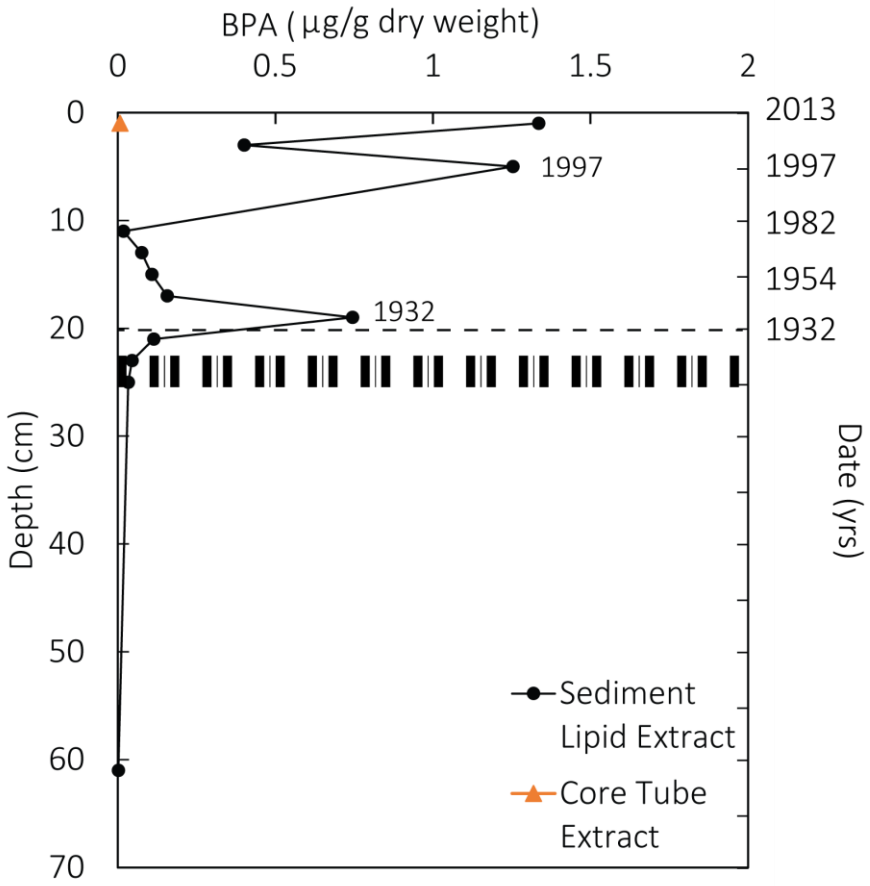

Figure 30. Historical profile of BPA in TLE (BPA concentration from core tube extract for reference; 6 ng/g). The dashed line demarcates zones before (below line) and after (above line) fires and logging at Douglas Lake. The scotch ruled line indicates the black mud (above) and brown mud (below) transition.

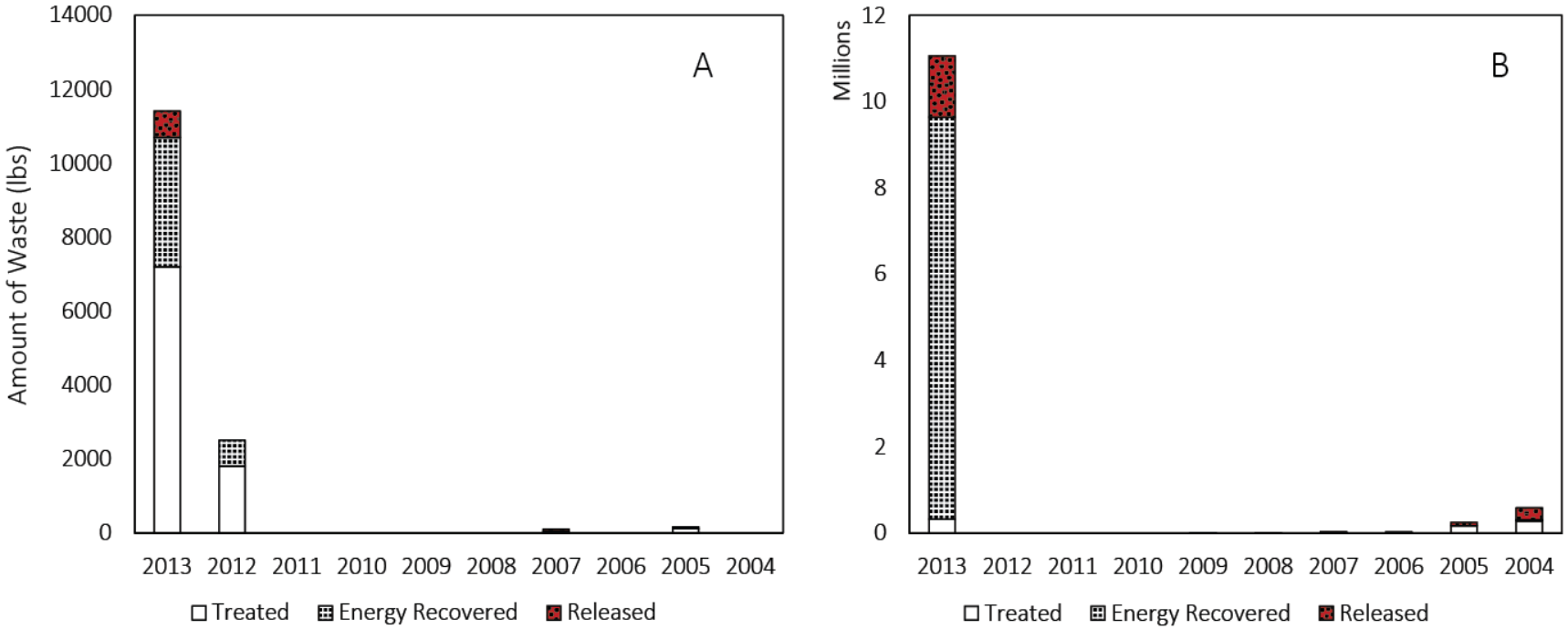

Figure 31. BPA waste generated (A) in Midland, MI and B) nationally. Both graphs symbolize the fate of BPA waste in industry. The waste has been: 1) transformed into compounds with the least practical effect on the environment (Treated); 2) converted into usable heat, electricity, or fuel through a variety of processes (Energy Recovered); or 3) released into the environment (Released).

The historical profile shows a third BPA peak at subsection DL-L2 x (16 –18 cm, 1932). Using the characteristic diffusion model (equation 11), it was found that in the ~81 year period between the peak and sediment sampling (1932–2013), previously-deposited BPA would have diffused 22.6 cm (50.56 cm prior to compaction). The third peak in the historic profile shows a characteristic diffusion peak with both upward and downward diffusion that is concomitant with rapid sedimentation (Fig. 30). This pattern consistent with a low value for the Guinasso-Schink mixing parameter, G (Guinasso & Schink, 1975). When G is small (relatively rapid sedimentation and little or no reworking), a packet of contamination will be buried before it can be reworked and its concentration distribution will be bell-shaped (Fig. 32).

Prior studies have noted that the distribution patterns of BPA might be related to TOC (Mortazavi et al., 2012; Rice et al., 2003). Total Organic Carbon (TOC) content of sediment has been shown to correlate significantly with the concentration of BPA. This is likely caused by charged attractions between organic sediment and BPA's phenolic moieties. Normalizing the BPA profile to TOC for Douglas Lake sediment may reduce the variability in the data.

There is also a potential for bioturbation which could have affected the temporal resolution and intensity of BPA signals. Cole (1953) reported on macrobenthic bioturbators sampled in the profundal zone (19.5 m deep, the maximum depth of Douglas Lake is ~24 m), including *Limnodrilus hoffmeisteri*, *Limnodrilus claparèdeianus* (species of aquatic worm), and feather midge larvae (*Tendipes plumosus*). While inhabiting laminated sediment, bioturbators tend to mottle lamina and homogenize stratigraphic signals (Martin, 1999). Given that there are well defined, seemingly non-homogenized stratigraphic markers (such as ^{210}Pb dates, ^{137}Cs activity, and *n*-alkane profiles) evident from sediment analysis, it is unlikely that BPA was affected by bioturbation.

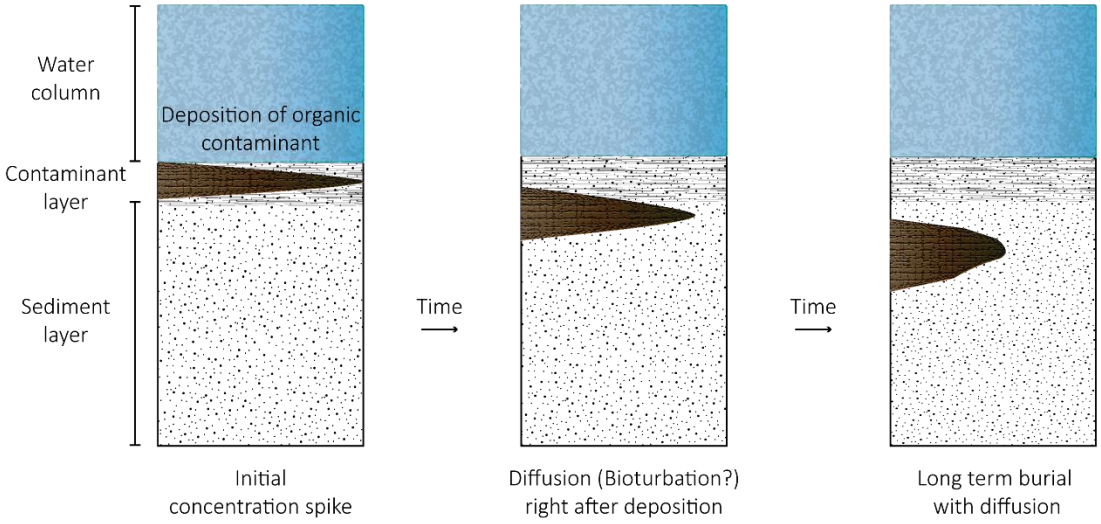

Figure 32. Concentration distribution (schematic) of contaminant in sediment undergoing box-model-type diffusion and possible bioturbation (modified from Robert Berner (1980) and Ronald Martin (1999))

If the initial concentration spike of BPA is preserved by rapid sedimentation under anoxic conditions, with little or no reworking as a result of bioturbation, then (owing to its polarity) will diffuse in a predictable pattern. This initial concentration preservation is evident from its bell curve shape (Fig. 30) and the characteristic diffusion length was calculated using equation 11.

3.3. HYSPLIT RESULTS

BPA is produced in Midland, Michigan. This is the only proximal source of BPA that may account for the anomalously high BPA concentration in Douglas Lake sediments. HYSPLIT was used to model a theoretical release of BPA from Midland, MI to Cheboygan County, MI. The results of the model showed that if 323 kg of BPA was released (in a 24 hour period, for this hypothetical scenario) about 1×10^{-8} mg/m^2 would be deposited in Douglas Lake (Fig. 33).

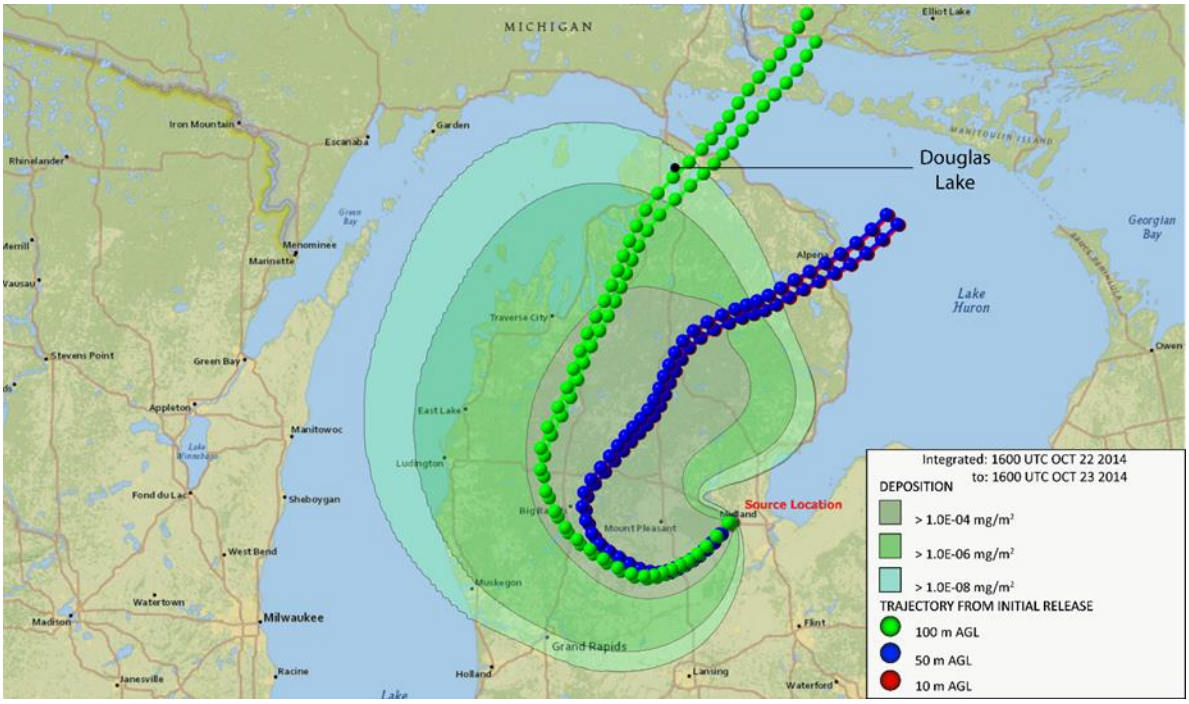

Figure 33. HYSPLIT model–generated map of BPA transport from Midland, MI towards Douglas Lake.

The variable for mass released used in the HYSPLIT model was obtained from the EPA's ECHO data for BPA released in 2013. Because the data resolution for mass release is annual, the assumption for the model was that the entire fugitive release of BPA occurred in a single day.

3.4. BPA AS A LAB CONTAMINANT

The concentration of BPA within TLE from Douglas Lake is nearly two orders of magnitude higher than values reported in other studies. There remains a distinct possibility of user–introduced contamination from the polycarbonate core tube or LDPE core tube cap that housed the sediment

core during transport to the laboratory at UIC. However, the lipid content of the core tube and core tube cap (Fig. 34) consists largely of phthalates (plasticizers), select alkanes, fatty acids and miniscule amounts of BPA (~0.0063 µg/g). Furthermore, the most abundant compounds in the core tube and cap, octadecyl 3-(3,5-di-tert-butyl-4-hydroxyphenyl) propionate (K-nox 1076, benzenepropanoic acid), and homosalate (respectively) are not detected in sediment lipid extract. Therefore, the core tube and cap are unlikely sources of the high BPA contamination.

Finally, 4-(1-methyl-1-phenylethyl)-phenol, a compound like BPA without its hydroxyl group, and 1-methyl-4-(1-methyethen-1-yl) benzene (Fig. 18, structures II and III) follow similar distribution patterns with BPA. These compounds which likely derive from pyrolysis of synthetic polymers (Moldoveanu, 2005), were not detected within the core tube or LDPE core cap.

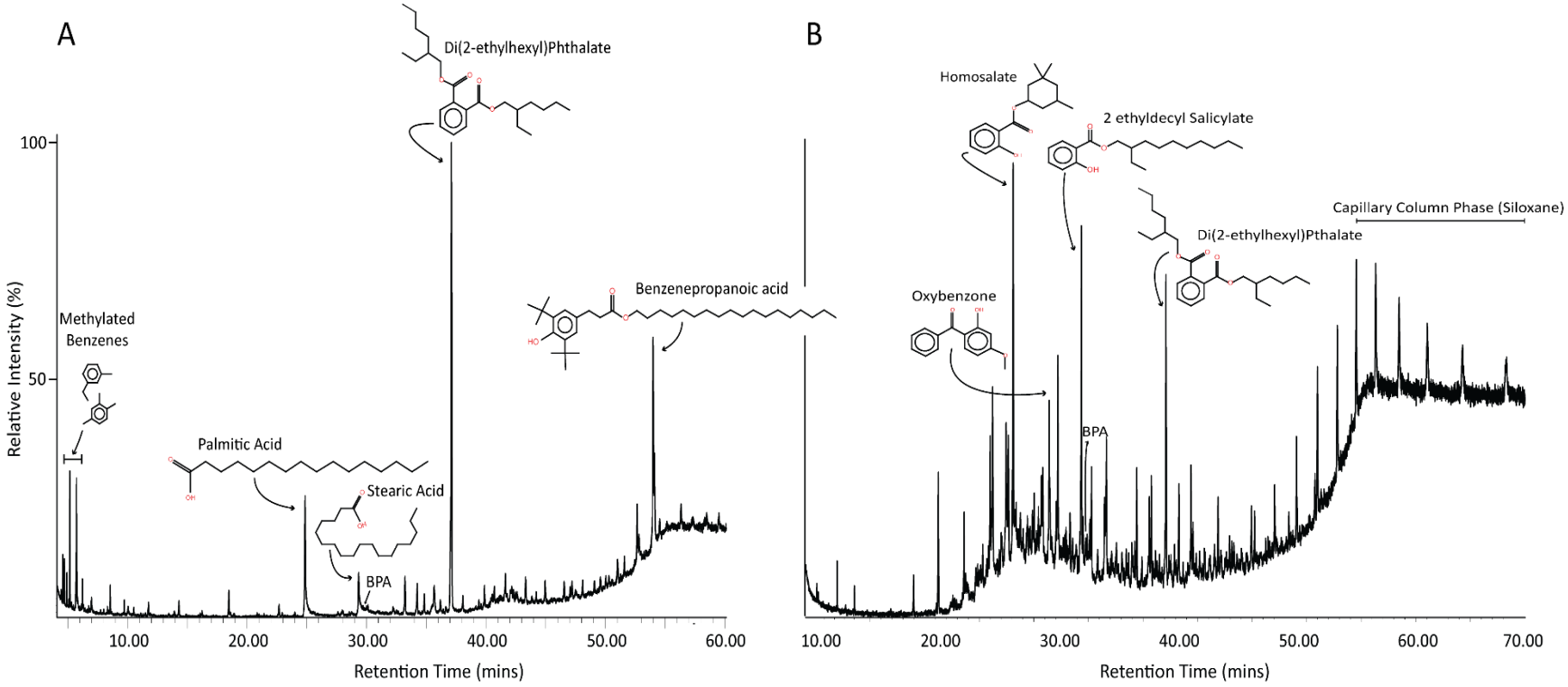

Figure 34. Total ion chromatogram of A) Low Density Polyethylene (LDPE) core tube. B) LDPE core tube cap. Several of the most abundant compounds have been identified by comparison of structures with in-house libraries.

4. CONCLUSION AND FUTURE STUDY

BPA is subject of continuing study but the classification of BPA as a compound of concern to public health remains the consensus amongst scientists. Evidence shows that BPA may be linked to endocrine–related disorders. The compound is produced and consumed worldwide, and as production continues to rise globally, concern that BPA pollution will become more serious concomitantly increases. BPA was detected in sediments from Douglas Lake with an average concentration of 111.8 ng/g dw sediment, over 180 times the North American average. Further work, including sediment coring from another depression at Douglas Lake, is needed to validate these values.

For future study, a more refined model with better constrained parameters should be employed in conjunction with data from the EPA's TRI and ECHO websites, and physically measured sediment concentrations. Other assumptions that need to be accounted for include prevailing wind conditions, the amount of degradation of BPA in the photic zone, and additional atmospheric transport from other facilities in the USA.

CHAPTER IV: SUMMARY AND CONCLUSIONS

Lacustrine accumulations of organic matter reflect both the primary source and possibly the amounts of the original matter deposited into the lake. Interpretations of the biomarkers within Douglas Lake were instrumental in reconstructing the paleolimnologic history of the lake, resolving minute changes in the total microbial biomass too sensitive for casual observation, and dramatic environmental changes previously reported in literature. Several biomarkers detected and referenced but not thoroughly discussed in this study could be useful for future biomarker research at the lake. For example, investigating the stereochemistry of steroids and hopanoids may prove useful in measuring the relative contribution of each respective class of organism to organic matter at Douglas Lake. Other biomarkers observed in minor concentrations may hold immeasurable potential for further investigations. For instance, apocarotenoids and other pigment fragments may serve two purposes: (1) they act as proxies for calculating the degradation rate of pigments in anoxic sediments. For example, there is an inverse relationship between loliolide and fucoxanthin as reported by Repeta (1989). This means that the more loliolide is detected (relative to its precursor pigment) the more fucoxanthin has degraded; (2) they represent, at least, an indirect contribution from diatoms, higher plants or other photosynthetic organisms (Das et al., 2009; El Hattab et al., 2008; Percot et al., 2009). Since useful lipidic information can be lost via photooxidative processes during settlement into lake sediment, lipids from various levels in the water column will reduce the dearth of biochemical information from Douglas Lake. Water from Douglas Lake was extracted using liquid-liquid chromatography, results were not discussed in this paper. However, the TIC and its accompanying identification table were provided (Appendix F).

Accumulated sediments also preserved the record of contamination in Douglas Lake. PAHs from forest fires were detected in quantifiable concentrations in sediment until ~1982. The other major

contaminant in the lake, BPA, was detected in surprisingly high concentrations. While BPA was quantified using proper extraction/quantification procedures, re-sampling and quantification using HPLC and standard EPA methodology would be preferential for proper validation. The HYSPLIT model used in this study was largely hypothetical but was a useful step for modelling the atmospheric transport of BPA to lakes.

APPENDIX A

TABLE VII. MASS OF PRE-EXTRACTED SEDIMENT SAMPLES.

Sample Name	Pre weighed Vial (g)	Vial with Sediment (g)	Net Weight (g)
DL-L2 i	100.83	103.78	2.95
DL-L2 ii	97.36	99.99	2.63
DL-L2 iii	98.56	100.27	1.71
DL-L2 iv	100.80	102.30	1.50
DL-L2 v	97.48	99.68	2.20
DL-L2 vi	97.37	99.77	2.40
DL-L2 vii	99.95	103.10	3.15
DL-L2 viii	98.75	102.42	3.67
DL-L2 ix	97.98	101.89	3.91
DL-L2 x	99.08	101.95	2.87
DL-L2 xi	97.33	102.38	5.05
DL-L2 xii	98.48	102.35	3.87
DL-L2 xiii	100.96	105.33	4.37
DL-L2 xiv	97.58	101.88	4.30
DL-L2 xv	98.45	102.61	4.16
DL-L2 xvi	97.12	99.47	2.35
DL-L2 xvii	100.20	104.69	4.49
DL-L2 xviii	98.71	103.34	4.63
DL-L2 xix	97.77	102.92	5.15
DL-L2 xx	97.79	102.62	4.83
DL-L2 xxi	99.86	104.67	4.81
DL-L2 xxii	97.24	102.22	4.98
DL-L2 xxiii	98.23	103.95	5.72
DL-L2 xxiv	97.47	103.64	6.17
DL-L2 xxv	98.34	104.23	5.89
DL-L2 xxvi	98.82	103.73	4.91
DL-L2 xxvii	98.46	102.72	4.26
DL-L2 xxviii	101.19	105.50	4.31
DL-L2 xxix	99.59	104.44	4.85
DL-L2 xxx	97.31	101.21	3.90
DL-L2 xxxi	97.65	101.05	3.40
DL-L2 xxxii	97.50	102.72	5.22

APPENDIX B

Table VIII. TLE MASS LOSS FOLLOWING ELEMENTAL SULFUR REMOVAL.

TLE prior to sulfur removal					TLE after sulfur removal					
Sample Name	Pre weighed Vial (g)	Vial with TLE (g)	Net Weight (g)	Net Weight (mg)	Pre weighed Vial (g)	Vial with TLE (g)	Net Weight (g)	Net Weight (mg)	Weight Change (%)	Weight Change (mg)
DL-L2 i	3.8611	3.8995	0.0384	38.4	4.0060	4.0255	0.0195	19.5	49.21875	18.9
DL-L2 ii	3.9038	3.9400	0.0362	36.2	4.0343	4.0515	0.0172	17.2	52.48619	19
DL-L2 iii	3.9064	3.9280	0.0216	21.6	4.0684	4.0795	0.0111	11.1	48.61111	10.5
DL-L2 vi	3.9258	3.9550	0.0292	29.2	4.0458	4.0556	0.0098	9.8	66.43836	19.4
DL-L2 vii	3.9655	3.9935	0.0280	28	4.0529	4.0667	0.0138	13.8	50.71429	14.2
DL-L2 viii	3.9021	3.9372	0.0351	35.1	4.0598	4.0736	0.0138	13.8	60.68376	21.3
DL-L2 ix	3.9175	3.9495	0.0320	32	4.0551	4.0705	0.0154	15.4	51.875	16.6
DL-L2 x	3.8597	3.8897	0.0300	30	4.0384	4.0490	0.0106	10.6	64.66667	19.4
DL-L2 xi	3.8894	3.9122	0.0228	22.8	4.0922	4.1064	0.0142	14.2	37.7193	8.6
DL-L2 xii	3.8869	3.9121	0.0252	25.2	4.0219	4.0327	0.0108	10.8	57.14286	14.4
DL-L2 xiii	3.8992	3.9510	0.0518	51.8	3.9605	3.9717	0.0112	11.2	78.37838	40.6
DL-L2 xiv	4.8009	4.8258	0.0249	24.9	3.9206	3.9305	0.0099	9.9	60.24096	15
DL-L2 xxix	3.8962	3.9196	0.0234	23.4	4.0367	4.0523	0.0156	15.6	33.33333	7.8
DL-L2 xxxi	4.0098	4.0245	0.0147	14.7	4.0403	4.0486	0.0083	8.3	43.53741	6.4

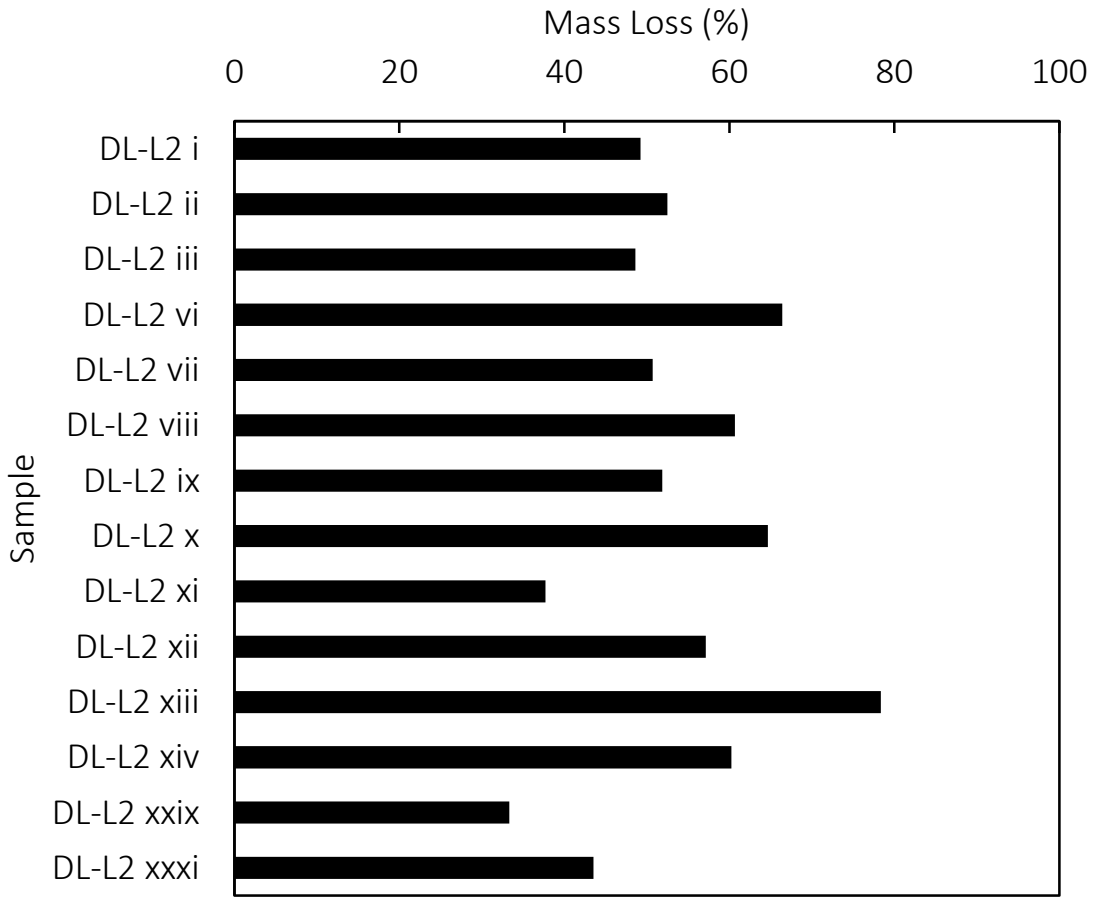

Figure 35. Percent of mass lost from TLE following removal of elemental sulfur.

APPENDIX C

Table IX. RADIONUCLIDE ACTIVITIES AND ERRORS.

Sample Name	Sample Weight (g)	Sample Height (mm)	Pb-210 Bq/Kg	Pb err Bq/Kg	Ra-226 Bq/Kg	Ra err Bq/Kg	Cs-137 Bq/Kg	Cs err Bq/Kg	Am-241 Bq/Kg	Am err Bq/Kg	Depth
DL-L2i	1.05	37	1276.19	34.7103	≤ 33.79	15.99739	80.40608	3.765991	≤ 4.47	2.12880	1
DL-L2ii	1	38	848.7436	33.1787	≤ 41.51	19.8828	107.2189	4.466066	≤ 4.95	2.33306	3
DL-L2iii	1.05	37	785.8127	32.511	52.63748	23.08335	119.8834	4.483287	≤ 4.43	2.09631	5
DL-L2iv	0.79	27	554.6914	36.3722	≤ 53.85	25.58424	126.1946	5.119852	≤ 6.32	3.00289	7
DL-L2v	1.44	38	489.6345	23.3070	≤ 34.46	16.50106	159.9377	4.167478	≤ 3.19	1.50484	9
DL-L2vi	1.34	38	415.1086	22.6885	≤ 41.72	19.60897	202.2389	4.601506	6.56294	1.53986	11
DL-L2vii	1.36	37	339.2986	20.6386	≤ 33.91	16.10613	197.1443	4.173931	8.51706	1.50814	13
DL-L2viii	1.06	38	221.487	14.3312	36.52146	12.01417	14.46232	1.483388	≤ 1.91	0.90626	15
DL-L2ix	1.07	39	163.8256	15.1134	≤ 25.48	12.13622	2.84658	0.955839	≤ 1.90	0.89970	17
DL-L2x	1.52	40	120.745	15.6379	≤ 28.23	13.51125	≤ 2.16	1.03316	≤ 2.14	1.02017	19

APPENDIX C (CONTINUED)

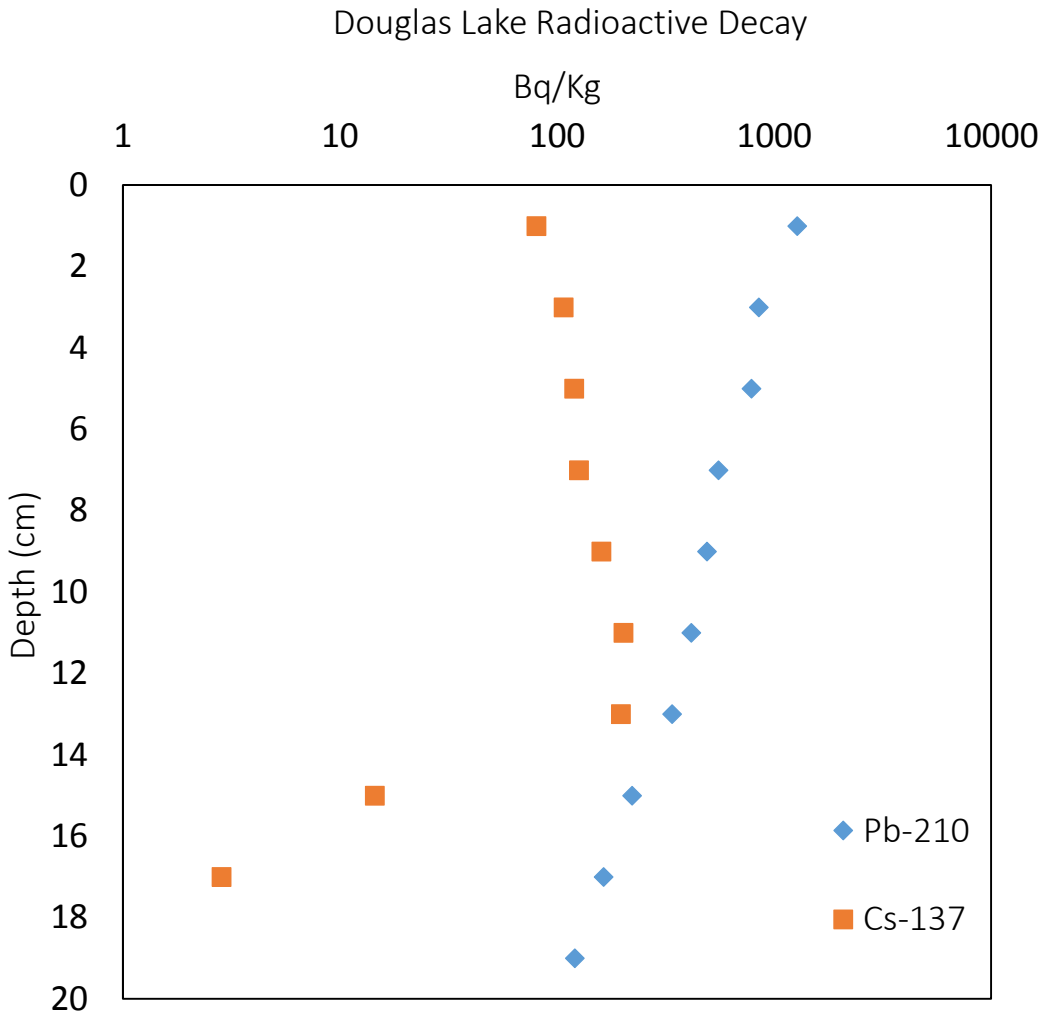

Figure 36. 210Pb and 137Cs radionuclide activity profile (graph in logarithmic scale).

APPENDIX D

TABLE X. CONCENTRATIONS OF MEASURABLE PAHS IN DOUGLAS LAKE. N – NAPHTHALENE, P – PHENANTHRENE, A – ANTHRACENE, FA – FLUORANTHENE, PY – PYRENE, B[GHI]FA – BENZO[G,H,I]FLUORANTHENE, B[A]A – BENZO[A]ANTHRACENE, C + TPN – CHRYSENE/TRIPHENYLENE, B[B]FA – BENZO[B]FLUORANTHENE, B[E]PY – BENZO[E]PYRENE, B[A]PY – BENZO[A]PYRENE, PE –PERYLENE, I[CD]PY – INDENO[C,D]PYRENE, B[GHI]PE – BENZO[G,H,I]PERYLENE, DB[AL]PY – DIBENZO(A,L)PYRENE, CO – CORONENE.

Sample	Concentration (µg/g dry sediment weight) by compound																
DL-L2	N	P	A	Fa	Py	B[ghi]Fa	B[a]A	C + TPn	B[b]Fa	B[e]Py	B[a]Py	Pe	I[cd]Py	B[ghi]Pe	Db[al]Py	Co	Total
vi	0.0030	0.0043	0.0011	0.0078	0.0047	0.0008	0.0014	0.0038	0.0090	0.0030	0.0018	0.0008	0.0042	0.0069	0.0001	0.0028	0.0554
vii	0.0035	0.0407	0.0187	0.1014	0.0634	0.0122	0.0124	0.0500	0.0823	0.0306	0.0212	0.0084	0.0424	0.0653	0.0077	0.0224	0.5824
viii	0.0053	0.0087	0.0021	0.0179	0.0130	0.0033	0.0027	0.0074	0.0167	0.0056	0.0037	0.0016	0.0075	0.0094	0.0013	0.0039	0.1102
ix	0.0019	0.0070	0.0029	0.0208	0.0107	0.0036	0.0041	0.0114	0.0326	0.0093	0.0079	0.0040	0.0166	0.0206	0.0057	0.0103	0.1694
x	0.0022	0.0128	0.0030	0.0267	0.0167	0.0057	0.0031	0.0123	0.0287	0.0080	0.0062	0.0035	0.0169	0.0168	0.0047	0.0096	0.1769
xi	0.0011	0.0087	0.0020	0.0211	0.0113	0.0045	0.0035	0.0146	0.0272	0.0084	0.0053	0.0035	0.0158	0.0206	0.0044	0.0079	0.1597
xii	0.0010	0.0028	0.0016	0.0144	0.0050	0.0034	0.0038	0.0104	0.0222	0.0066	0.0041	0.0026	0.0134	0.0130	0.0035	0.0070	0.1147
xiii	0.0014	0.0056	0.0020	0.0137	0.0114	0.0038	0.0021	0.0048	0.0159	0.0046	0.0028	0.0020	0.0083	0.0110	0.0019	0.0049	0.0961
xxxi	0.0037	0.0000	0.0000	0.0003	0.0001	0.0000	0.0000	0.0001	0.0000	0.0000	0.0000	0.0023	0.0000	0.0000	0.0000	0.0000	0.0065
	0.0231	0.0905	0.0334	0.2241	0.1363	0.0373	0.0330	0.1147	0.2345	0.0761	0.0530	0.0287	0.1251	0.1635	0.0294	0.0687	1.4713

APPENDIX E

TABLE XI. EPA ECHO BPA WASTE MANAGEMENT DATA.

Year	TRI Reporters	Waste management			
		Treated	Energy Recovered	Released	Total
2013	Regional: 1	7200	3500	713	11413
	National: 3115	325378	9317995	1421098	11064471
2012	Regional: 1	1813	700	0	2513
	National: N.D.	N.D.	N.D.	N.D.	N.D.
2011	Regional: N.D.	N.D.	N.D.	N.D.	N.D.
	National: N.D.	N.D.	N.D.	N.D.	N.D.
2010	Regional: N.D.	N.D.	N.D.	N.D.	N.D.
	National: N.D.	N.D.	N.D.	N.D.	N.D.
2009	Regional: N.D.	N.D.	N.D.	N.D.	N.D.
	National: 375	592.78	8135	1746.58	10474.36
2008	Regional: N.D.	N.D.	N.D.	N.D.	N.D.
	National: 379	1764.29	3100	4396.04	9260.33
2007	Regional: 1	56	0	54	110
	National: 388	19066	4382	9481.1	32929.1
2006	Regional: N.D.	N.D.	N.D.	N.D.	N.D.
	National: 364	2231.7	21197	6822.3	30251
2005	Regional: 1	120	0	52	172
	National: 362	174215	0	79315.45	253530.45
2004	Regional: N.D.	N.D.	N.D.	N.D.	N.D.
	National: 358	289491	23168	277643	590302

APPENDIX F

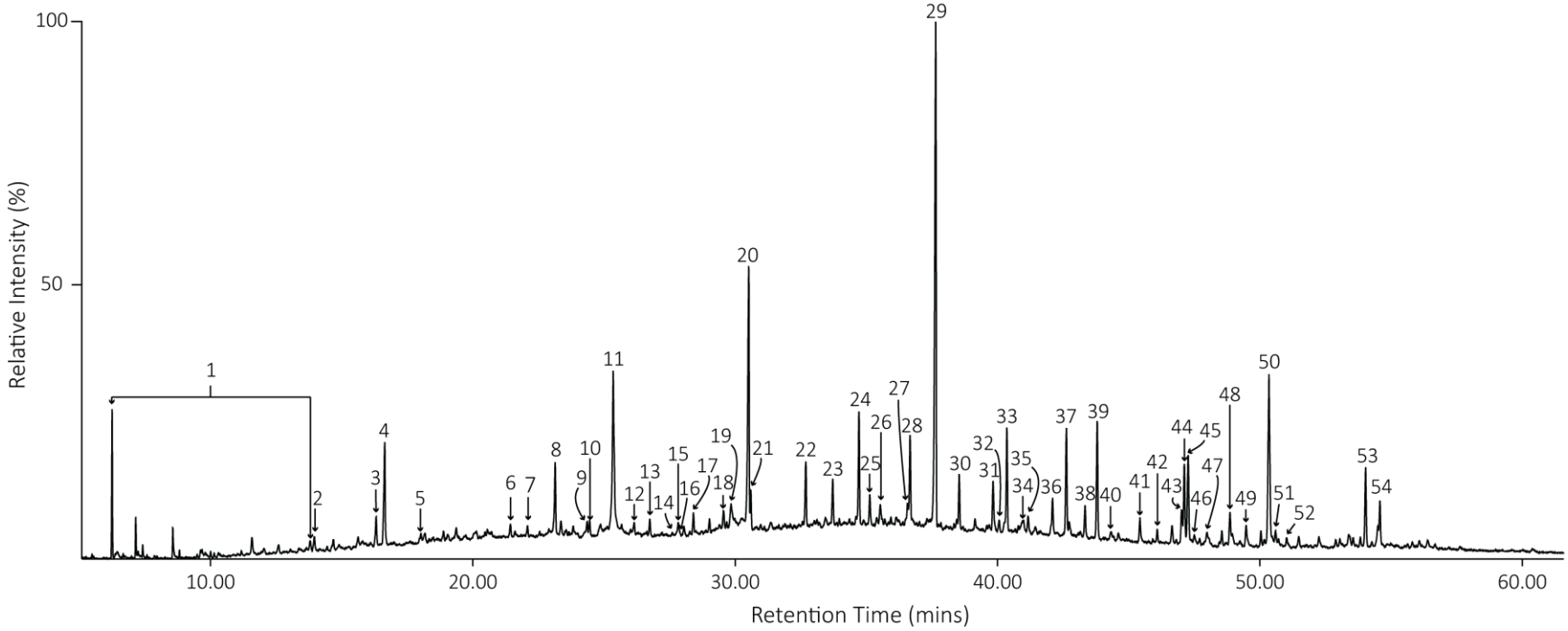

Figure 37. TIC of the total lipid extract of water samples from Douglas Lake.

APPENDIX F (CONTINUED)

TABLE XII. IDENTIFICATION OF NUMBERED PEAKS IN FIGURE 37, SHOWING TIC OF WATER EXTRACTS FROM DOUGLAS LAKE.

Peak	Compound	Peak	Compound	Peak	Compound
1	Oxidized cyclohexane compounds	26	OP3EO	51	23,24-Bisnorchola-5,17(20)-dien-3β-ol
2	2,6-Dimethyl benzothiazole	27	2-(4-methylbenzenesulfonate) - related	52	Hexadecanoic acid hexadecyl ester
3	N,N-Diethyl toluamide	28	Pentacosane	53	Papyriferic acid - related
4	Ethyl phthalate	29	Di-(2-eethylhexyl)phthalate	54	Unknown plasticizer + hopanoid
5	Dihydromethyljasmonate	30	Hexacosane		
6	(1,1' Biphenyl)-2,5-diol	31	Monounsaturated alcohol 1		
7	Isopropyl myristate	32	Phthalate		
8	Isobutyl phthalate	33	Heptacosane		
9	7,9-di-tert-butyl-1-oxaspiro(4.5)deca-6,9-diene-2,8-dione	34	2-[2-[2-[4-(2,4,4-trimethylpentan-2-yl)phenoxy]ethoxy...ethanol		
10	Methyl palmitate	35	Phthalate		
11	Butyl phthalate	36	Octacosane		
12	Eicosane	37	Squalene		
13	Hexadecanoic acid	38	Monounsaturated alcohol 2		
14	Fluoranthene	39	Nonacosane		
15	Sclareolide-like	40	Phthalate		
16	Benzonitrile ? (MW-303)	41	Triacontane		
17	Heneicosane	42	Monounsaturated alcohol 3		
18	Octylphenol diethoxylate (OP2EO)	43	Hentriacontane		
19	Octadecanoic acid	44	Nonacosan-15-ol		
20	Citric acid, tributyl ester	45	Cholest-5-en-3β-ol		
21	Docosane	46	Phthalate		
22	Tricosane	47	Ergosta-5,24-dien-3β-ol		
23	Butyl benzyl phthalate (BBP)	48	Stigmasta-5,24-dien-3β-ol (Fucosterol)		
24	Tetracosane	49	Stigmasta-5,22-dien-3β-ol		
25	Tributoxyethyl phosphate	50	Stigmast-5-en-3β-ol		

VITA

NAME

Nnamdi Lionel Mojekwu

EDUCATION

ArcGIS Certificate, UIC	2015
B.Sc., Earth and Environmental Sciences, UIC	2008 – 2012

HONORS

LAS Dean's List, UIC	August 2011
LAS Dean's List, UIC	August 2012
Outstanding Teaching Assistant Award, UIC	May 2014
Outstanding Teaching Assistant Award, NAGT	June 2014

TEACHING EXPERIENCE

Teaching Assistant	2013 – 2015

EXPERIENCE

Research Assistant, UIC	11/2010 – 08/2011
Researcher, UIC	01/2012 – 05/2015

EQUIPMENT AND LABORATORY SKILLS

Basic lab skills (chemical preparations, basic instrumentation etc.), gas chromatography, mass spectrometry, column chromatography, Soxhlet extraction, centrifuge (standard, high speed), rotatory evaporator, preparation and cleaning of lab apparatus and glassware, marine sediment sampling (with percussion corer), GC-MS Data Analysis Software (HP Chemstation, AMDIS, OpenChrom), MS Office Suite, Adobe Creative Suite, ArcGIS, Google Earth Pro, HYSPLIT Atmospheric Modelling, Chemsketch.

MEMBERSHIPS

Geological Society of America

REFERENCES

Al-Qudah, M. a. (2013). Chemical Composition of Essential oil from Jordanian Lupinus varius L. *Arabian Journal of Chemistry*, *6*(2), 225–227. doi:10.1016/j.arabjc.2011.01.012

Andresen, N. A. (1976). *Recent Diatoms from Douglas Lake, Cheboygan County, Michigan*. University of Michigan, Ann Arbor.

Appleby, P. G. (2008). Three Decades of Dating Recent Sediments by Fallout Radionuclides: A Review. *The Holocene*, *18*(1), 83–93. doi:10.1177/0959683607085598

Appleby, P. G., & Oldfield, F. (1983). The Assessment of 210Pb Data from Sites with Varying Sediment Accumulation Rates. *Hydrobiologia*, *103*(1), 29–35.

Bakhtiari, A. R., Zakaria, M. P., Yaziz, M. I., Lajis, M. N. H., Bi, X., & Rahim, M. C. A. (2009). Vertical Distribution and Source Identification of Polycyclic Aromatic Hydrocarbons in Anoxic Sediment Cores of Chini Lake, Malaysia: Perylene as Indicator of Land Plant-Derived Hydrocarbons. *Applied Geochemistry*, *24*(9), 1777–1787. doi:10.1016/j.apgeochem.2009.05.008

Barreca, S., Bastone, S., Caponetti, E., Martino, D. F. C., & Orecchio, S. (2014). Determination of Selected Polyaromatic Hydrocarbons by Gas Chromatography – Mass Spectrometry for the Analysis of Wood to Establish the Cause of Sinking of an Old Vessel (Scauri Wreck) by Fire. *Microchemical Journal*, *117*, 116–121.

Bazin, M., & Saunder, G. W. (1971). The Hypolimnetic Oxygen deficit as an index of Eutrophication in Douglas Lake, Michigan. *Michigan Academician*, *3*(4), 91–106.

Belt, S., Allard, G., Masse, G., Robert, J.-M., & Rowland, S. (2000). Highly Branched Isoprenoids (HBIs): Identification of the most common and abundant Sedimentary Isomers. *Geochimica et Cosmochimica Acta*, *64*(22), 3839–3851.

Berner, R. A. (1980). *Early Diagenesis: A Theoretical Approach*. *Princeton Series in Geochemistry*. Retrieved from http://books.google.com/books?id=weRFglCVBkUC&pgis=1

Blomqvist, P., McNamee, M. S., Andersson, P., & Lönnermark, A. (2011). Polycyclic Aromatic Hydrocarbons (PAHs) Quantified in Large-Scale Fire Experiments. *Fire Technology*, *48*(2), 513–528. doi:10.1007/s10694-011-0242-9

Brassell, S. C., Lewis, C., de Leeuw, J. W., & Sinninghe Damsté, J. S. (1986). Isoprenoid Thiophenes: Novel Products of Sediment Diagenesis. *Nature*, *320*(13), 160–162. Retrieved from papers://d389027f-1c90-43ee-8f36-77ce4678000f/Paper/p254

Bray, E. E., & Evans, E. D. (1961). Distribution of n-Paraffins as a clue to Recognition of Source Beds. *Geochimica et Cosmochimica Acta*, *22*(1), 2–15. doi:10.1016/0016-7037(61)90069-2

Bromilow, M., Diem, T., Fellbam, S., Fortino, S., Parsons, C., Stamplis, Z., & Steffler, M. (2012). *Aquatic Vegetation Survey 2012 for Douglas Lake*.

Brophy, J. J., Goldsack, R. J., Wu, M. Z., Fookes, C. J. R., & Forster, P. I. (2000). The Steam Volatile Oil of Wollemia nobilis and its Comparison with other Members of the Araucariaceae (Agathis and Araucaria). *Biochemical Systematics and Ecology*, *28*(6), 563–578. doi:10.1016/S0305-1978(99)00090-3

Bush, R. T., & McInerney, F. A. (2013). Leaf Wax n-Alkane Distributions in and across Modern Plants: Implications for Paleoecology and Chemotaxonomy. *Geochimica et Cosmochimica Acta*, *117*, 161–179. doi:10.1016/j.gca.2013.04.016

Castañeda, I. S., & Schouten, S. (2011). A review of Molecular Organic Proxies for examining Modern and Ancient Lacustrine Environments. *Quaternary Science Reviews*, *30*(21-22), 2851–2891. doi:10.1016/j.quascirev.2011.07.009

Castañeda, I. S., Werne, J. P., & Johnson, T. C. (2009). Influence of Climate Change on Algal Community Structure and Primary Productivity of Lake Malawi (East Africa) from the Last Glacial Maximum to Present. *Limnology and Oceanography*, *54*(6), 2431–2447. doi:10.4319/lo.2009.54.6_part_2.2431

Coates, R. C., Podell, S., Korobeynikov, A., Lapidus, A., Pevzner, P., Sherman, D. H., … Gerwick, W. H. (2014). Characterization of Cyanobacterial Hydrocarbon Composition and Distribution of Biosynthetic Pathways. *PLoS ONE*, *9*(1), e851. doi:10.1371/journal.pone.0085140

Cole, G. (1953). Notes on the Vertical Distribution of Organisms in the Profundal Sediments of Douglas Lake, Michigan. *The American Midland Naturalist*, *49*(1), 252–256.

Cranwell, P. (1973). Branched-Chain and Cyclopropanoid Acids in a Recent Sediment. *Chemical Geology*, *11*, 307–313.

Cranwell, P. A., Eglinton, G., & Robinson, N. (1987). Lipids of Aquatic Organisms as Potential Contributors to Lacustrine Sediments—II. *Organic Geochemistry*, *11*(6), 513–527. doi:10.1016/0146-6380(87)90007-6

Cwalinski, T. A. (2004). Status of the Fishery Resource Report. *Michigan Department of Natural Resources*.

Das, S. K., Routh, J., & Roychoudhury, A. N. (2009). Biomarker Evidence of Macrophyte and Plankton Community Changes in Zeekoevlei, a Shallow Lake in South Africa. *Journal of Paleolimnology*, *41*(3), 507–521. doi:10.1007/s10933-008-9241-3

De Mesmay, R., Metzger, P., Grossi, V., & Derenne, S. (2008). Mono- and Dicyclic Unsaturated Triterpenoid Hydrocarbons in Sediments from Lake Masoko (Tanzania) widely extend the Botryococcene Family. *Organic Geochemistry*, *39*(7), 879–893. doi:10.1016/j.orggeochem.2008.01.024

Dekker, M. H., Piersma, T., & Sinninghe Damsté, J. S. (2000). Molecular Analysis of Intact Preen Waxes of Calidris canutus (Aves: Scolopacidae) by Gas Chromatography/Mass Spectrometry. *Lipids*, *35*(5), 533–541. doi:10.1007/s11745-000-553-7

Didyk, B. M., Simoneit, B. R. T., Brassell, S. C., & Eglinton, G. (1978). Organic Geochemical Indicators of Palaeoenvironmental conditions of Sedimentation. *Nature*, *272*, 217–221.

Drooge, B. L. Van. (2004). *Long-Range Atmospheric Transport and Fate of Persistent Organic Pollutants in Remote Mountain Areas*.

Duan, Y. (2000). Organic Geochemistry of Recent Marine Sediments from the Nansha Sea, China. *Organic Geochemistry*, *31*, 159–157.

Eggleton, F. (1931). A Limnological Study of the Profundal Bottom Fauna of certain Fresh-Water Lakes. *Ecological Monographs*, *1*(3), 231–331.

El Hattab, M., Culioli, G., Valls, R., Richou, M., & Piovetti, L. (2008). Apo-fucoxanthinoids and Loliolide from the Brown Alga Cladostephus spongiosus f. verticillatus (Heterokonta, Sphacelariales). *Biochemical Systematics and Ecology*, *36*(5-6), 447–451. doi:10.1016/j.bse.2007.08.016

El-Shahawi, M. S., Hamza, A., Bashammakh, a S., & Al-Saggaf, W. T. (2010). An Overview on the Accumulation, Distribution, Transformations, Toxicity and Analytical Methods for the Monitoring of Persistent Organic Pollutants. *Talanta*, *80*(5), 1587–1597. doi:10.1016/j.talanta.2009.09.055

Erler, C., & Novak, J. (2010). Bisphenol A Exposure: Human Risk and Health Policy. *Journal of Pediatric Nursing*, *25*(5), 400–407. doi:10.1016/j.pedn.2009.05.006

Ficken, K. J., Li, B., Swain, D. L., & Eglinton, G. (2000). An n-Alkane Proxy for the Sedimentary Input of Submerged /floating Freshwater Aquatic Macrophytes. *Organic Geochemistry*, *31*, 745–749.

Fiege, H., Voges, H.-W., Hamamoto, T., Umemura, S., Iwata, T., Miki, H., … Paulu, W. (2000). Phenol Derivatives. In *Ullmann's Encyclopedia of Industrial Chemistry.* Wiley-VCH. doi:10.1002/14356007.a19_313

Francis, D. (1997). Bryozoan Statoblasts in the Recent Sediments of Douglas Lake, Michigan. *Journal of Paleolimnology*, *17*, 255–261.

Francis, D. (2001). A Record of Hypolimnetic Oxygen Conditions in a Temperate Lake from Chemical and Chironomid Remains. *Journal of Paleolimnology*, *25*, 351–365.

Fu, P., & Kawamura, K. (2010). Ubiquity of bisphenol A in the atmosphere. *Environmental Pollution*, *158*(10), 3138–3143. doi:10.1016/j.envpol.2010.06.040

Fukushima, K., Yasukawa, M., Muto, N., Uemura, H., & Ishiwatari, R. (1992). Formation of C20 isoprenoid thiophenes in modern sediments. *Organic Geochemistry*, *18*(1), 83–91. doi:10.1016/0146-6380(92)90146-O

Fuller, D. R., Stemberger, R., & Gannon, J. E. (1977). Limnetic Rotifers as Indicators of Trophic Change. *J. Elisha Mitchell Sci. Soc.*, *93*, 104–113.

Gao, M., Simoneit, B. R. T., Gantar, M., & Jaffé, R. (2007). Occurrence and Distribution of Novel Botryococcene Hydrocarbons in Freshwater Wetlands of the Florida Everglades. *Chemosphere*, *70*(2), 224–236. doi:10.1016/j.chemosphere.2007.06.056

Gelpi, E., Oró, J., Schneider, H. J., & Bennett, E. O. (1968). Olefins of high molecular weight in two microscopic algae. *Science (New York, N.Y.)*, *161*(842), 700–702. doi:10.1126/science.161.3842.700

Gelpi, E., Schneider, H., Mann, J., & Oró, J. (1970). Hydrocarbons of Geochemical Significance in Microscopic Algae. *Phytochemistry*, *9*(3), 603–612. doi:10.1016/S0031-9422(00)85701-5

George, S. C., Volk, H., Dutkiewicz, A., Ridley, J., & Buick, R. (2008). Preservation of hydrocarbons and biomarkers in oil trapped inside fluid inclusions for >2 billion years. *Geochimica et Cosmochimica Acta*, *72*(3), 844–870. doi:10.1016/j.gca.2007.11.021

Gold, A., Gannon, J., & Paddock, M. W. (1976). *Douglas Lake Profile. A report for the National Science Foundation*.

Grice, K., Gibbison, R., Atkinson, J. E., Schwark, L., Eckardt, C. B., & Maxwell, J. R. (1996). Maleimides (1H-pyrrole-2,5-diones) as Molecular Indicators of Anoxygenic Photosynthesis in Ancient Water Columns. *Geochimica et Cosmochimica Acta*, *60*(20), 3913–3924. doi:10.1016/0016-7037(96)00199-8

Grice, K., Schouten, S., Nissenbaum, A., Charrach, J., & Sinninghe Damsté, J. S. (1998). Isotopically Heavy Carbon in the C21 to C25 regular Isoprenoids in Halite-rich Deposits from the Sdom Formation, Dead Sea Basin, Israel. *Organic Geochemistry*, *28*(6), 349–359. doi:10.1016/S0146-6380(98)00006-0

Grossi, V., Beker, B., Geenevasen, J. a J., Schouten, S., Raphel, D., Fontaine, M. F., & Sinninghe Damsté, J. S. (2004). C 25 Highly Branched Isoprenoid Alkenes from the Marine Benthic Diatom Pleurosigma strigosum. *Phytochemistry*, *65*(22), 3049–3055. doi:10.1016/j.phytochem.2004.09.002

Guinasso, N. L., & Schink, D. R. (1975). Quantitative Estimates of Biological Mixing Rates in Abyssal Sediments. *Journal of Geophysical Research*. doi:10.1029/JC080i021p03032

Hautevelle, Y., Michels, R., Lannuzel, F., Malartre, F., & Trouiller, A. (2006). Confined Pyrolysis of Extant Land Plants: A Contribution to Palaeochemotaxonomy. *Organic Geochemistry*, *37*(11), 1546–1561. doi:10.1016/j.orggeochem.2006.06.016

Haynes, R. R., & Barre Hellquist, C. B. (1978). The Distribution of the Aquatic Vascular Flora of Douglas Lake, Cheboygan County, Michigan. *Michigan Botanist*, *17*(4), 183–191.

Heemken, O. P., Reincke, H., Stachel, B., & Theobald, N. (2001). The Occurrence of Xenoestrogens in the Elbe River and the North Sea. *Chemosphere*, *45*(3), 245–259. doi:10.1016/S0045-6535(00)00570-1

Heusser, G., Laubenstein, M., & Neder, H. (2006). Low-level Germanium Gamma-Ray Spectrometry at the Bq/kg Level and Future Developments towards Higher Sensitivity. *Radioactivity in the Environment*, *8*, 495–510.

Hogarh, J. N., Seike, N., Kobara, Y., & Masunaga, S. (2012). Atmospheric polychlorinated naphthalenes in Ghana. *Environmental Science & Technology*, *46*(5), 2600–6. doi:10.1021/es2035762

Holtvoeth, J., Vogel, H., Wagner, B., & Wolff, G. a. (2010). Lipid biomarkers in Holocene and glacial sediments from ancient Lake Ohrid (Macedonia, Albania). *Biogeosciences*, *7*(11), 3473–3489. doi:10.5194/bg-7-3473-2010

Huang, Y. Q., Wong, C. K. C., Zheng, J. S., Bouwman, H., Barra, R., Wahlström, B., … Wong, M. H. (2012). Bisphenol A (BPA) in China: A Review of Sources, Environmental Levels, and Potential Human Health Impacts. *Environment International*, *42*(1), 91–99. doi:10.1016/j.envint.2011.04.010

Huang, Y., Street-Perrott, F. A., Perrott, R. A., Metzger, P., & Eglinton, G. (1999). Glacial-Interglacial Environmental Changes inferred from Molecular and Compound-Specific δ13C Analyses of Sediments from Sacred Lake, Mt. Kenya. *Geochimica et Cosmochimica Acta*, *63*(9), 1383–1404. doi:10.1016/S0016-7037(99)00074-5

Hughes, W. B., Holba, A. G., & Dzou, L. I. P. (1995). The ratios of dibenzothiophene to phenanthrene and pristane to phytane as indicators of depositional environment and lithology of petroleum source rocks. *Geochimica et Cosmochimica Acta*. doi:10.1016/0016-7037(95)00225-O

Huszar, V. L. D. M., & Caraco, N. F. (1998). The Relationship Between Phytoplankton Composition and Physical-Chemical Variables: A Comparison of Taxonomic and Morphological-Functional Descriptors in six Temperate Lakes. *Freshwater Biology*, *40*(4), 679–696. doi:10.1046/j.1365-2427.1998.00369.x

Ide, H., & Toki, S. (1970). Metabolism of β-Ionone: Isolation, Characterization and Identification of the Metabolites in the Urine of Rabbits. *Journal of Biochemistry*, *119*, 281–287.

Jaffé, R., Mead, R., Hernandez, M. E., Peralba, M. C., & DiGuida, O. a. (2001). Origin and Transport of Sedimentary Organic Matter in Two Subtropical Estuaries: A Comparative, Biomarker-based Study. *Organic Geochemistry*, *32*(4), 507–526. doi:10.1016/S0146-6380(00)00192-3

Jarman, W. M., & Ballschmiter, K. (2012). From Coal to DDT: The History of the Development of the Pesticide DDT from Synthetic Dyes till Silent Spring. *Endeavour*, *36*(4), 131–42. doi:10.1016/j.endeavour.2012.10.003

Jeter, H. W. (2000). Determining the Ages of Recent Sediments Using Measurements of Trace Radioactivity. *Terra et Aqua*, *78*, 21–28.

Kenig, F., & Huc, A. Y. (1990). Incorporation of Sulfur into Recent Organic Matter in a Carbonate Environment (Abu Dhabi, United Arab Emirates). In *Geochemistry of Sulfur in Fossil Fuels* (Vol. 429, p. Washington, DC (US)).

Kenig, F., Huc, A. Y., Purser, B. H., & Oudin, J.-L. (1990). Sedimentation, distribution and diagenesis of organic matter in a recent carbonate environment, Abu Dhabi, U.A.E. *Organic Geochemistry*, *16*(4-6), 735–747. doi:10.1016/0146-6380(90)90113-E

Kenig, F., & Sinninghe Damsté, J. S. (1995). Molecular Indicators for Palaeoenvironmental change in a Messinian Evaporitic Sequence (Vena del Gesso, Italy). II: High-resolution Variations in Abundances and 13C contents of free and Sulphur-bound Carbon Skeletons in a Single Marl Bed. *Science*, *23*(6), 485–526.

Kilburn, P. D. (1957). *Historical Development and Structure of the Aspen, Jack Pine and Oak Vegetation Types on Sandy Soils in Northern Lower Michigan*.

Killops, S. D., & Massoud, M. S. (1992). Polycyclic Aromatic Hydrocarbons of Pyrolytic Origin in Ancient Sediments: Evidence for Jurassic Vegetation Fires. *Organic Geochemistry*, *18*(1), 1–7. doi:10.1016/0146-6380(92)90137-M

Klečka, G. M., Staples, C. a., Clark, K. E., van der Hoeven, N., Thomas, D. E., & Hentges, S. G. (2009). Exposure Analysis of Bisphenol A in Surface Water Systems in North America and Europe. *Environmental Science & Technology*, *43*(16), 6145–6150. doi:10.1021/es900598e

Kolpin, D. W., Kolpin, D. W., Furlong, E. T., Furlong, E. T., Meyer, M. T., & Meyer, M. T. (2002). Pharmaceuticals, Hormones, and other Organic Wastewater Contaminants in U.S. Streams. *Environmental Science & Technology*, *36*(6), 1202–1211. doi:10.1021/es011055j

Köster, J., Volkman, J. K., Rullkötter, J., Scholz-Böttcher, B. M., Rethmeier, J., & Fischer, U. (1999). Mono-, Di- and Trimethyl-Branched Alkanes in Cultures of the Filamentous Cyanobacterium Calothrix scopulorum. *Organic Geochemistry*, *30*(11), 1367–1379. doi:10.1016/S0146-6380(99)00110-2

Laflamme, R. E., & Hites, R. a. (1979). Tetra- and pentacyclic, naturally-occurring, aromatic hydrocarbons in recent sediments. *Geochimica et Cosmochimica Acta*, *43*(10), 1687–1691. doi:10.1016/0016-7037(79)90188-1

Liao, C., Liu, F., Moon, H. B., Yamashita, N., Yun, S., & Kannan, K. (2012). Bisphenol Analogues in Sediments from Industrialized Areas in the United States, Japan, and Korea: Spatial and

Temporal Distributions. *Environmental Science and Technology*, *46*(21), 11558–11565. doi:10.1021/es303191g

Lima, A. L. C., Eglinton, T. I., & Reddy, C. M. (2003). High-resolution record of pyrogenic polycyclic aromatic hydrocarbon deposition during the 20th century. *Environmental Science and Technology*, *37*(1), 53–61. doi:10.1021/es025895p

Lind, O. T. (1987). Spatial and temporal variation in hypolimnetic oxygen deficits of a multidepression lake. *Limnology and Oceanography*, *32*(3), 740–744. doi:10.4319/lo.1987.32.3.0740

Livsey, A., Douglas, A. G., & Connan, J. (1984). Diterpenoid Hydrocarbons in Sediments from an Offshore (Labrador) Well. *Organic Geochemistry*, *6*, 73–81. doi:10.1016/0146-6380(84)90028-7

Lu, Y., & Meyers, P. A. (2009). Organic Geochemistry Sediment Lipid Biomarkers as Recorders of the Contamination and Cultural Eutrophication of Lake Erie, 1909 – 2003. *Organic Geochemistry*, *40*(8), 912–921. doi:10.1016/j.orggeochem.2009.04.012

Magliano, D. J., & Lyons, J. G. (2013). Bisphenol A and Diabetes, Insulin Resistance, Cardiovascular Disease and Obesity: Controversy in a (Plastic) cup? *The Journal of Clinical Endocrinology and Metabolism*, *98*(2), 502–504. doi:10.1210/jc.2012-3058

Martin, R. E. (1999). Taphonomy: A Process Approach. In *Cambridge University Press* (pp. 161–182).

Marzi, R., Torkelson, B. E., & Olson, R. K. (1993). A Revised Carbon Preference Index. *Organic Geochemistry*, *20*(8), 1303–1306. doi:10.1016/0146-6380(93)90016-5

Matsunaga, S., & Morita, R. (1983). Hopenol-B, A Triterpene alcohol from Euphorbia supina. *Phytochemistry*, *22*(1885), 605–606.

Meredith, W., Snape, C. E., Carr, A. D., Nytoft, H. P., & Love, G. D. (2008). The Occurrence of Unusual Hopenes in Hydropyrolysates generated from Severely Biodegraded oil Seep Asphaltenes. *Organic Geochemistry*, *39*(8), 1243–1248. doi:10.1016/j.orggeochem.2008.01.022

Metzger, P., Casadevall, E., & Coute, A. (1988). Botryococcene Distribution in Strains of Green Alga Botryococcus braunii. *Phytochemistry*, *27*(5), 1383–1388.

Metzger, P., Casadevall, E., Pouet, M. J., & Pouet, Y. (1985). Structures of Some Botryococcenes: From the B-Race of the Green Alga Botryococcus Braunii. *Phytochemistry*, *24*(12), 2995–3002.

Meyers, P. A. (2003). Applications of Organic Geochemistry to Paleolimnological Reconstructions : A Summary of Examples from the Laurentian Great Lakes. *Organic Geochemistry*, *34*, 261–289.

Meyers, P. A., & Ishiwatari, R. (1993). Lacustrine Organic Geochemistry - Overview of Indicators of Organic Matter Sources and Diagenesis in Lake Sediments. *Organic Geochemistry*, *20*(7), 867–900.

Mill, T., & Mabey, W. (1985). Photochemical Transformations. In *Environmental Exposure from Chemicals, Volume 1* (pp. 175–216). CRC Press.

Moldoveanu, S. (2005). *Analytical Pyrolysis of Synthetic Organic Polymers*. Elsevier.

Mortazavi, S., Riyahi Bakhtiari, A., Sari, A. E., Bahramifar, N., & Rahbarizade, F. (2012). Phenolic Endocrine Disrupting Chemicals (EDCs) in Anzali Wetland, Iran: Elevated Concentrations of 4-nonylphenol, Octhylphenol and Bisphenol A. *Marine Pollution Bulletin*, *64*(5), 1067–1073. doi:10.1016/j.marpolbul.2012.02.010

Muri, G., & Wakeham, S. G. (2006). Organic Matter and Lipids in Sediments of Lake Bled (NW Slovenia): Source and Effect of Anoxic and Oxic Depositional Regimes. *Organic Geochemistry*, *37*(12), 1664–1679. doi:10.1016/j.orggeochem.2006.07.016

Muschitiello, F., Andersson, A., Wohlfarth, B., & Smittenberg, R. H. (2015). The C20 Highly Branched Isoprenoid Biomarker – A new Diatom-sourced Proxy for Summer Trophic Conditions? *Organic Geochemistry*, *81*, 27–33. doi:10.1016/j.orggeochem.2015.01.007

Nichols, J. E., Booth, R. K., Jackson, S. T., Pendall, E. G., & Huang, Y. (2006). Paleohydrologic reconstruction based on n-alkane distributions in ombrotrophic peat. *Organic Geochemistry*, *37*(11), 1505–1513. doi:10.1016/j.orggeochem.2006.06.020

Noller, S. J. (2000). Lead-210 Geochronology. *Quaternary Geology*, *210*, 115–120. doi:10.1029/RF004p0115

Page, D. S., Boehm, P. D., Douglas, G. S., Bence, A. E., Burns, W. A., & Mankiewicz, P. J. (1999). Pyrogenic Polycyclic Aromatic Hydrocarbons in Sediments Record Past Human Activity: A Case Study in Prince William Sound, Alaska. *Marine Pollution Bulletin*, *38*(4), 247–260. doi:10.1016/S0025-326X(98)00142-8

Pearce, G. E. S., Harradine, P. J., Talbot, H. M., & Maxwell, J. R. (1998). Sedimentary Sterols and Steryl Chlorin Esters: Distribution Differences and Significance. *Organic Geochemistry*, *28*, 3–10. doi:10.1016/S0146-6380(97)00124-1

Percot, A., Yalcin, A., Aysel, V., Erduğan, H., Dural, B., & Güven, K. C. (2009). Loliolide in Marine Algae. *Natural Poduct Research*, *23*(5), 460–465. doi:10.1080/14786410802076069

Phinney, H. K. (1946). A Peculiar Lake Sediment of Algal Origin. *University of Notre Dame*, *35*(2), 453–459.

Rao, Z., Wu, Y., Zhu, Z., Jia, G., & Henderson, A. (2011). Is the Maximum Carbon Number of Long-Chain n-Alkanes an Indicator of Grassland or Forest? Evidence from Surface Soils and

Modern Plants. *Chinese Science Bulletin*, *56*(16), 1714–1720. doi:10.1007/s11434-011-4418-y

Rashby, S. E., Sessions, A. L., Summons, R. E., & Newman, D. K. (2007). Biosynthesis of 2-Methylbacteriohopanepolyols by an Anoxygenic Phototroph. *Proceedings of the National Academy of Sciences of the United States of America*, *104*(38), 15099–15104. doi:10.1073/pnas.0704912104

Repeta, D. J. (1989). Carotenoid Diagenesis in recent Marine Sediments: II. Degradation of Fucoxanthin to Loliolide. *Geochimica et Cosmochimica Acta*, *53*(3), 699–707. doi:10.1016/0016-7037(89)90012-4

Rezg, R., El-Fazaa, S., Gharbi, N., & Mornagui, B. (2014). Bisphenol A and Human Chronic Diseases: Current Evidences, Possible Mechanisms, and future Perspectives. *Environment International*, *64*, 83–90. doi:10.1016/j.envint.2013.12.007

Rice, C. P., Samson, P. J., & Noguchit, G. E. (1986). Atmospheric Transport of Toxaphene to Lake Michigan. *Environmental Science & Technology*, *20*(11), 1109–1116.

Rice, C. P., Schmitz-Afonso, I., Loyo-Rosales, J. E., Link, E., Thoma, R., Fay, L., … Camp, M. J. (2003). Alkylphenol and Alkylphenol-ethoxylates in Carp, Water, and Sediment from the Cuyahoga River, Ohio. *Environmental Science and Technology*, *37*(17), 3747–3754. doi:10.1021/es034105o

Rielley, G., Collier, R. J., Jones, D. M., & Eglinton, G. (1991). The biogeochemistry of Ellesmere Lake, U.K.—I: source correlation of leaf wax inputs to the sedimentary lipid record. *Organic Geochemistry*, *17*(6), 901–912. doi:10.1016/0146-6380(91)90031-E

Ritchie, J., & Mchenry, J. R. (1990). Application of Radioactive Fallout Cesium-137 for Measuring Soil Erosion and Sediment Accumulation Rates and Patterns : A Review. *Journal of Environmental Quality*, *233*, 215–233.

Ritter, L., Solomon, K. R., Forget, J., & Stemeroff, M. (2007). Persistent organic pollutants. *United Nations Environment Programme*.

Robson, J. N., & Rowland, S. J. (1988). Biodegradation of Highly Branched Isoprenoid Hydrocarbons: A possible explanation of Sedimentary Abundance. *Organic Geochemistry*, *13*(4-6), 691–695. doi:10.1016/0146-6380(88)90090-3

Roger, M., Ritchie, J. C., & Gill, A. C. (1973). Accumulation of Fallout Cesium 137 in Soils and Sediments in Selected Watersheds and Sediments in Selected Watersheds. *Water Resource Research*, *9*(3), 676–686.

Rosner, D., & Markowitz, G. (2013). Persistent Pollutants: A Brief History of the Discovery of the Widespread Toxicity of Chlorinated Hydrocarbons. *Environmental Research*, *120*, 126–33. doi:10.1016/j.envres.2012.08.011

Rowland, S. J., & Robson, J. N. (1990). The Widespread Occurrence of Highly Branched Acyclic C20, C25 and C30 Hydrocarbons in Recent Sediments and Biota—A Review. *Marine Environmental Research*, *30*(3), 191–216. doi:10.1016/0141-1136(90)90019-K

Sheehan, D. M. (2000). Activity of Environmentally Relevant Low Doses of Endocrine Disruptors and the Bisphenol A Controversy: Initial Results Confirmed. *Experimental Biology and Medicine*, *224*, 57–60.

Shiea, J., Brassell, S. C., & Ward, D. M. (1990). Mid-chain Branched Mono- and dimethyl Alkanes in Hot Spring Cyanobacterial Mats: A direct Biogenic Source for Branched Alkanes in Ancient Sediments? *Organic Geochemistry*, *15*(3), 223–231. doi:10.1016/0146-6380(90)90001-G

Simoneit, B. R. T. (2002). *Biomass Burning - A Review of Organic Tracers for Smoke from Incomplete Combustion*. *Applied Geochemistry* (Vol. 17). doi:10.1016/S0883-2927(01)00061-0

Sinninghe Damsté, J. S., Baas, M., Geenevasen, J. A. J., & Kenig, F. (2005). Structural Identification of Sedimentary C 21 and C 22 Highly Branched Isoprenoid Alkanes. *Organic Geochemistry*, *36*, 511–517. doi:10.1016/j.orggeochem.2004.11.005

Sinninghe Damsté, J. S., Muyzer, G., Abbas, B., Rampen, S. W., Massé, G., Allard, W. G., … Schouten, S. (2004). The Rise of the Rhizosolenid Diatoms. *Science (New York, N.Y.)*, *304*(5670), 584–587. doi:10.1126/science.1096806

Sinninghe Damsté, J. S., van Koert, E. R., Kock-van Dalen, A. C., de Leeuw, J. W., & Schenck, P. A. (1989). Characterisation of Highly Branched Isoprenoid Thiophenes occurring in Sediments and Immature Crude Oils. *Organic Geochemistry*, *14*(5), 555–567. doi:10.1016/0146-6380(89)90035-1

Smittenberg, R. H., Baas, M., Schouten, S., & Sinninghe Damsté, J. S. (2005). The demise of the alga Botryococcus braunii from a Norwegian fjord was due to early eutrophication. *The Holocene*, *15*(1), 133–140. doi:10.1191/0959683605hl786rp

Spyckerelle, C., Greiner, A., Albrecht, P., & Ourisson, G. (1977). Aromatic hydrocarbons from geological sources. Part III. *Journal of Chemical Research*, 3746–3777.

Stoermer, E. (1977). Post Pleistocene Diatom Succession in Douglas Lake, Michigan. *Journal of Phycology*, *13*, 73–80.

Summons, R. E., Jahnke, L. L., Hope, J. M., & Logan, G. A. (1999). 2-Methylhopanoids as Biomarkers for Cyanobacterial Oxygenic Photosynthesis. *Nature*, *400*(6744), 554–557. doi:10.1038/23005

Szafranek, B. M., & Synak, E. E. (2006). Cuticular Waxes from Potato (Solanum tuberosum) Leaves. *Phytochemistry*, *67*(1), 80–90. doi:10.1016/j.phytochem.2005.10.012

Ten Haven, H. L., de Leeuw, J. W., Rullkötter, J., & Sinninghe Damsté, J. S. (1987). Restricted Utility of the Pristane/Phytane ratio as a Palaeoenvironmental Indicator. *Nature*, *330*(17), 641–643.

Ten Haven, H. L., Peakman, T. M., & Rullkötter, J. (1992). Early Diagenetic Transformation of Higher-plant Triterpenoids in Deep-sea Sediments from Baffin Bay. *Geochimica et Cosmochimica Acta*, *56*(5), 2001–2024. doi:10.1016/0016-7037(92)90326-E

Tissot, B. P., & Welte, D. H. (1984). Diagenesis, Catagenesis and Metagenesis of Organic Matter. In *Petroleum Formation and Occurrence* (pp. 69–73). doi:1 0.1 007/978-3-642-96446-6

Tsai, W.-T. (2006a). Human Health Risk on Environmental Exposure to Bisphenol A: A Review. *Journal of Environmental Science and Health. Part C, Environmental Carcinogenesis & Ecotoxicology Reviews*, *24*(2), 225–255. doi:10.1080/10590500600936482

Tsai, W.-T. (2006b). Human Health Risk on Environmental Exposure to Bisphenol-A: A Review. *Journal of Environmental Science and Health, Part C: Environmental Carcinogenesis & Ecotoxicology Reviews*, *24*(2), 225–55. doi:10.1080/10590500600936482

Turner, L. J., & Delorme, L. D. (1996). Assessment of 210Pb Data from Canadian Lakes using the CIC and CRS Models. *Environmental Geology*, *28*(2), 78–87. doi:10.1007/s002540050080

Turusov, V., Rakitsky, V., & Tomatis, L. (2002). Dichlorodiphenyltrichloroethane (DDT): Ubiquity, Persistence, and Risks. *Environmental Health Perspectives*, *110*(2), 125–128. doi:10.1289/ehp.02110125

Vandenberg, L. N., Maffini, M. V, Sonnenschein, C., Rubin, B. S., & Soto, A. M. (2009). Bisphenol-A and the Great Divide: a Review of Controversies in the Field of Endocrine Disruption. *Endocrine Reviews*, *30*(1), 75–95. doi:10.1210/er.2008-0021

Vogel, S. (2009). The Politics of Plastics: The Making and Unmaking of Bisphenol A “Safety”. *American Journal of Public Health*, *99*, 559–566. doi:10.2105/AJPH.2008.159228

Volkman, J. K. (1986). A review of Sterol Markers for Marine and Terrigenous Organic Matter. *Organic Geochemistry*, *9*(2), 83–99. doi:10.1016/0146-6380(86)90089-6

Volkman, J. K. (2003). Sterols in Microorganisms. *Applied Microbiology and Biotechnology*, *4*, 495–506. doi:10.1007/s00253-002-1172-8

Volkman, J. K. (2005). Sterols and other triterpenoids: Source specificity and evolution of biosynthetic pathways. *Organic Geochemistry*, *36*(2), 139–159. doi:10.1016/j.orggeochem.2004.06.013

Volkman, J. K., Barrett, S. M., Blackburn, S. I., Mansour, M. P., Sikes, E. L., & Gelin, F. (1998). Microalgal Biomarkers : A Review of Recent Research Developments. *Organic Geochemistry*, *29*(5), 1163–1179.

Voss, E. G. (1956). A History of Floristics in the Douglas Lake Region (Emmet and Cheboygan counties), Michigan, with an account of Rejected Records. *Journal of the Scientific Laboratories*, *44*, 16–75.

Wakeham, S. G., Sinninghe Damsté, J. S., Kohnen, M. E. L., & De Leeuw, J. W. (1995). Organic Sulfur Compounds formed during Early Diagenesis in Black Sea Sediments. *Geochimica et Cosmochimica Acta*, *59*(3), 521–533. doi:10.1016/0016-7037(94)00361-O

Wilson, I., & Putzcer, J. E. (1942). Pollen Study of Sediments from Douglas Lake, Cheboygan County and Middle Fish Lake, Montmorency County, Michigan. *Proceedings of the Indiana Academy of Science*, *52*, 87–92.

Xu, Y., & Jaffé, R. (2008). Biomarker-based Paleo-record of Environmental change for an Eutrophic, Tropical Freshwater Lake, Lake Valencia, Venezuela. *Journal of Paleolimnology*, *40*(1), 179–194. doi:10.1007/s10933-007-9150-x

Yon, D., & Maxwell, J. (1982). 2,6,10-Trimethyl-7-(3-methylbutyl)-dodecane, A Novel Sedimentary Biological Marker Compound. *Tetrahedron Letters*, *23*(20), 2143–2146.

Yunker, M. B., Macdonald, R. W., Vingarzan, R., Mitchell, H., Goyette, D., & Sylvestre, S. (2002). PAHs in the Fraser River Basin a Critical appraisal of PAH ratios as indicators of PAH source and composition. *Organic Geochemistry*, *33*, 489–515.

Zincke, T. (1905). Mittheilungen aus dem chemischen Laboratorium der Universitat Marburg. *Justus Leibigs Annals Chemie*, *343*, 75–99.